COLLISION EFFICIENCY OF A POLLUTANT PARTICLE ONTO A LONG CYLINDER IN LOW REYNOLDS NUMBER FLUID FLOW

by

Saeed Hashemi Mohammadabad

Department of Civil Engineering and Applied Mechanics
McGill University
Montreal, Canada

July 1996

A THESIS SUBMITTED TO THE FACULTY OF GRADUATE STUDIES
AND RESEARCH IN PARTIAL FULFILMENT OF THE REQUIREMENTS
FOR THE DEGREE OF MASTER OF ENGINEERING

ISBN 0-612-19867-7

Canada

COLLISION EFFICIENCY OF

A POLLUTANT PARTICLE ONTO A LONG CYLINDER

IN HIS NAME. THE MOST HIGH

SUMMARY

A method for calculating the collision efficiency of a small pollutant particle onto a solid long circular cylinder in a low Reynolds number fluid flow with inertia effects is presented. The cylinder is considered at rest in a uniform undisturbed flow at infinity, in the direction perpendicular to the cylinder axis.

Assuming that the Reynolds number R based on cylinder radius b is very small but not zero ($R << 1$), and the Reynolds number Re based on cylinder length l is of order unity, the force per unit length of the cylinder, correct to the order of R, is obtained, first for a general flow direction and then for the case of flow perpendicular to the cylinder axis. This is done by using the Navier-Stokes equations in long slender bodies theory and applying matched asymptotic expansions in terms of the ratio κ of radius to body length. Flow field around the cylinder is calculated and the equation of particle motion is developed by applying Newton's second law of motion. The initial particle velocity far from the cylinder is calculated analytically and the particle trajectory course is solved numerically as an initial value problem by using Richardson Extrapolation and the Bulirsch-Stoer method.

The collision Efficiency E is obtained by trial and error and is plotted against the dimensionless particle parameter p for different values of R (from 10^{-6} to 1). The numerical calculations show that the curves have a tendency to move to the right and become like a straight-line as R gets very small. The points at which E is less than 0.005 are also predicted.

SOMMAIRE

Une méthode qui calcule l'efficacité de la collision d'une petite particule de polluant avec d'un long cylindre circulaire solide, dans un écoulement fluide dont le nombre de Reynolds est bas, avec les effets des forces d'inertie, est présentée. Le cylindre est considéré au repos dans un écoulement uniforme infini, dans la direction perpendiculaire à l'axe du cylindre.

En présumant que le nombre de Reynolds R basé sur le rayon du cylindre b est très petit ($R << 1$), mais différent de zéro, et que le nombre de Reynolds Re basé sur la longueur du cylindre l, est de l'ordre de l'unité, la force par unité de longueur de cylindre,du même ordre que R, est obtenue en premier pour une direction générale de l'écoulement et alors pour le cas d'un écoulement perpendiculaire à l'axe du cylindre. Ceci est effectué en utilisant la théorie des corps longs et minces et en appliquant l'expansion asymptotique en termes du rapport κ du rayon à la longueur du corps. Le champ d'écoulement autour du cylindre est calculé et l'équation de mouvement de la particule est développée en appliquant la deuxième loi de mouvement de Newton. La vitesse initiale de la particule, loin du cylindre, est calculée analytiquement et la trajectoire de la route est résolue numériquement comme un problème à valeur initiale en utilisant l'extrapolation de Richardson et la méthode de Bulirsch-Stoer.

L'efficacité de la collision E est obtenu par essais et erreurs et est mis en courbes en fonction du paramètre adimensionnel de la particule p pour différents R (de 10^{-6} à 1). Les calculs numériques montrent que les courbes ont tendance à se déplacer vers la droite et deviennent des droites quand R devient très petit. Les points pour lesquels l'efficacité est inférieure à 0.005 sont aussi prédits.

TABLE OF CONTENTS

LIST OF FIGURES AND TABLES

ACKNOWLEDGEMENTS

The author wishes to express his deep regret of the death of his supervisor, late professor R. G. Cox, on July 31, 1995. In addition to his expertise in analytical Fluid Mechanics and extensive knowledge in different other fields, Professor Cox had a high rank in humanity as well. He never stopped thinking about his students even when it was almost impossible to communicate, during his illness. After about a year of his death, it is to him that this thesis is dedicated.

The author is grateful to the Ministry of Culture and Higher Education of the Islamic Republic of Iran for providing him a fellowship. The work in this thesis was also funded in part by NSERC.

Thanks must also be given to Professor T. G. M. van de Ven who accepted to supervise me after the sad death of professor Cox and provided valuable guidance during writing this thesis.

Special thanks to my good friend, Mr. Kourosh Mohammadi, for his French translation of the summary.

Lastly, but most importantly, the author would like to thank his family who helped to keep his spirit up during long hours of work.

Chapter 1

INTRODUCTION

The removal of suspended particles from a carrier fluid is of great interest in many industries. The first step in the design of a filter involves obtaining a detailed knowledge of the fluid dynamics of the flow. The motion of fluid around a fiber or a slender body has long received considerable attention and, particularly, flow at low Reynolds number has been extensively studied analytically. In this research, a method for developing the hydrodynamic forces acting on an isolated long cylinder and deriving the flow field around the cylinder is presented. We also use the obtained results to develop the equations governing the motion of a tiny pollutant particle toward the cylinder. Solving the particle equations of motion, numerically, we calculate the collision efficiency of the particle onto the cylinder and plot the result into graphs.

Although the applications of this work are specific, they are found in different industries such as deposition of particles onto (single) pulp fibers in papermaking suspensions, in the retention of particles in the forming paper sheet during the papermaking process, and even in the removal of metallic grains from the lubricating oil of an internal combustion engine. Generally, this work can be applied in pulp fibers, asbestos fibers, fibrous filters, and wool and cloth industries.

1.1 STATEMENT OF THE PROBLEM

Consider an isolated long circular cylinder at rest in a uniform flow of velocity U in the direction perpendicular to the cylinder axis, at infinity. The radius of the cylinder being b and its length being l (long enough to neglect the ends effects). The Reynolds

number based on the radius of the cylinder R is very small but not zero ($R << 1$) and the Reynolds number based on the length of the cylinder Re is of order unity. Thus, inertia effects are considered. A very small solid spherical particle is released far from the cylinder. The specifications of the particle are characterized as a particle parameter p. The collision efficiency of the particle onto the cylinder is our final objective in this research. Because of the long length of the cylinder, every unit length of the cylinder, far from the ends, can be dealt with exactly the same. Then, by definition, the collision efficiency E, for each unit length of the cylinder, is the ratio of the largest amount of initial x_3' (shown as X_∞' in figure 1.1) over b so that if we release the particle at X_∞', it just and just touches the surface of the cylinder. Hence the problem turns out to be a two dimensional problem.

Neglecting all hydrodynamic and colloidal interactions, the number of potential collisions f_c per unit length of the cylinder per second, when the cylinder radius b is much larger than the particle radius a, is given by

$$f_c = 2\,n\,U\,b,$$

where n is the number of pollutant particles per unit volume. The number of pollutant particles that can be captured by the cylinder per unit length of the cylinder per second is given by

$$f = E f_c,$$

with the collision efficiency E given by

$$E = \frac{X_\infty'}{b}.$$

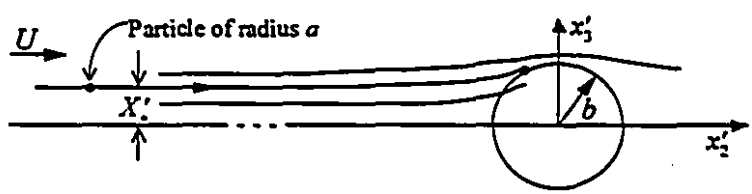

Figure 1.1 Statement of the problem (cross-section)

Since our interest is not only in the results, but also in the analytical method of solution, in order to find the forces per unit length and flow field around the cylinder, we need to study and develop the necessary equations from the basic theories of long slender bodies. Applying the modified results for the case of our cylinder, we will be able, then, to develop a set of differential equations expressing the trajectory of the particle.

In 1970, neglecting inertia effects, the creeping flow equations for a general direction of velocity was solved by R. G. Cox. The result was a power series in $\left(\frac{1}{\ln\kappa}\right)$, correct to the order of $\left(\frac{1}{\ln\kappa}\right)^3$, where $\kappa = \frac{b}{l} << 1$. In 1980, R. E. Johnson solved the same problem but satisfying an integral equation correct to the order of κ^{+1} ($Re = 0$, and $R = 0$).

R. E. Khayat and R. G. Cox considered inertia effects in 1989. They solved the case with

$$Re \equiv \frac{lU}{\nu} = O(1), \quad \text{and} \quad R \equiv \frac{bU}{\nu} = \kappa Re << 1,$$

and obtained the force per unit length on body as a power series in $\left(\frac{1}{\ln\kappa}\right)$, correct to the order of $\left(\frac{1}{\ln\kappa}\right)^3$, for Re small or of order unity.

In the present research, we first concentrate on the same problem as that of R. E. Khayat and R. G. Cox (long slender body with circular cross-section) and find the force per unit length, but as an *integral equation.*

We will make an expansion in κ (correct to the order of κ^{+1}) treating Re as a parameter so that if $Re \to 0$, we must have the same result as that of R. E. Johnson (1980). Then, we will find the flow field based on such a drag force on a slender body.

Applying the obtained result for the case of a long circular cylinder, we will find the flow field around the cylinder. It is worth mentioning that obtaining the same result as in previous studies for the same conditions but with different methods is the strength of these studies and increases the reliability of the results. Thereafter, it is possible to obtain the trajectory equations for a particle released in such a flow field, far from the cylinder. Having the equations for the path of a particle toward the cylinder, the collision efficiency is calculated numerically for a series of R's and p's.

1.2 OBJECTIVES

As mentioned earlier, our final objective is to calculate the collision efficiency of a particle onto the cylinder. Our approach in this research is that we deal with the problem analytically, go as far as we can, and then solve the rest numerically. Therefore, since the analytical portion of solution is of our interest too, we set up our objectives in different stages as follows.

1) Deriving the drag force per unit length of an isolated slender body, considering inertia effects and correct to the order of κ^{-1}, as an *integral equation* and ensuring it is the same as R. E. Johnson's result (1980) for $Re \rightarrow 0$, as it should be.
2) Developing hydrodynamic forces on the cylinder, based on what we obtained in the previous stage for a slender body, first for a general flow direction and then for the flow perpendicular to the cylinder axis. This must be the same as the result obtained by Khayat & Cox (1989).
3) Having the drag forces on the cylinder, we develop the flow field around the cylinder for the flow perpendicular to the cylinder axis.
4) Deriving the equations governing the motion of a particle as a set of differential equations.
5) Solving particle equations of motion, numerically, in order to calculate the collision efficiency of the particle onto the cylinder. This is to be done for different Reynolds number R (from 10^{-6} to 1) and different values of the particle parameter p. Since we

make the assumption of $R << 1$, the case $R = 1$ is not going to be valid but we include this just to see the behavior of the solution. The case $R = 0.1$ is somewhere in between and suspicious. It should be investigated too.

6) By plotting the collision efficiency E against the particle parameter p, we should realize
   i) what behavior the plotted graphs show. It is expected that they should move to right as R gets very small. But do they move to right to a certain curve or go to infinity or become like almost a straight-line?
   ii) what the maximum value of p is for $E \to 0$. This values tell us, for each R, the minimum value of p we should keep in order to have an impact with the lowest efficiency.

1.3 THESIS ORGANIZATION AND OUR APPROACH

After some introductory information including the statement of the problem, we set up our objectives for the different stages of work in chapter one. Our main approach in this research is that we deal with the problem analytically, go as far as we can, and then solve the rest numerically. In chapter 2, some of the previous studies related to the problem on hand are summarized. These include the collection of pollutant, described in papers in computational fluid dynamics, and the motion of long slender bodies as the basic theory of developing the flow field around the cylinder. The interrelation between this work and previous studies is also explained.

Chapter three is a quite analytical chapter devoted to the development of the equations. After a more detailed explanation of the problem, we concentrate on the flow around long slender bodies. Inner and outer region variables are introduced, non-dimensionalized, and the drag force on the body and the flow field are developed by matching between outer and inner solutions. Then as an example of long slender bodies, the fluid motion around the cylinder is discussed. Deriving the hydrodynamic forces on the cylinder for a general flow direction is done analytically by solving the integral equations developed for a slender body. The advantage of solutions as integral equations

(instead of power series) is that they can be directly solved for bodies which poses a certain symmetry (like a cylinder). The force and the flow field for the case of flow perpendicular to the cylinder axis are found by matching the asymptotic expansions. In the last section of this chapter, the motion of a tiny particle in the flow is investigated. Using Newton's second law of motion, the equations governing the trajectory course of particle are obtained, analytically, by applying the results from the previous section.

The main idea of chapter four is to introduce the numerical method to be used in solving the equations of motion of the particle. To start any initial value problem, initial values must be determined. Calculation of the initial velocities, far in the outer region, is the only analytical section of this chapter. Then, after comparing different methods for solving an initial value problem, Richardson extrapolation and the Bulirsch-Stoer method is chosen and discussed.

In chapter five, we first explain what we are doing in the numerical calculations. Optimizing the solution and error control in a numerical solution are other topics discussed in this chapter. Then, the numerical results are presented, partly in table form and fully as different graphs for different Reynolds numbers R. Discussion about these results is the subject of the last part of this chapter.

Conclusion and suggestions for future work are the ideas of chapter six. The relationship between the final results, the results obtained in each chapter and section and our objectives expressed in chapter one is discussed and shown. Interesting and useful topics to continue this work are explained as suggestions for future studies.

The next part, Appendix A, includes the source program which has been used to obtain the results, presented in chapter five, and also the tables produced by the program as their outputs.

The last part of this thesis, Appendix B, is a list f the nomenclature. A list of all symbols used throughout the thesis is presented.

Chapter 2

SUMMARY OF PREVIOUS STUDIES

There have been a tremendous number of research studies on low Reynolds number fluid flow particularly after C.-L.-M.-H. Navier, and Sir G. G. Stokes formulated their well-known equations, ordinarily called the *Navier-Stokes equations*, independently in 1822 and 1845, respectively. However, there are only a few problems in which it is possible to solve exactly the creeping motion equations for flow around a single isolated solid body. When it comes to inertia effects, of course, the number of cases with exact solutions are even less. Since our interest, in this research, is not only in the results, but the analytical method of solving is also of importance, what we discuss here is mostly related to solving the flow field and drag forces on slender bodies as the basis for finding the equation of motion of a particle colliding with the slender body, analytically. The rest of the problem, to calculate the collision efficiency, is solved numerically and there is usually no available analytical solution for it. Some of the previous studies, related to the problem on hand, are summarized in this chapter.

2.1 COLLECTION OF POLLUTANT

2.1.1 Explanation of Theory

Fonda and Herne, in the 1940s, numerically evaluated the collision efficiency, E, as a function of the particle parameter, p, for impact of pollutant on a falling rain or mist drop. A falling rain drop has the same flow around it as a solid sphere since $\frac{\mu_{water}}{\mu_{air}} \cong 50-100 >> 1$ (neglecting inside circulation of the drop). Because of the likeness of this problem with our problem and in order to get familiar with the problem solving procedure, this case is going to be explained along with more details than the others.

Consider a drop of radius R sedimenting with velocity V.

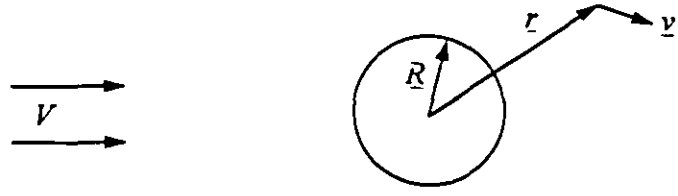

Figure 2.1 A falling rain drop

The velocity field around drop $\underline{v}(\underline{r})$ must be, by dimensional analysis, of the form

$$\underline{v} = V\underline{f}\left(\frac{\underline{r}}{R}, \frac{VR}{\nu}\right), \tag{2,1}$$

where ν = kinematic viscosity, and if $Re \equiv \frac{VR}{\nu} << 1$, we have creeping flow.

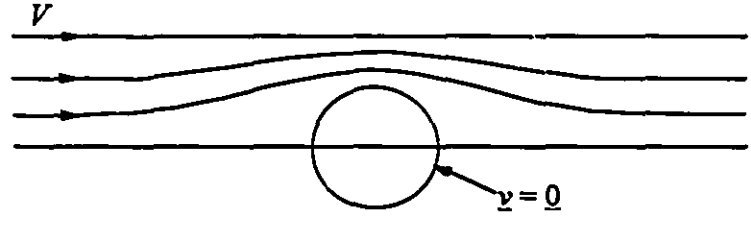

Figure 2.2 Velocity field around the sphere

Where $Re >> 1$, the flow is inviscid flow ahead of the drop and since V is a uniform velocity far enough from the sphere, we have irrotational flow, described by

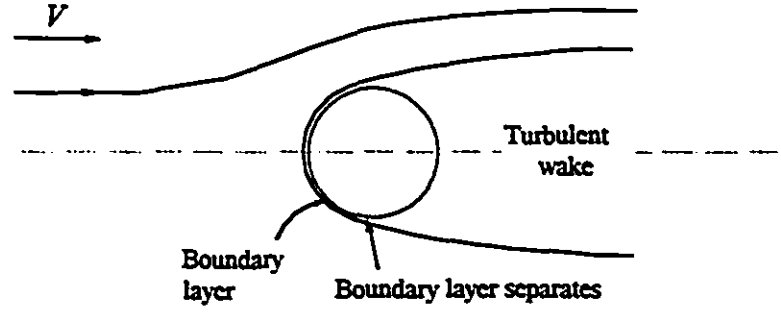

Figure 2.3 Inviscid flow

$$-\nabla p = \rho \underline{u} \cdot \nabla \underline{u} \qquad \nabla \cdot \underline{u} = 0, \tag{2.2}$$

where ρ = density of the fluid

$\underline{u}$ = velocity field

p = pressure field

∇ = Nabla operator $\left(\frac{\partial}{\partial x_1}\underline{i} + \frac{\partial}{\partial x_2}\underline{j} + \frac{\partial}{\partial x_3}\underline{k}\right)$

Taking the curl ($\nabla\times$), to get rid of p

$$\underline{0} = \rho\left(\underline{u}.\nabla\underline{\omega} + \underline{\omega}.\nabla\underline{u}\right) \qquad \underline{\omega} = \nabla \times \underline{u}\ , \tag{2.3}$$

$$\frac{D\underline{\omega}}{Dt} = \frac{\partial\underline{\omega}}{\partial t} + \underline{u}.\nabla\underline{\omega} = -\underline{\omega}.\nabla\underline{u} \quad \Rightarrow \quad \frac{D\underline{\omega}}{Dt} = \underline{0}\ , \tag{2.4}$$

where $\underline{\omega}$ = vorticity

$\frac{D\underline{\omega}}{Dt}$ = Lagrangian derivative

$\frac{\partial\underline{\omega}}{\partial t} = 0$ (unsteady term)

In fact, since $\underline{\omega} = \underline{0}$ for upstream, $\underline{\omega} = \underline{0}$ everywhere. In other words, the viscous term in the Navier-Stokes equations is neglected, for $Re >> 1$, so there is no cause of diffusion for vorticity.

$$\because \quad \nabla \times \underline{u} = \underline{0} \qquad \underline{u} = \nabla\phi\ , \tag{2.5}$$

$$\nabla.\underline{u} = 0 \quad \Rightarrow \quad \nabla^2\phi = 0\ , \tag{2.6}$$

where ϕ = velocity potential and with $u_n = \frac{\partial\phi}{\partial n} = 0$ at the drop surface.

If the pollutant is in the form of *small solid particles* of radius a (where $a << R$), the position $\underline{r}$ of a single particle is given by

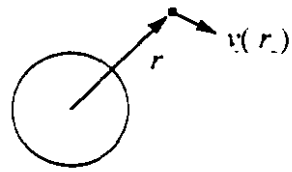

Figure 2.4 Small solid pollutant

$$\left(\tfrac{4}{3}\pi a^3 \rho_s\right)\underline{\ddot{r}} = 6\pi\mu\, a\left[\underline{v}(\underline{r}) - \underline{\dot{r}}\right], \tag{2,7}$$

where a = radius of particle

ρ_s = density of particle

$\underline{\ddot{r}}$ = acceleration of particle relative to the constant coordinates on the sphere

μ = viscosity of the fluid

$\underline{v}(\underline{r})$ = velocity of fluid relative to the sphere

$\underline{\dot{r}}$ = velocity of particle relative to the sphere

In the right hand side of the equation (2,7), the result of Stokes problem (falling sphere) is used (drag forces on a spherical solid body, F = 6πμ aU, where Re = 0 and U is the constant velocity of sphere relative to fluid, but in here we use the expression of velocity of fluid relative to particle, instead). We are also assuming here that the particle radius a is sufficiently small so that inertia effects in the fluid for flow around it are negligible.

Defining dimensionless quantities

$$\underline{r}^* = \frac{\underline{r}}{R} \qquad t^* = \frac{tV}{R} \qquad v^* = \frac{\underline{v}}{V}, \tag{2,8}$$

so that t is time and $\underline{v}^* = \underline{v}^*\left(\underline{r}^*, Re\right)$. Hence the particle motion is given by

$$\mathrm{p}\frac{d^2\underline{r}^*}{dt^{*2}} = -\frac{d\underline{r}^*}{dt^*} + \underline{v}^*\left(\underline{r}^*, Re\right), \tag{2,9}$$

where the particle parameter, $\mathrm{p} = \dfrac{2\rho_s a^2 V}{9\mu R}$.

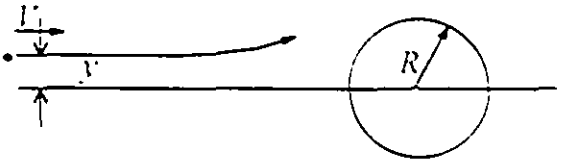

Figure 2.5 Particle orbit

Thus the particle orbit depends only on initial position $\frac{y}{R}$, p, and Re.

If y is less than some y_c, the particle collides with the drop. Otherwise if $y > y_c$, it misses the drop. Hence y_c is the height of the highest point at which if we release the particle in infinity, we will still get an impact.

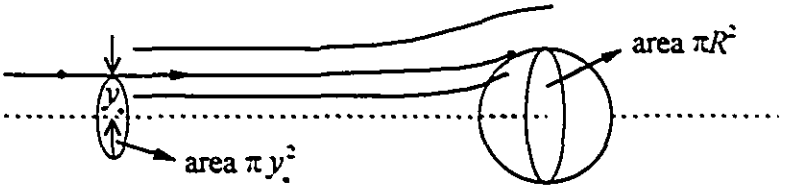

Figure 2.6 Collision efficiency and y_c

By definition, the collision efficiency is $E = \left(\frac{\pi y_c^2}{\pi R^2}\right) = \left(\frac{y_c}{R}\right)^2$. Then E *depends on* p *and* Re *only*, with $0 \le E \le 1$ ($E > 1$ are not considered).

As mentioned earlier, Fonda and Horne evaluated $E = E$ (p) numerically for

(a) Creeping flow $\underline{v}^* = \underline{v}^*(\underline{r}^*)$ around drop (for $Re \ll 1$).

(b) Potential flow $\underline{v}^* = \underline{v}^*(\underline{r}^*)$ around drop (for $Re \gg 1$).

The result of their numerical calculations, assembled in a graph, was more or less similar to what is presented in chapter 5.

2.1.2 Effects Not Included in the Above Theory

(a) Effect of finite (non-zero) size of particle.

(b) The intermediate Reynolds numbers are totally neglected. That is, for instance, for creeping flow ($Re << 1$), inertia effects are ignored.

(c) When a particle gets close to the drop surface the hydrodynamic interaction of particle with drop surface will result in a change of trajectory [actually including (c) would result in $E = 0$].

(d) Intermolecular (van der Waals) forces and electrostatic forces between a particle and the drop or other colloidal forces.

(e) Deformation of the drop surface as the particle gets close to it. The particle may
bounce - no capture,
penetrate the surface or
be captured at the surface.

(f) For the inviscid case ($Re >> 1$) effects of boundary layer and wake [i.e. they change value of $\underline{v}^*(\underline{r}^*)$].

(g) Effect of gravity on the particle.

(h) Brownian motion of the particle (diffusion portion of motion). Diffusion may dominate over convection with very small particles.

(i) Shape of particle will modify many of the above effects.

2.1.3 Papers in Computational Fluid Dynamics

Many theoretical papers have been appearing in recent years aimed at numerical calculation of particle collection , collection efficiency, or particle depcsition rates and the like. Basically, a computational approach is suitable when

(a) There is a particular interest in results (not in the method of solving).

(b) The answer is more or less already known before we start.

The present research is not classified as a numerical approach, instead, the obtained results can be useful for future computational solutions in this area. However, because of the similarity in subjects, a few papers in computational fluid dynamics are introduced in this section.

In 1981, Z. Adamczyk and T. G. M. van de Ven predicted particle deposition rates from a dilute suspension of Brownian particles flowing past an isolated cylindrical collector as well as through a fibrous filter. They took into account colloidal interactions (dispersion and double-layer forces) and also external forces (gravity and electrostatic).

They considered deposition of spherical particles dispersed uniformly in a uniform laminar stream and an infinitely long (to ignore end effects) cylindrical collector placed perpendicular to the main stream direction. So, the problem of obtaining the fluid velocity field became in essence two-dimensional and the stream function ψ was sufficient to describe it. For flow around a cylindrical collector, they considered several cases for which the stream function is already developed via Oseen's hypothesis (inertia effects considered). However, for flow in a fibrous filter composed of cylindrical particles (much more complex) the creeping motion equation derived by neglecting fluid inertia was used.

Neglecting interparticle interactions, they focused their attention upon the role of colloidal and external forces in particle deposition onto a cylindrical collector. A complete transport equation was solved numerically by using the implicit weighted-average Crank-Nicolson scheme and the accuracy was checked by varying the mesh size and accepting the results with relative difference less than 10^{-5}.

C. Mclaughlin, P. McComber and A. Gakwaya (1986) presented a method for calculating the collection efficiency of particles by a row of cylinders in a viscous fluid. The Navier-Stokes equation was solved by the finite element method to determine the carrier gas velocity field. Then, the particle equation of motion was also solved by the finite element method to find the particle velocity of impact. Finally, the collection efficiency was obtained by integration of the intercepted particles on the cylinder surface. Their numerical calculations covered three gas Reynolds numbers Re_D = 0.2, 2.0, and 10.

In 1989 and 1991, D. B. Ingham and M. L. Hildyard examined the entry flow and the trajectories of small solid particles into a fibrous filter modeled as a single row or cascade of cylinders. Both large (potential) and zero(creeping) Reynolds number flows

through the cascade of cylinders were treated using the Boundary Element Method (BEM). Viscous effects, for the case of potential flow, and inertia effects, in creeping flow, were ignored. For potential flow it was found that the single fiber collection efficiency of the first row was increased by adding a second row and further increased as the row separation was reduced. The opposite effect was observed for creeping flow.

2.2 THE MOTION OF LONG SLENDER BODIES

To find the equations of particle path, we need to have the equations governing the flow field around a collector. Therefore, as the analytic basis for developing the particle trajectory, researches related to the theory of long slender bodies are considered very briefly in this section. Through an analytic calculation one can find the drag force on a unit length of a slender body which is the main element to solve the flow field around such a body.

In 1970, R.G. Cox, considered the case of a general flow (velocity in any direction) with

$$Re \equiv \frac{lU}{\nu} = 0, \qquad \text{and} \qquad R \equiv \frac{bU}{\nu} = \kappa Re = 0.$$

where l being the length of body, U the uniform velocity far from body, and $\kappa = \frac{b}{l} << 1$.

Neglecting inertia effects, the creeping flow equations (2,10) was solved for a circular cross-section

$$\left.\begin{aligned} \mu \nabla^2 \underline{u} - \nabla p = 0 \\ \nabla . \underline{u} = 0 \end{aligned}\right\}. \tag{2,10}$$

The result was a power series in $\left(\frac{1}{\ln\kappa}\right)$, correct to the order of $\left(\frac{1}{\ln\kappa}\right)^3$ as

$$\underline{f}(s) = \frac{f_0}{\ln\kappa} + \frac{f_1}{(\ln\kappa)^2} + O\left(\frac{1}{\ln\kappa}\right)^3, \tag{2,11}$$

where $\underline{f}(s)$ is the force per unit length of body at a position $s = \frac{s'}{l}$ (see figure 2.7).

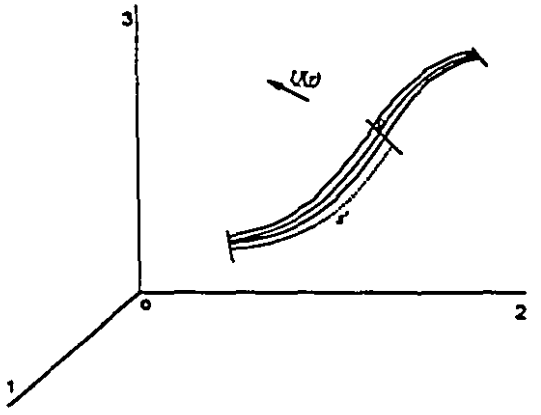

Figure 2.7 Slender body

In 1970, G. K. Batchelor, improved the solution of forces on slender bodies for non-circular cross-section. R. E. Johnson (1980) solved the same problem (circular cross-section, Re =0, and $R = 0$) but satisfying an integral equation. He also obtained the forces on the body correct to order κ^{+1} i.e.

$$F = \mu l U\left[\left(\frac{k_1}{\ln\kappa} + \frac{k_2}{(\ln\kappa)^2} + \ldots\right) + O(\kappa)\right]. \qquad (2,12)$$

Then R. E. Khayat and R. G. Cox considered inertia effects in 1989. They solved the case with a body at rest in a uniform undisturbed flow at infinity, a circular cross-section, and

$$Re \equiv \frac{lU}{\nu} = O(1), \quad \text{and} \quad R \equiv \frac{bU}{\nu} = \kappa Re << 1,$$

where $\kappa = \frac{b}{l} << 1$.

They obtained the force per unit length on body as:

(a) A power series in $\left(\frac{1}{\ln\kappa}\right)$, correct to the order of $\left(\frac{1}{\ln\kappa}\right)^3$, for Re small or of order unity

$$\underline{f}(s)=\frac{f_o(Re)}{\ln\kappa}+\frac{f_1(Re)}{(\ln\kappa)^2}+O\left(\frac{1}{\ln\kappa}\right)^3, \qquad (2,13)$$

where $\underline{f}(s)$ is a function of Re and the parameter κ .

(b) A power series in $\left(\frac{1}{\ln R}\right)$, correct to the order of $\left(\frac{1}{\ln R}\right)^3$, for Re large or of order unity

$$\underline{f}(s)=\frac{F_o(Re)}{\ln R}+\frac{F_1(Re)}{(\ln R)^2}+O\left(\frac{1}{\ln R}\right)^3, \qquad (2,14)$$

where $\underline{f}(s)$ is a function of Re and R.

In the present research, we first concentrate on the same problem as that of R. E. Khayat and R. G. Cox (long slender body with circular cross-section) and find the force per unit length, but as an *integral equation*. We will examine

$$\kappa=\frac{b}{l}\ll 1, \quad \text{and} \quad R\ll 1,$$

with

$$Re=\frac{R}{\kappa} \text{ of order unity.}$$

We will make an expansion in κ (correct to the order of κ^{+1}) treating Re as a parameter so that if $Re \to 0$, we must have the same result as that of R. E. Johnson (1980). Then, we will find the flow field based on such a drag force on a slender body. Applying the obtained result for the case of a long circular cylinder, we will find the flow field around the cylinder. It is worth mentioning that obtaining the same result as previous studies for the same conditions but different methods is a point of strength of the involved studies which increases the reliability of the results. Thereafter, developing the trajectory equations for a particle released in such a flow field, far from the cylinder, is possible. Having the equations for the path of a particle toward the cylinder, the collision efficiency is calculated numerically for a series of R's and p's.

Chapter 3

DEVELOPMENT OF EQUATIONS

3.1 EXPLANATION OF THE PROBLEM

Consider an isolated long solid cylinder with a circular cross-section which does not vary along the cylinder, the length of the cylinder being l and its radius being b. The cylinder is placed in an incompressible fluid undergoing a given uniform undisturbed flow of velocity U, perpendicular to the cylinder axis. The Reynolds number R based on the radius of the cylinder is very small ($R = \frac{bU}{\nu} << 1$) but not zero. Thus, the inertia effects of the fluid are taken into account. A very small solid spherical particle of radius a is released far enough from the cylinder. The collision efficiency of the particle on the cylinder is going to be calculated in this research.

Since the cylinder is assumed to be long enough to neglect the ends effects, every unit length of the cylinder, far from the ends, can be dealt with exactly the same. Then, by definition, the collision efficiency E, for each unit length of the cylinder, is the ratio of the largest amount of initial x_3' (shown as X_*' in figure 3.1) over b so that if we release the particle at X_*', it causes an impact on the surface of the cylinder. Hence the problem turns out to be a two dimensional problem.

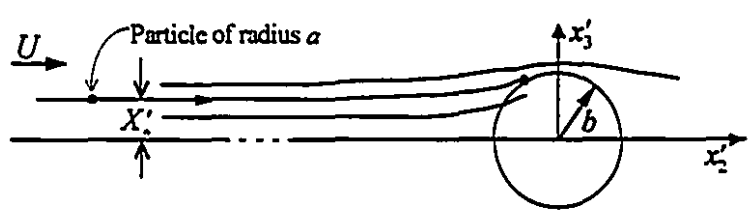

Figure 3.1 General problem (cross-section)

$$E = \frac{X'}{b}, \quad \text{for any particular } R \text{ and p.}$$

On the other hand, the flow field, streamlines, and particle trajectory are all symmetric about the equatorial plane which is parallel to the undisturbed velocity direction U, and passes through the center of the cylinder. Thus the above portion of the equatorial plane is merely considered.

In the case that x_3', the height of initial position of the particle from the equatorial plane (initial x_3'), is greater than X_c', the particle will miss the cylinder and if it is equal or less than some X_c', the particle will collide with the cylinder. It is worth mentioning that for each flow condition (different Reynolds number R) and any particle parameter p, there is a particular X_c' to be found out. In other words, if we change either R or particle parameter p, X_c' will change too.

As was mentioned in chapter 2, past researches which are related somehow to this work are not rare, but they have mostly followed a numerical approach from almost the beginning of the problem. In this research, however, the problem is going to be dealt with analytically as far as possible and after obtaining the equations of trajectory of the particle analytically, the result, the collision efficiency, for different Reynolds numbers R and particle characteristics p, will be calculated numerically by a quite reliable and powerful method, discussed in chapter 4. In this manner, the reliability of the results, introduced in chapter 5, is strongly secured.

A long isolated circular cylinder is one of the examples of long slender bodies problems which have been discussed in Fluid Mechanics for a long time. In order to find the forces per unit length and flow field around the cylinder, we need to study and develop the necessary equations from the basic theories of long slender bodies in brief. Applying the modified results for the case of our cylinder, we will be able, then, to develop a set of differential equations expressing the trajectory of the particle.

3.2 THE FLOW AROUND LONG SLENDER BODIES IN A VISCOUS FLUID

Consider a long slender body S of circular cross-section, the length of the body being l and a characteristic value of the cross-sectional radius being b. This body may be assumed bent in any manner whatsoever so that the radius of bending curvature at all points is of order l. The distance along the body centre-line measured from an arbitrary point like one end is s' (see figure 3.2) and a dimensionless quantity s is given by

$$s = \frac{s'}{l} \tag{3.1}$$

so that $0 \le s \le 1$ (the dimensionless distance along the body centre-line measured from one end), and the two ends of the body S being $s = 0$ and $s = 1$. The circular cross-section-radius at any point of the center line is generally taken to be $b\lambda(s)$, where $\lambda(s)$ is a dimensionless function of s. For a circular cylinder the radius b is constant and $\lambda(s)$ is equal to 1.

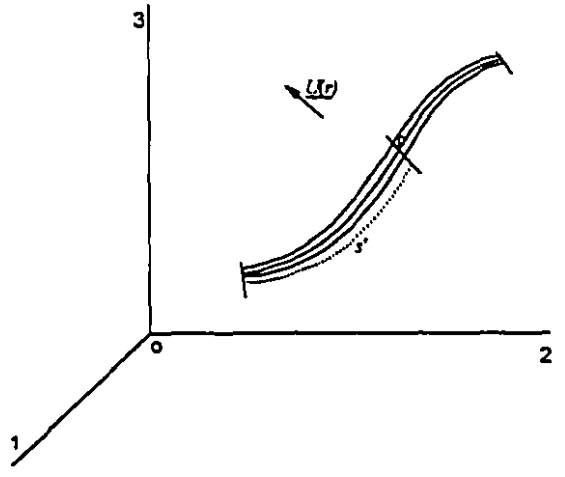

Figure 3.2 A long slender body at rest in a fluid with flow field *U(r)*

Dimensionless quantities will be used (unless otherwise stated) based upon the length l (a few miles), the fluid viscosity μ and a characteristic velocity U. The vector $\underline{r}$ (underlined variables are vectors) is now defined as a dimensionless position of a general point relative to a fixed set of rectangular Cartesian coordinates with origin O. The body S is considered placed in an undisturbed flow field with dimensionless value $\underline{U}(\underline{r})$.

At a general point P on the body centerline, we define a set of local Cartesian axes $(\bar{x}',\bar{y}',\bar{z}')$ and a set of local cylindrical polar coordinates $(\bar{\rho}',\theta,\bar{z}')$ with origin at P and the $\bar{z}'$ axis tangent to the body centerline as is shown in figure 3.3. Expansions of the velocity and pressure fields for the flow about the slender body are made in terms of the parameter $\kappa = \frac{b}{l} << 1$, that is the body is slender.

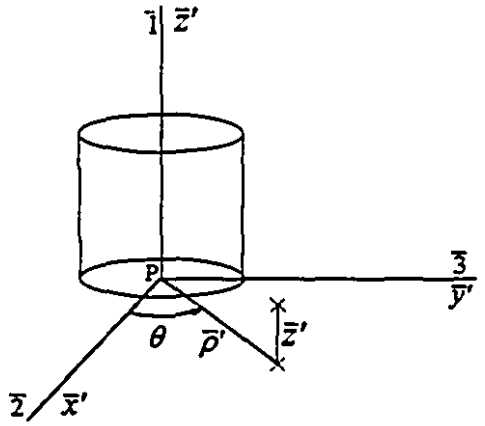

Figure 3.3 The local cylindrical coordinate system at the point P

The body is considered at rest in a fluid (of viscosity μ and density ρ) in which there is a uniform undisturbed flow field of (dimensional) velocity $\underline{U}$. Associated with $\underline{U}$ is the constant free-stream pressure which, without loss of generality, can be taken to be zero. We are interested in obtaining the drag force on the body in the limit as $\kappa \to 0$ with the Reynolds number $Re \equiv \frac{lU}{\nu} = \frac{\rho lU}{\mu}$ based on the body length assumed to be of order unity. The Reynolds number $R \equiv \frac{\rho bU}{\mu}$ is based on the body cross-sectional dimension. Thus

$$\kappa << 1, \quad R << 1, \quad Re = \frac{R}{\kappa} \text{ (of order unity)} \tag{3,2}$$

We will make expansions of the velocity and pressure field in terms of κ (correct to the order of κ^{+1}) treating Re as a parameter. However, one should note that this type of expansion must be singular since the flow locally around the long thin body must be

very nearly the flow around an infinite cylinder at zero Reynolds number R, and it is well known (Stokes' paradox) that it is impossible for such a flow field (u, p) to satisfy the equations of motion and at the same time to satisfy the no slip condition $u = 0$ on the surface of an infinite circular cylinder and also to make the velocity u tend to the uniform flow at infinity. So, we will use *The Matched Asymptotic Expansion Technique* which is a kind of perturbation method, and through that, we will solve the equations for two regions (inner and outer). Matching the results of these two regions, we will get an overall solution for the problem.

3.2.1 Non-Dimensionalizing

3.2.1.1 Outer Region

We use quantities made dimensionless by ρ, U, μ, and l. The dimensionless position vector $\underline{r}$, flow velocity $\underline{u}$ and pressure p are defined in terms of the corresponding dimensional quantities $\underline{r}'$, $\underline{u}'$, and p' as follows:

$$\underline{r} = \frac{\underline{r}'}{l} \ , \ \underline{u} = \frac{\underline{u}'}{U} \ , \ p = \frac{l\,p'}{\mu\,U} \tag{3,3}$$

where $U = |\underline{U}|$. Unless otherwise stated, we use *unprimed* variables to denote dimensionless quantities. The vector $\underline{r}$ is the dimensionless position vector of a general point relative to a fixed set of rectangular Cartesian coordinates with origin O (see figure 3.2) so that the body centreline itself is given by $\underline{r} = \underline{R}(s)$.

The dimensional fluid velocity $\underline{u}'$ and the pressure p', for both inner and outer regions, satisfy the Navier-Stokes' equations as follows:

$$\left.\begin{aligned} \rho\,\underline{u}'.\nabla'\underline{u}' &= \mu\nabla'^2\underline{u}' - \nabla' p' \\ \nabla'.\,\underline{u}' &= 0 \end{aligned}\right\} \tag{3,4}$$

with boundary conditions

$$\left.\begin{aligned} \underline{u}' &= 0 \qquad \text{on the body surface} \\ \underline{u}' &\to \underline{U} \qquad \text{as} \quad |\underline{r}'| \to \infty. \end{aligned}\right\} \tag{3.5}$$

The governing equations of momentum and continuity for the dimensionless velocity $\underline{u}$, and pressure p in the outer region can be obtained by placing outer region variables in the above equations. They are of the form

$$\left.\begin{aligned} Re\ \underline{u}.\nabla\underline{u} &= \nabla^2\underline{u} - \nabla p, \\ \nabla.\ \underline{u} &= 0. \end{aligned}\right\} \tag{3.6}$$

We have to solve the above equation as an expansion in κ using the boundary conditions

$$\left.\begin{aligned} \underline{u} &\to \underline{e} \qquad \text{as} \quad \underline{r} \to \infty \\ \underline{u} &= \underline{0} \qquad \text{on the body surface,} \end{aligned}\right\} \tag{3.7}$$

where $\underline{e}$ is the unit vector in the direction of the uniform undisturbed flow. This will require obtaining a solution as an outer expansion in κ valid in a region (the outer region) where $\underline{r}$ is of order unity. As mentioned, in the outer region lengths are made dimensionless by l, and as $\kappa \to 0$, the body becomes a line singularity $\underline{r} = \underline{R}(s)$ (see figure 3.4).

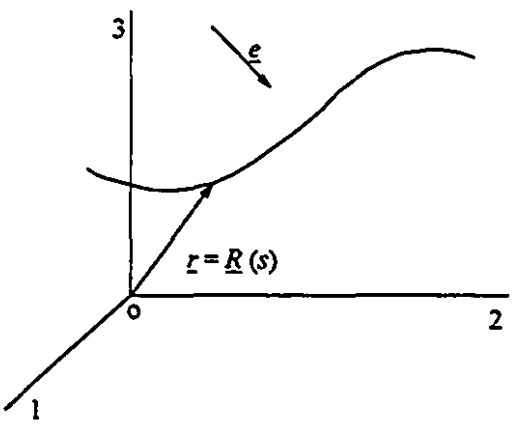

Figure 3.4 In the outer region the body becomes a line singularity

In the outer region, the velocity can be written, generally, as

$$\underline{u} = \underline{e} + \underline{u}_1(\kappa, \underline{r}), \tag{3.8}$$

where $\underline{e} = \dfrac{\underline{U}}{|\underline{U}|}$, and $\underline{u}_1 \to \underline{0}$ as $\kappa \to 0$.

If we apply the velocity from equation (3.8) into the equations(3.6), we will get Oseen's equations for the outer region:

$$\left.\begin{aligned} Re\ \underline{e}.\nabla\underline{u}_1 &= \nabla^2\underline{u}_1 - \nabla p_1, \\ \nabla.\ \underline{u}_1 &= 0. \end{aligned}\right\} \tag{3.9}$$

With the boundary conditions $\underline{u}_1 \to \underline{0}$ as $|\underline{r}| \to \infty$. It is worth mentioning that the boundary condition on $\underline{r} = \underline{R}(s)$ can be obtained only by matching.

3.2.1.2 Inner Region

In the inner region, we use quantities made dimensionless by ρ, U, μ, and b. The dimensionless position vector $\overline{\underline{r}}$, flow velocity $\overline{\underline{u}}$ and pressure $\overline{p}$ are defined in terms of the corresponding dimensional quantities $\underline{r}'$, $\underline{u}'$, and p', and also in terms of dimensionless outer variables. Using $\kappa = \dfrac{b}{l}$, we define:

$$\overline{\underline{r}} = \frac{\underline{r}' - \underline{R}'_P}{b} = \frac{\underline{r}' - \underline{R}'_P}{l\left(\frac{b}{l}\right)} = \frac{1}{\kappa}\left(\frac{\underline{r}'}{l} - \frac{\underline{R}'_P}{l}\right)$$

$$\overline{\underline{r}} = \frac{\underline{r} - \underline{R}_P}{\kappa} \tag{3.10}$$

$$\overline{\underline{u}} = \underline{u} \tag{3.11}$$

$$\overline{p} = \frac{p'}{\left(\mu\frac{U}{b}\right)} = \frac{b}{l}\frac{p'}{\mu\frac{U}{l}}$$

$$\overline{p} = \kappa p \tag{3.12}$$

Therefore we have two sets of dimensionless variables. Outer region variables in the form of $\underline{u}$, $\underline{r}$, and p, and inner region variables with an overbar sign as $\underline{\bar{r}}$, $\underline{\bar{u}}$, and $\bar{p}$.

At any point P on $\underline{r} = \underline{R}_P$ (see figure 3.5) of the body centreline one may define an inner expansion in κ for which $\underline{\bar{r}}$ is used as the independent variable and $\underline{\bar{u}}$ and $\bar{p}$ as dependent variables.

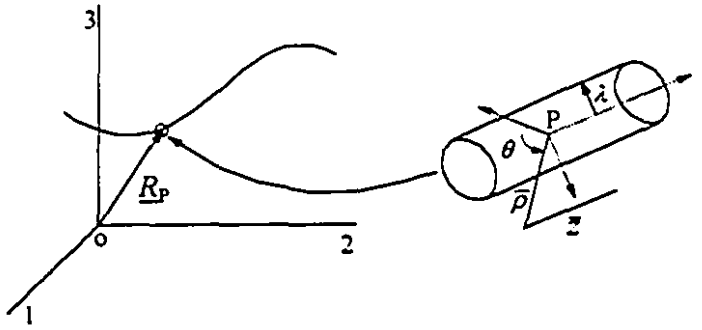

Figure 3.5 Inner region and cylindrical polar coordinates

In a Cartesian coordinate system, the position vector in the inner region $\underline{\bar{r}} = (\bar{x}, \bar{y}, \bar{z})$, where the $\bar{x}$, $\bar{y}$, and $\bar{z}$ are respectively $\bar{x}'$, $\bar{y}'$, and $\bar{z}'$ made dimensionless by b (see figure 3.3). In the inner expansion at each point P of the centreline, the unit of length is b and as $\kappa \to 0$, the body becomes very much like a cylinder of infinite length (since $l \to \infty$). Actually, one has an infinite number of inner expansions corresponding to each point of the centreline of the body. However all such inner expansions may be considered simultaneously by taking a general point P of the body centreline. The inner expansion at such a point is then matched onto the solution for the outer expansion at the same point P.

Relative to the inner dimensionless coordinates $\bar{x}, \bar{y}$, and $\bar{z}$, a dimensionless cylindrical polar coordinate system $(\bar{\rho}, \theta, \bar{z})$, is defined (see figure 3.3) with $\bar{\rho} = \dfrac{\bar{\rho}'}{b}$, so that

$$\bar{x} = \bar{\rho} \cos\theta, \quad \bar{y} = \bar{\rho} \sin\theta. \tag{3,13}$$

3.2.2 Matched Asymptotic Expansion

3.2.2.1 Inner Expansion

At a general point P of the body centreline consider now the inner expansion. The flow field ($\underline{\bar{u}}$ and $\bar{p}$) in the vicinity of the point P is to be computed by solving the governing motion equations (3,6), using inner variables described above, i.e.

$$\left.\begin{aligned} \kappa\, Re\, \underline{\bar{u}}.\bar{\nabla}\underline{\bar{u}} &= \bar{\nabla}^2\underline{\bar{u}} - \bar{\nabla}\bar{p}, \\ \bar{\nabla}.\underline{\bar{u}} &= 0, \end{aligned}\right\} \tag{3,14}$$

with $\underline{\bar{u}} = 0$ on the body surface, where $\bar{\rho} = \lambda$ in cylindrical polar coordinates $(\bar{\rho}, \theta, \bar{z})$, (see figure 3.5). It is worth mentioning that the boundary condition at $\bar{\rho} \to \infty$ is to be obtained by matching.

Assuming that $\lambda(s)$ varies slowly with s, (in case of an infinite circular cylinder $\lambda(s)=1$), the value of $\underline{\bar{u}}$ may then, at the lowest order, be calculated in the same manner as for $Re = 0$ (Cox, 1970). The general solution for equations (3,14) will be

$$\left.\begin{aligned} \bar{u}_{\bar{\rho}} &= C(\kappa)\{1-\lambda^2\bar{\rho}^{-2}-2\ln(\frac{\bar{\rho}}{\lambda})\}\cos\theta \\ &\quad + D(\kappa)\{1-\lambda^2\bar{\rho}^{-2}-2\ln(\frac{\bar{\rho}}{\lambda})\}\sin\theta, \\ \bar{u}_{\theta} &= C(\kappa)\{1-\lambda^2\bar{\rho}^{-2}+2\ln(\frac{\bar{\rho}}{\lambda})\}\cos\theta \\ &\quad + D(\kappa)\{-1+\lambda^2\bar{\rho}^{-2}-2\ln(\frac{\bar{\rho}}{\lambda})\}\sin\theta, \\ \bar{u}_{\bar{z}} &= E(\kappa)\ln(\frac{\bar{\rho}}{\lambda}), \\ \bar{p} &= C(\kappa)\{4\bar{\rho}^{-1}\cos\theta\} + D(\kappa)\{4\bar{\rho}^{-1}\sin\theta\} + \kappa F(\kappa), \end{aligned}\right\} \tag{3,15}$$

where C, D, and E are arbitrary constants independent of the coordinate system, but they can be dependent on κ. In the equations (3,15), no other terms can appear since terms in

$\bar{u}_\rho, \bar{u}_\theta$ like $\bar{\rho}^{-1}$ can not appear as they would have to match onto terms in κ^{-1} in the outer expansion.

We assume $C(\kappa)$, $D(\kappa)$, and $E(\kappa)$ are such that as $\kappa \to 0$

$$C(\kappa) \to 0, \qquad D(\kappa) \to 0, \qquad E(\kappa) \to 0. \tag{3,16}$$

Using polar axes (ρ, θ, z), corresponding to the $(\bar{\rho}, \theta, \bar{z})$ axes so that

$$\rho = \kappa\bar{\rho} \quad \text{and} \quad z = \kappa\bar{z}, \tag{3,17}$$

the inner boundary conditions on the outer flow field $(\underline{u}, p)$, has the following form:

$$\left.\begin{aligned}
u_\rho &\sim \{C(\kappa)(-2\ln\rho)\cos\theta + D(\kappa)(-2\ln\rho)\sin\theta\} \\
&\quad + \left[C(\kappa)\{2\ln(\kappa\lambda)+1\}\cos\theta + D(\kappa)\{2\ln(\kappa\lambda)+1\}\sin\theta\right] + O(\kappa^2), \\
u_\theta &\sim \{C(\kappa)(2\ln\rho)\sin\theta + D(\kappa)(-2\ln\rho)\cos\theta\} \\
&\quad + \left[C(\kappa)\{-2\ln(\kappa\lambda)+1\}\sin\theta + D(\kappa)\{2\ln(\kappa\lambda)-1\}\cos\theta\right] + O(\kappa^2), \\
u_z &\sim \{E(\kappa)\ln\rho\} + E(\kappa)\{-\ln(\kappa\lambda)\}, \\
p &\sim \left[C(\kappa)\cos\theta + D(\kappa)\sin\theta\right](4\rho^{-1}) + F(\kappa).
\end{aligned}\right\} \tag{3,18}$$

Here $C(\kappa)$, $D(\kappa)$, $E(\kappa)$, and $F(\kappa)$ will depend on s, the position on the body centreline.

3.2.2.2 Outer Expansion

We recall that the outer flow field $(\underline{u}, p)$ satisfies (3,6) with the outer boundary condition that $\underline{u} \to \underline{e}$ as $\underline{r} \to \infty$ (where $\underline{e}$ is a unit vector in undisturbed flow direction). The outer flow field $(\underline{u}, p)$ has an expansion of the form

$$\underline{u} = \underline{e} + \underline{u}_1(\kappa) + \ldots, \qquad p = 0 + p_1(\kappa) + \ldots, \tag{3,19}$$

where $(\underline{u}_1, p_1) \to (\underline{0}, 0)$ as $\kappa \to 0$.

At a general point P on the line singularity $\underline{r} = \underline{R}(s)$ it is convenient to take a set of

rectangular Cartesian axes with unit base vectors $\underline{i}_z$, $\underline{i}_x$, and $\underline{i}_y$ which lie in the same direction as the $(\bar{z},\bar{x},\bar{y})$-axes at P (see figure 3.3) Thus $\underline{i}_z$ lies in the direction of the tangent to $\underline{r} = \underline{R}(s)$ at P. Since $\bar{x}$ and $\bar{y}$ axes are arbitrary, one may choose, for convenient, $\underline{i}_x$ to lie in the plane containing $\underline{i}_z$ and the velocity vector $\underline{e}$ (see figure 3.6).

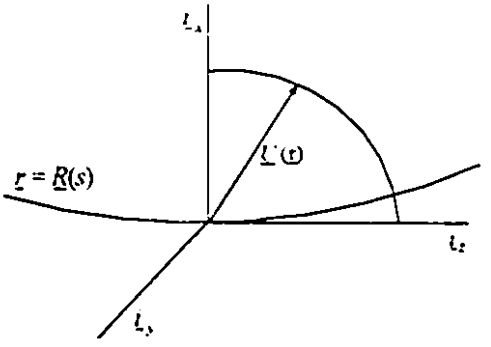

Figure 3.6 The system of axes with unit base vectors $\underline{i}_x$, $\underline{i}_y$, $\underline{i}_z$

Thus the unit vectors $\underline{i}_z$, $\underline{i}_x$, and $\underline{i}_y$ are

$$\underline{i}_z = \underline{t}, \quad \underline{i}_x = \frac{\underline{e}.(\underline{I} - \underline{tt})}{\left(1 - |\underline{e}.\underline{t}|^2\right)^{\frac{1}{2}}}, \quad \underline{i}_y = \frac{\underline{t} \times \underline{e}}{\left(1 - |\underline{e}.\underline{t}|^2\right)^{\frac{1}{2}}}, \tag{3,20}$$

where $\underline{t} = \dfrac{d\underline{R}}{ds}$ is a unit vector in the tangent direction and $\underline{I}$ is the idemfactor.

From the form of $\underline{u}$ as one approaches the centreline, we see (Cox 1970) that the singular part of $(\underline{u}_1, p_1)$ represents a line of force on $\underline{r} = \underline{R}(s)$

$$\underline{f}^*(s) = 8\pi C(\kappa, s)\underline{i}_x + 8\pi D(\kappa, s)\underline{i}_y - 2\pi E(\kappa, s)\underline{i}_z, \tag{3,21}$$

where $\bar{x} = \bar{\rho}\cos\theta$, $\bar{y} = \bar{\rho}\sin\theta$, thus

$$\underline{f}^*(s) = 2\pi\{4C(\kappa, s)\underline{i}_x + 4D(\kappa, s)\underline{i}_y - E(\kappa, s)\underline{i}_z\}. \tag{3,22}$$

Taking variables (3,20), we can write

$$\underline{f}^*(s) = 2\pi\left[\frac{4C(\kappa,s)\underline{e}.(\underline{I}-\underline{t}\underline{t}) + 4D(\kappa,s)\,\underline{t}\times\underline{e}}{\left(1-|\underline{e}.\underline{t}|^2\right)^{1/2}} - E(\kappa,s)\,\underline{t}\right]. \tag{3,23}$$

We require $\underline{u}_1 \to 0$ as $\underline{r} \to \infty$ so that $\underline{u}_1$ is the flow due to the line distribution of force $\underline{f}^*(s)$. That is

$$(u_1)_i = \frac{1}{8\pi}\int_0^1 g_{ij}(\underline{r}-\underline{\hat{R}})\underline{f}^*(\hat{s})\,d\hat{s}, \tag{3,24}$$

where $\hat{s}$ is a dummy variable expressing the dimensionless distance along the body centreline to a general point (see figure 3.7), $\underline{\hat{R}} = \underline{R}(\hat{s})$, and the function $g_{ij}(\underline{r})$ and the radial distance from the origin r are respectively defined by

$$g_{ij}(\underline{r}) = \delta_{ij}\nabla^2\psi(\underline{r}) - \frac{\partial^2\psi(\underline{r})}{\partial r_i\,\partial r_j}. \tag{3,25}$$

$$r = (r_j\ r_j)^{1/2} = |\underline{r}| \tag{3,26}$$[1]

and where $\psi(\underline{r})$, stream function, is defined by

$$\psi(\underline{r}) = \frac{2}{Re}\int_0^{\frac{1}{2}Re(r-\underline{e}.\underline{r})}\frac{1-e^{-\alpha}}{\alpha}d\alpha. \tag{3,27}$$

The corresponding pressure is

$$p_1 = \frac{1}{4\pi}\int_0^1 \frac{(r_j-\hat{R}_j)}{|\underline{r}-\underline{\hat{R}}|^3} f_j^*(\hat{s})\,d\hat{s}, \tag{3,28}$$

where the local axes are defined so that the point P is the origin and $\hat{r}_1$ is in the direction of tangent to the body at the point P (see figure 3.7).

---

[1] Repeated indices refer to summation over the index unless otherwise specified.

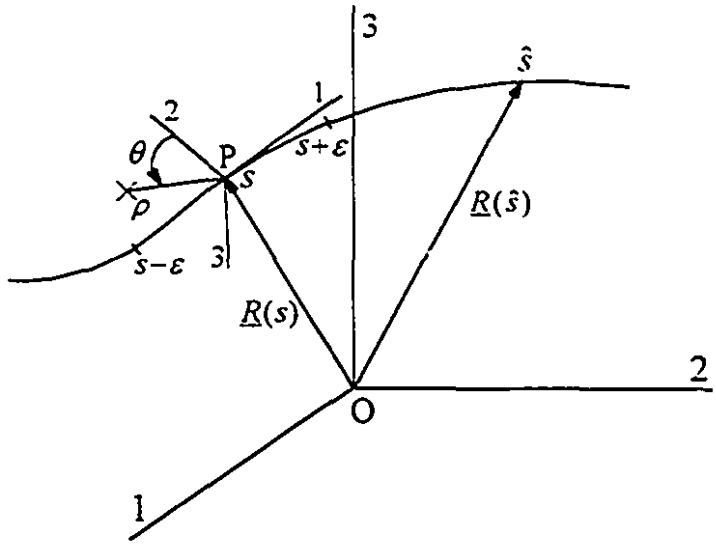

Figure 3.7 Local axes at the point P

Here $\underline{R}(\hat{s})$ is the position vector for any general point from origin O, where $\alpha \le \hat{s} \le \beta$, with α and β as two ends of the body. The position vector $\underline{R}(s)$ is the same as $\underline{R}(\hat{s})$, but specifically for the point P. Since the integrands for $\underline{u}_1$ and p_1 become singular on the line of force, we write

$$(u_1)_i = J_i + J_i^*, \qquad p_1 = H + H^* \tag{3.29}$$

where J_i and H are the integrals taken over the intervals $(0,\ s-\varepsilon)$ and $(s+\varepsilon,\ 1)$ and J_i^* and H^* are the integrals taken over the remaining interval $(s-\varepsilon,\ s+\varepsilon)$. Therefore,

$$J_i(s) = \frac{1}{8\pi}\left\{\int_0^{s-\varepsilon} + \int_{s-\varepsilon}^{1}\right\} g_{ij}\left(\underline{r} - \underline{R}(\hat{s})\right) f_j^*(\hat{s})\, d\hat{s}, \tag{3.30}$$

$$J_i^*(s) = \frac{1}{8\pi}\int_{s-\varepsilon}^{s-\varepsilon} g_{ij}\left(\underline{r} - \underline{R}(\hat{s})\right) f_j^*(\hat{s})\, d\hat{s}, \tag{3.31}$$

$$H(s) = \frac{1}{4\pi}\left\{\int_0^{s-\varepsilon} + \int_{s-\varepsilon}^{1}\right\} \frac{(r_j - R_j(\hat{s}))}{\left|\underline{r} - \underline{R}(\hat{s})\right|^3} f_j^*(\hat{s})\, d\hat{s}, \tag{3.32}$$

$$H^*(s) = \frac{1}{4\pi}\int_{s-\varepsilon}^{s+\varepsilon} \frac{\left(r_j - R_j(\hat{s})\right)}{\left|\underline{r} - \underline{R}(\hat{s})\right|^3} f_j^*(\hat{s})\, d\hat{s}. \tag{3,33}$$

The quantity $\varepsilon > 0$ is assumed to be an arbitrary constant and very much smaller than unity. Since the integrands only become singular at $\hat{s} = s$, if $\underline{r}$ relies on the line singularity ($\underline{r} \to \underline{R}(s)$), it follows that the integrals J_i and H have integrands with no singularity, although the values of these integrals will tend to infinity as $\varepsilon \to 0$. Since $\varepsilon << 1$, the integrals J_i^* and H^* may be simplified if one notes that $s \approx \hat{s}$ in the range of integration. Therefore,

$$J_i^* \sim \frac{1}{8\pi} f_j^*(s)\, I_{ij} \qquad\qquad H^* \sim \frac{1}{4\pi} f_j^*(s)\, I_j \ , \tag{3,34}$$

where

$$\left.\begin{aligned} I_{ij} &= \int_{s-\varepsilon}^{s+\varepsilon} g_{ij}(\underline{r} - \hat{\underline{R}})\, d\hat{s}, \\ I_j &= \int_{s-\varepsilon}^{s+\varepsilon} \frac{(r_j - \hat{R}_j)}{\left|\underline{r} - \hat{\underline{R}}\right|^3}\, d\hat{s}, \end{aligned}\right\} \tag{3,35}$$

where $\hat{\underline{R}} = \underline{R}(\hat{s})$.

By considering figure 3.7

$$r_1 = R_1(s), \quad r_2 = R_2(s) + \rho\cos\theta, \qquad r_3 = R_3(s) + \rho\sin\theta \tag{3,36}$$

we can write

$$\left.\begin{aligned} R_1(\hat{s}) &= R_1(s) + \frac{dR_1(s)}{ds}(\hat{s}-s) + \frac{1}{2}\frac{d^2R_1(s)}{ds^2}(\hat{s}-s)^2 + \ldots, \\ R_2(\hat{s}) &= R_2(s) + \frac{dR_2(s)}{ds}(\hat{s}-s) + \frac{1}{2}\frac{d^2R_2(s)}{ds^2}(\hat{s}-s)^2 + \ldots, \\ R_3(\hat{s}) &= R_3(s) + \frac{dR_3(s)}{ds}(\hat{s}-s) + \frac{1}{2}\frac{d^2R_3(s)}{ds^2}(\hat{s}-s)^2 + \ldots, \end{aligned}\right\} \tag{3,37}$$

but $\frac{dR_i}{ds} = t_i = \delta_{i1}$, and also $\frac{d\underline{R}}{ds} = \underline{t}$ is a unit vector. Then

$$\frac{d\underline{R}}{ds}\cdot\frac{d\underline{R}}{ds}=1,$$

$$\frac{d\underline{R}}{ds}\cdot\frac{d^2\underline{R}}{ds^2}=0 \qquad \text{or} \qquad \delta_{i1}\frac{d^2R_i}{ds^2}=0,$$

$$\frac{d^2R_1}{ds^2}=0$$

Using the above quantities in order to find components of I_j

$$\left.\begin{aligned}(\underline{r}-\underline{R}(\hat{s}))_1 &= -(\hat{s}-s)+O(\hat{s}-s)^3,\\ (\underline{r}-\underline{R}(\hat{s}))_2 &= \rho\cos\theta-\frac{1}{2}\frac{d^2R_2}{ds^2}(\hat{s}-s)^2+\ldots,\\ (\underline{r}-\underline{R}(\hat{s}))_3 &= \rho\sin\theta-\frac{1}{2}\frac{d^2R_3}{ds^2}(\hat{s}-s)^2+\ldots.\end{aligned}\right\} \tag{3,38}$$

Applying these quantities into $\left|\underline{r}-\underline{R}(\hat{s})\right|^3$, and letting

$$\hat{s}-s=\rho x, \qquad d\hat{s}=\rho dx, \tag{3,39}$$

we will get

$$I_1=-\rho^{-1}\int_{-\varepsilon/\rho}^{\varepsilon/\rho}\frac{x}{(1+x^2)^{3/2}}dx+O\left[\rho\int_{-\varepsilon/\rho}^{\varepsilon/\rho}\frac{x^3\,dx}{(1+x^2)^{3/2}},\rho\int_{-\varepsilon/\rho}^{\varepsilon/\rho}\frac{x^5\,dx}{(1+x^2)^{5/2}},\rho\int_{-\varepsilon/\rho}^{\varepsilon/\rho}\frac{x^3\,dx}{(1+x^2)^{5/2}}\right], \tag{3,40}$$

as $\rho\to 0$ for a fixed ε, we have

$$I_1=-\rho^{-1}\int_{-\infty}^{\infty}\frac{x}{(1+x^2)^{3/2}}dx+O\left[\varepsilon,\varepsilon,\int_{-\infty}^{\infty}\frac{x^3\,dx}{(1+x^2)^{5/2}}\right]. \tag{3,41}$$

Thus, one should include the *O*rder ($\varepsilon^0\rho^0$) term. Then we take

$$\left|\underline{r}-\underline{R}(\hat{s})\right|^2=\left\{(\hat{s}-s)^2+\rho^2\right\}-\left(\cos\theta\frac{d^2R_2}{ds^2}+\sin\theta\frac{d^2R_3}{ds^2}\right)\rho(\hat{s}-s)^2, \tag{3,42}$$

$$\left|\underline{r}-\underline{R}(\hat{s})\right|^{-3}=\left\{(\hat{s}-s)^2+\rho^2\right\}^{-3/2}+\frac{3}{2}\left(\cos\theta\frac{d^2R_2}{ds^2}+\sin\theta\frac{d^2R_3}{ds^2}\right)\frac{\rho(\hat{s}-s)^2}{\left\{(\hat{s}-s)^2+\rho^2\right\}^{5/2}}+\ldots. \tag{3,43}$$

Thus,

$$I_1 = \int_{s-\varepsilon}^{s+\varepsilon}\left[-\frac{(\hat{s}-s)}{\left\{(\hat{s}-s)^2+\rho^2\right\}^{3/2}} - \frac{3}{2}\left(\cos\theta\,\frac{d^2R_2}{ds^2} + \sin\theta\,\frac{d^2R_3}{ds^2}\right)\frac{\rho(\hat{s}-s)^3}{\left\{(\hat{s}-s)^2+\rho^2\right\}^{5/2}} + \ldots\right] d\hat{s} \qquad (3,44)$$

$$= \int_{-\varepsilon/\rho}^{+\varepsilon/\rho}\left[-\frac{\rho^2 x}{\rho^3(1+x^2)^{3/2}} - \frac{3}{2}\left(\cos\theta\,\frac{d^2R_2}{ds^2} + \sin\theta\,\frac{d^2R_3}{ds^2}\right)\frac{\rho^5 x^3}{\rho^5(1+x^2)^{5/2}} + \ldots\right] dx \qquad (3,45)$$

$$\sim -\rho^{-1}\int_{-\infty}^{+\infty}\frac{x}{(1+x^2)^{3/2}}\,dx - \frac{3}{2}\left(\cos\theta\,\frac{d^2R_2}{ds^2} + \sin\theta\,\frac{d^2R_3}{ds^2}\right)\int_{-\infty}^{+\infty}\frac{x^3 dx}{(1+x^2)^{5/2}} + \ldots \qquad (3,46)$$

Since both integrals are zero, by symmetry,

$$I_1 \to 0 \quad \text{as} \quad \rho \to 0. \qquad (3,47)$$

We evaluate I_2 in the same manner

$$I_2 = \int_{s-\varepsilon}^{s+\varepsilon}\left[\frac{\rho\cos\theta}{\left\{(\hat{s}-s)^2+\rho^2\right\}^{3/2}} + O\left\{\frac{\rho^2(\hat{s}-s)^4}{\left\{(\hat{s}-s)^2+\rho^2\right\}^{5/2}}, \frac{\rho^3(\hat{s}-s)^2}{\left\{(\hat{s}-s)^2+\rho^2\right\}^{5/2}}, \frac{\rho(\hat{s}-s)^2}{\left\{(\hat{s}-s)^2+\rho^2\right\}^{3/2}}\right\}\right] d\hat{s}$$

$$= \int_{-\varepsilon/\rho}^{+\varepsilon/\rho}\left[\frac{\rho^2\cos\theta}{\rho^3(1+x^2)^{3/2}} + O\left\{\frac{\rho^7 x^4}{\rho^5(1+x^2)^{5/2}}, \frac{\rho^6 x^2}{\rho^5(1+x^2)^{5/2}}, \frac{\rho^4 x^2}{\rho^3(1+x^2)^{3/2}}\right\}\right] dx$$

$$I_2 \sim \rho^{-1}\cos\theta\int_{-\infty}^{+\infty}\frac{dx}{(1+x^2)^{3/2}} + O\left\{\rho^2\ln\varepsilon, \rho^2\ln\rho, \rho\,\rho\ln\rho, \rho\ln\varepsilon\right\}, \qquad (3,48)$$

and since

$$\int_{-\infty}^{+\infty}\frac{dx}{(1+x^2)^{3/2}} = \int_{-\pi/2}^{\pi/2}\frac{\sec^2\theta\,d\theta}{\sec^3\theta} = \int_{-\pi/2}^{\pi/2}\cos\theta\,d\theta = +2, \qquad (3,49)$$

we have

$$I_2 \sim 2\rho^{-1}\cos\theta + O(\rho^0) \qquad \text{as} \qquad \rho \to 0. \qquad (3,50)$$

Similarly for I_3, we obtain

$$I_3 \sim 2\rho^{-1}\sin\theta + O(\rho^0) \qquad \text{as} \qquad \rho \to 0. \qquad (3,51)$$

Now, by inserting I_2 and I_3 into expression (3,34), we have as $\varepsilon \to 0$

$$H^* \sim \frac{1}{4\pi} 2\rho^{-1} \left\{ \cos\theta \, f_2^*(s) + \sin\theta \, f_3^*(s) \right\} + O(\rho^0), \tag{3,52}$$

and as $\rho \to 0$

$$p_1 \sim \frac{1}{4\pi} 2\rho^{-1} \left\{ \cos\theta \, f_2^*(s) + \sin\theta \, f_3^*(s) \right\} + H(s) + O(1), \tag{3,53}$$

or by using equation (3,32)

$$\begin{aligned} p_1 \sim & \frac{1}{2\pi\rho} \left\{ \cos\theta \, f_2^*(s) + \sin\theta \, f_3^*(s) \right\} \\ & + \frac{1}{4\pi} \left\{ \int_0^{s-\varepsilon} + \int_{s+\varepsilon}^{1} \right\} \frac{(r_j - R_j(\hat{s}))}{\left| \underline{r} - \underline{R}(\hat{s}) \right|^3} f_j^*(\hat{s}) \, d\hat{s} + O(1) \end{aligned} \tag{3,54}$$

Matching onto inner expansion of p in expression (3,18) requires

$$C(\kappa) = \frac{1}{8\pi} f_2^*(s), \qquad D(\kappa) = \frac{1}{8\pi} f_3^*(s), \tag{3,55}$$

$$F(\kappa) = \frac{1}{4\pi} \left\{ \int_0^{s-\varepsilon} + \int_{s+\varepsilon}^{1} \right\} \frac{(r_j - R_j(\hat{s}))}{\left| \underline{r} - \underline{R}(\hat{s}) \right|^3} f_j^*(\hat{s}) \, d\hat{s}. \tag{3,56}$$

Now, we concentrate on the function g_{ij}, see equation (3,25)

$$\frac{1 - e^{-\alpha}}{\alpha} \sim \frac{1 - \left\{ 1 - \alpha + \frac{\alpha^2}{2!} - \frac{\alpha^3}{3!} + \ldots \right\}}{\alpha} = 1 - \frac{\alpha}{2!} + \frac{\alpha^2}{3!} - \ldots, \tag{3,57}$$

$$\int_0^{\alpha} \frac{1 - e^{-\alpha}}{\alpha} d\alpha = \alpha - \frac{\alpha^2}{2.2!} + \frac{\alpha^3}{3.3!} - \ldots. \tag{3,58}$$

Thus as $\underline{r} \to 0$, we have

$$\psi \sim (r - \underline{e}.\underline{r}) - \frac{1}{8} Re (r - \underline{e}.\underline{r})^2 + \frac{1}{72} Re^2 (r - \underline{e}.\underline{r})^3 - \ldots, \tag{3,59}$$

$$\psi_{,i} \sim \left(\frac{r_i}{r} - e_i \right) - \frac{1}{4} Re (r - e_k r_k) \left(\frac{r_i}{r} - e_i \right) + \ldots, \tag{3,60}$$

where $\psi_{,i}$ denotes $\frac{\partial \psi}{\partial r_i}$ and $\psi_{,ij} = \frac{\partial^2 \psi}{\partial r_i \partial r_j}$

$$\psi_{,ij} \sim \left(\frac{\delta_{ij}}{r} - \frac{r_i r_j}{r^3}\right) - \frac{1}{4} Re\left\{(r - e_k r_k)\left(\frac{\delta_{ij}}{r} - \frac{r_i r_j}{r^3}\right) + \left(\frac{r_j}{r} - e_j\right)\left(\frac{r_i}{r} - e_i\right)\right\} + \ldots \qquad (3,61)$$

$$\psi_{,ii} \sim -\frac{2}{r} - \frac{1}{4} Re\left\{2 - \frac{2 e_k r_k}{r} + 1 - 2\frac{r_i e_i}{r} + 1\right\} + \ldots, \qquad (3,62)$$

and also

$$\psi_{,kk} \sim 2r^{-1} - Re\left(1 - \frac{r_k e_k}{r}\right) + \ldots. \qquad (3,63)$$

Since we have $g_{ij} = \delta_{ij}\psi_{,kk} - \psi_{,ij}$, we will obtain

$$g_{ij} \sim -\left(\frac{\delta_{ij}}{r} + \frac{r_i r_j}{r^3}\right) + \frac{1}{4} Re\left\{-3\delta_{ij} + 3\frac{e_k r_k \delta_{ij}}{r} + \frac{e_k r_k r_i r_j}{r^3} - \frac{e_j r_i}{r} - \frac{e_i r_j}{r} + e_i e_j\right\} + \ldots. \qquad (3,64)$$

Thus, the term in Re^{-1} is bounded as $r \to 0$ so that it gives a contribution to I_{ij} (see equation (3,35)) of order ε^{-1} and so $Re^{-1} \to 0$ as $\varepsilon \to 0$. The term in Re^0 gives

$$g_{ij} \sim \left\{\delta_{ij}\left|\underline{r} - \underline{R}(\hat{s})\right|^{-1} + \left(r_i - R_i(\hat{s})\right)\left(r_j - R_j(\hat{s})\right)\left|\underline{r} - \underline{R}(\hat{s})\right|^{-3}\right\} + \ldots. \qquad (3,65)$$

Now, we can evaluate different elements of the tensor g_{ij}

$$g_{11} = \left[\frac{1}{\left\{(\hat{s}-s)^2 + \rho^2\right\}^{1/2}} + \frac{(\hat{s}-s)^2}{\left\{(\hat{s}-s)^2 + \rho^2\right\}^{3/2}}\right] + \ldots,$$

$$g_{22} = \left[\frac{1}{\left\{(\hat{s}-s)^2 + \rho^2\right\}^{1/2}} + \frac{\rho^2 \cos^2\theta}{\left\{(\hat{s}-s)^2 + \rho^2\right\}^{3/2}}\right] + \ldots,$$

$$g_{33} = \left[\frac{1}{\left\{(\hat{s}-s)^2 + \rho^2\right\}^{1/2}} + \frac{\rho^2 \sin^2\theta}{\left\{(\hat{s}-s)^2 + \rho^2\right\}^{3/2}}\right] + \ldots,$$

$$g_{12} = g_{21} = -\frac{(\hat{s}-s)\rho\cos\theta}{\left\{(\hat{s}-s)^2 + \rho^2\right\}^{3/2}} + \ldots,$$

$$g_{13} = g_{31} = -\frac{(\hat{s}-s)\rho\sin\theta}{\left\{(\hat{s}-s)^2+\rho^2\right\}^{3/2}}+\ldots,$$

$$g_{23} = g_{32} = -\frac{\rho^2\sin\theta\cos\theta}{\left\{(\hat{s}-s)^2+\rho^2\right\}^{3/2}}+\ldots. \tag{3,66}$$

By inserting these values into I_{ij} (see equation (3,35)), it can be shown that

$$I_{11} = -\frac{2\varepsilon}{\sqrt{\varepsilon^2+\rho^2}} + 2\ln\left(\frac{\sqrt{\varepsilon^2+\rho^2}+\varepsilon}{\sqrt{\varepsilon^2+\rho^2}-\varepsilon}\right), \tag{3,67}$$

and as $\rho \to 0$ we have

$$I_{11} \sim -4\ln\rho + \left\{4\ln\varepsilon - 2 + 4\ln 2\right\}+\ldots. \tag{3,68}$$

Similarly, we get

$$I_{22} \sim -2\ln\rho + \left\{2\ln\varepsilon + 2\ln 2 + 2\cos^2\theta\right\}+\ldots,$$

$$I_{33} \sim -2\ln\rho + \left\{2\ln\varepsilon + 2\ln 2 + 2\sin^2\theta\right\}+\ldots,$$

$$I_{23} = I_{32} \sim 2\sin\theta\cos\theta+\ldots,$$

$$I_{12} = I_{21} \sim 0,$$

$$I_{13} = I_{31} \sim 0. \tag{3,69}$$

Thus, for equation (3,34), as $\rho \to 0$, we have

$$J_i^* \sim \frac{1}{8\pi} f_j^*(s) I_{ij}\ , \tag{3,34}$$

$$J_i^* \sim \frac{1}{8\pi}\left\{I_{i1} f_1^*(s) + I_{i2} f_2^*(s) + I_{i3} f_3^*(s)\right\},$$

giving

$$J_1^* \sim \frac{1}{8\pi}\left[-4\ln\rho + \left\{4\ln(2\varepsilon) - 2\right\}+\ldots\right] f_1^*(s),$$

$$J_2^* \sim \frac{1}{8\pi}\left[\left\{-2\ln\rho + \left(2\ln(2\varepsilon) + 2\cos^2\theta\right)+\ldots\right\} f_2^*(s) + 2\sin\theta\cos\theta\, f_3^*(s)+\ldots\right],$$

$$J_1^* \sim \frac{1}{8\pi}\left[\left\{-2\ln\rho+\left(2\ln(2\varepsilon)+2\sin^2\theta\right)+\ldots\right\}f_3^*(s)+2\sin\theta\cos\theta f_2^*(s)+\ldots\right].$$

Therefore, as $\rho \to 0$, based on equation (3.29), we get

$$(u_1)_1 \sim -\frac{1}{2\pi}f_1^*(s)\ln\rho+\left[\frac{1}{4\pi}\left(2\ln(2\varepsilon)-1\right)f_1^*(s)+J_1(s)\right]+\ldots,$$

$$(u_1)_2 \sim -\frac{1}{4\pi}f_2^*(s)\ln\rho+\left[\frac{1}{4\pi}\left(\ln(2\varepsilon)+\cos^2\theta\right)f_2^*(s)+\frac{1}{4\pi}\sin\theta\cos\theta f_3^*(s)J_2(s)\right]+\ldots,$$

$$(u_1)_3 \sim -\frac{1}{4\pi}f_3^*(s)\ln\rho+\left[\frac{1}{4\pi}\left(\ln(2\varepsilon)+\sin^2\theta\right)f_3^*(s)+\frac{1}{4\pi}\sin\theta\cos\theta f_2^*(s)J_3(s)\right]+\ldots.$$

Now, we may use these quantities into outer region velocity field equation (see equation (3.19)); so that

$$\left.\begin{aligned}
u_1 &\sim -\frac{1}{2\pi}f_1^*(s)\ln\rho+\left[e_1+\frac{1}{4\pi}\left(2\ln(2\varepsilon)-1\right)f_1^*(s)+J_1(s)\right]+\ldots\\
u_2 &\sim -\frac{1}{4\pi}f_2^*(s)\ln\rho+\left[e_2+\frac{1}{4\pi}\left(\ln(2\varepsilon)+\cos^2\theta\right)f_2^*(s)+\frac{1}{4\pi}\sin\theta\cos\theta f_3^*(s)J_2(s)\right]+\ldots,\\
u_3 &\sim -\frac{1}{4\pi}f_3^*(s)\ln\rho+\left[e_3+\frac{1}{4\pi}\left(\ln(2\varepsilon)+\sin^2\theta\right)f_3^*(s)+\frac{1}{4\pi}\sin\theta\cos\theta f_2^*(s)J_3(s)\right]+\ldots.
\end{aligned}\right\} \quad (3,70)$$

In terms of the polar coordinate system (ρ,θ,z), (see figure 3.8) we generally have

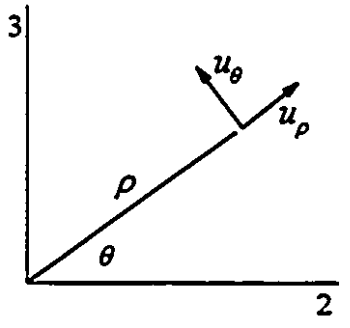

Figure 3.8 Transfer to the polar coordinate system

$$\left.\begin{aligned}
u_\rho &= u_2\cos\theta+u_3\sin\theta,\\
u_\theta &= -u_2\sin\theta+u_3\cos\theta,\\
u_z &= u_1,
\end{aligned}\right\}$$

thus, the outer region velocity fields will act like

$$u_\rho \sim -\frac{1}{4\pi}\left\{f_2^*(s)\cos\theta + f_3^*(s)\sin\theta\right\}\ln\rho + \left\{e_2 + \frac{1}{4\pi}\left(\ln(2\varepsilon)+1\right)f_2^*(s) + J_2(s)\right\}\cos\theta$$
$$+\left\{e_3 + \frac{1}{4\pi}\left(\ln(2\varepsilon)+1\right)f_3^*(s) + J_3(s)\right\}\sin\theta + \ldots, \tag{3,71}$$

$$u_\theta \sim -\frac{1}{4\pi}\left\{-f_2^*(s)\sin\theta + f_3^*(s)\cos\theta\right\}\ln\rho - \left\{e_2 + \frac{1}{4\pi}\ln(2\varepsilon)\,f_2^*(s) + J_2(s)\right\}\sin\theta$$
$$+\left\{e_3 + \frac{1}{4\pi}\ln(2\varepsilon)\,f_3^*(s) + J_3(s)\right\}\cos\theta + \ldots, \tag{3,72}$$

$$u_z \sim -\frac{1}{2\pi}f_1^*(s)\ln\rho + \left[e_1 + \frac{1}{4\pi}\left(2\ln(2\varepsilon)-1\right)f_1^*(s) + J_1(s)\right] + \ldots. \tag{3,73}$$

Matching at order $\ln\rho$ onto the inner expansion velocity fields, expressions (3,18), we obtain the following

$$\left.\begin{aligned} C(\kappa) &= \frac{1}{8\pi}f_2^*(s) \\ D(\kappa) &= \frac{1}{8\pi}f_3^*(s) \\ E(\kappa) &= -\frac{1}{2\pi}f_1^*(s) \end{aligned}\right\} \tag{3,74}$$

The values of $C(\kappa)$ and $D(\kappa)$ agrees with equations (3,55), obtained earlier by matching the pressure. Similarly, matching at order ρ^0 gives

$$C(\kappa)\left\{2\ln(\kappa\lambda)+1\right\} = e_2 + \frac{1}{4\pi}\left(\ln(2\varepsilon)+1\right)f_2^*(s) + J_2(s), \tag{3,75}$$

$$D(\kappa)\left\{2\ln(\kappa\lambda)+1\right\} = e_3 + \frac{1}{4\pi}\left(\ln(2\varepsilon)+1\right)f_3^*(s) + J_3(s), \tag{3,76}$$

$$C(\kappa)\left\{2\ln(\kappa\lambda)-1\right\} = e_2 + \frac{1}{4\pi}\left(\ln(2\varepsilon)+1\right)f_2^*(s) + J_2(s), \tag{3,77}$$

$$D(\kappa)\left\{2\ln(\kappa\lambda)-1\right\} = e_3 + \frac{1}{4\pi}\left(\ln(2\varepsilon)+1\right)f_3^*(s) + J_3(s), \tag{3,78}$$

$$-E(\kappa)\ln(\kappa\lambda) = e_1 + \frac{1}{4\pi}\left(2\ln(2\varepsilon) - 1\right) f_1^*(s) + J_1(s). \tag{3,79}$$

Substituting the values of $\underline{f}^*(s)$ from (3,74) i.e.

$$\left.\begin{aligned} f_1^*(s) &= -2\pi\, E(\kappa) \\ f_2^*(s) &= +8\pi\, C(\kappa) \\ f_3^*(s) &= +8\pi\, D(\kappa) \end{aligned}\right\} \tag{3,80}$$

we obtain from either equation (3,75) or (3,77)

$$C(\kappa)\left\{2\ln\left(\frac{\kappa\lambda}{2\varepsilon}\right) - 1\right\} = e_2 + J_2(s), \tag{3,81}$$

and from either equation (3,76) or (3,78)

$$D(\kappa)\left\{2\ln\left(\frac{\kappa\lambda}{2\varepsilon}\right) - 1\right\} = e_3 + J_3(s), \tag{3,82}$$

and from (3,79)

$$E(\kappa)\left\{-\ln\left(\frac{\kappa\lambda}{2\varepsilon}\right) - \frac{1}{2}\right\} = e_1 + J_1(s). \tag{3,83}$$

3.2.3 Force per unit Length of the Body

From the inner expansion solution, we calculate the force per unit length of the body as $\mu U \underline{f}(s)$; where $\underline{f}(s)$ is the dimensionless force per unit length on the body exerted by the fluid and $\underline{f}^*(s)$ being the dimensionless force per unit length on the fluid exerted by the body.

$$\underline{f}(s) = -\underline{f}^*(s)$$

In inner region $\overline{u}$ and $\overline{p}$ are given by equations (3,15) in cylindrical polar coordinates. The rate of strain tensor $e_{ij} = \frac{1}{2}(u_{i,j} + u_{j,i})$ will be

$$e_{\bar{\rho}\bar{\rho}} = \frac{\partial \overline{u}_{\bar{\rho}}}{\partial \bar{\rho}} = C(\kappa)\left\{2\lambda^2\bar{\rho}^{-3} - 2\bar{\rho}^{-1}\right\}\cos\theta + D(\kappa)\left\{2\lambda^2\bar{\rho}^{-3} - 2\bar{\rho}^{-1}\right\}\sin\theta,$$

$$e_{\theta\bar{\rho}} = \frac{1}{2}\left\{\frac{\partial \bar{u}_\theta}{\partial \bar{\rho}} + \frac{1}{\bar{\rho}}\frac{\partial \bar{u}_{\bar{\rho}}}{\partial \theta} - \frac{\bar{u}_\theta}{\bar{\rho}}\right\} = C(\kappa)\left\{2\lambda^2\bar{\rho}^{-3}\sin\theta\right\} + D(\kappa)\left\{-2\lambda^2\bar{\rho}^{-3}\cos\theta\right\},$$

$$e_{z\bar{\rho}} = \frac{1}{2}\left\{\frac{\partial \bar{u}_z}{\partial \bar{\rho}} + \frac{\partial \bar{u}_{\bar{\rho}}}{\partial \bar{z}}\right\} = \frac{1}{2}E(\kappa)\bar{\rho}^{-1},$$

so that considering $\bar{\rho} = \lambda$ on the cylinder surface, the stress tensor $\sigma_{ij} = -p\delta_{ij} + 2e_{ij}$ has the values

$$\left.\begin{aligned}\sigma_{\bar{\rho}\bar{\rho}} &= -4\lambda^{-1}\left(C(\kappa)\cos\theta + D(\kappa)\sin\theta\right),\\ \sigma_{\theta\bar{\rho}} &= 4\lambda^{-1}\left(C(\kappa)\sin\theta - D(\kappa)\cos\theta\right),\\ \sigma_{z\bar{\rho}} &= \lambda^{-1}E(\kappa).\end{aligned}\right\} \tag{3,84}$$

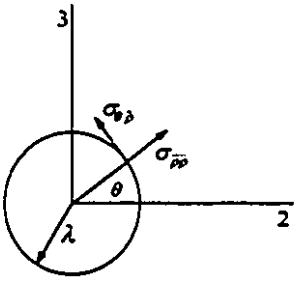

Figure 3.9 Stress tensor on the cylinder surface

Thus force per unit length $\underline{f}$ on the body is given by

$$f_1 = \left\{\lambda^{-1}E(\kappa)\right\}2\pi\lambda = 2\pi E(\kappa),$$

$$f_2 = \int_0^{2\pi}\left\{\sigma_{\bar{\rho}\bar{\rho}}\cos\theta - \sigma_{\theta\bar{\rho}}\sin\theta\right\}\lambda\, d\theta = -8\pi C(\kappa),$$

$$f_3 = \int_0^{2\pi}\left\{\sigma_{\theta\bar{\rho}}\cos\theta - \sigma_{\bar{\rho}\bar{\rho}}\sin\theta\right\}\lambda\, d\theta = -8\pi D(\kappa),$$

that is

$$\left.\begin{aligned}f_1(s) &= 2\pi E(\kappa),\\ f_2(s) &= -8\pi C(\kappa),\\ f_3(s) &= -8\pi D(\kappa),\end{aligned}\right\} \tag{3,85}$$

which when compared with equations (3,80) gives

$$\underline{f}(s) = -\underline{f}^{*}(s)$$

as expected.

Thus the equations (3,81), (3,82), and (3,83) may be written in the form

$$\left.\begin{aligned} f_1(s)\left\{\ln\left(\frac{\kappa\lambda}{2\varepsilon}\right)+\frac{1}{2}\right\} &= -2\pi\left(e_1 + J_1(s)\right), \\ f_2(s)\left\{2\ln\left(\frac{\kappa\lambda}{2\varepsilon}\right)-1\right\} &= -8\pi\left(e_2 + J_2(s)\right), \\ f_3(s)\left\{2\ln\left(\frac{\kappa\lambda}{2\varepsilon}\right)-1\right\} &= -8\pi\left(e_3 + J_3(s)\right), \end{aligned}\right\} \tag{3,86}$$

where by equation (3,30), we have

$$J_i(s) = -\frac{1}{8\pi}\left\{\int_0^{s-\varepsilon} + \int_{s+\varepsilon}^{1}\right\} g_{ij}\left(\underline{r} - \underline{R}(\hat{s})\right) f_j(\hat{s})\, d\hat{s}.$$

Thus, if replace $\underline{r}$ by $\underline{R}(s)$ in $J_i(s)$, since there is no singularity at $\underline{r} = \underline{R}(s)$ for $J_i(s)$, we will have

$$\left.\begin{aligned} f_1(s)\left\{2\ln\left(\frac{\kappa\lambda}{2\varepsilon}\right)+1\right\} &= -4\pi\, e_1 + \frac{1}{2}\left\{\int_0^{s-\varepsilon} + \int_{s+\varepsilon}^{1}\right\} g_{1j}\left(\underline{R}(s) - \underline{R}(\hat{s})\right) f_j(\hat{s})\, d\hat{s}, \\ f_2(s)\left\{2\ln\left(\frac{\kappa\lambda}{2\varepsilon}\right)-1\right\} &= -8\pi\, e_2 + \left\{\int_0^{s-\varepsilon} + \int_{s+\varepsilon}^{1}\right\} g_{2j}\left(\underline{R}(s) - \underline{R}(\hat{s})\right) f_j(\hat{s})\, d\hat{s}, \\ f_3(s)\left\{2\ln\left(\frac{\kappa\lambda}{2\varepsilon}\right)-1\right\} &= -8\pi\, e_3 + \left\{\int_0^{s-\varepsilon} + \int_{s+\varepsilon}^{1}\right\} g_{3j}\left(\underline{R}(s) - \underline{R}(\hat{s})\right) f_j(\hat{s})\, d\hat{s}, \end{aligned}\right\} \tag{3,87}$$

and since

$$\left\{\int_0^{s-\varepsilon} + \int_{s+\varepsilon}^{1}\right\} \frac{d\hat{s}}{|s-\hat{s}|} = -2\ln\varepsilon + \ln[s(1-s)],$$

we may write

$$2f_i(s)\ln\varepsilon = f_i(s)\ln[s(1-s)] - \left\{\int_0^{s-\varepsilon} + \int_{s+\varepsilon}^{1}\right\} \frac{f_i(s)\,d\hat{s}}{|s-\hat{s}|}.$$

Thus, the equations (3,87) may be written in the form

$$\left.\begin{aligned}
f_1(s)\left\{2\ln\left(\frac{\kappa\lambda}{2\sqrt{s(1-s)}}\right)-1\right\} &= -4\pi e_1 + \frac{1}{2}\left\{\int_0^{s-\varepsilon} + \int_{s+\varepsilon}^{1}\right\}\left(g_{1j}\left(\underline{R}-\underline{\hat{R}}\right)f_j(\hat{s}) - \frac{2f_1(s)}{|s-\hat{s}|}\right)d\hat{s},\\
f_2(s)\left\{2\ln\left(\frac{\kappa\lambda}{2\sqrt{s(1-s)}}\right)-1\right\} &= -8\pi e_2 + \left\{\int_0^{s-\varepsilon} + \int_{s+\varepsilon}^{1}\right\}\left(g_{2j}\left(\underline{R}-\underline{\hat{R}}\right)f_j(\hat{s}) - \frac{f_2(s)}{|s-\hat{s}|}\right)d\hat{s},\\
f_3(s)\left\{2\ln\left(\frac{\kappa\lambda}{2\sqrt{s(1-s)}}\right)-1\right\} &= -8\pi e_3 + \left\{\int_0^{s-\varepsilon} + \int_{s+\varepsilon}^{1}\right\}\left(g_{3j}\left(\underline{R}-\underline{\hat{R}}\right)f_j(\hat{s}) - \frac{f_3(s)}{|s-\hat{s}|}\right)d\hat{s}.
\end{aligned}\right\} \qquad (3.88)$$

However, from set equations of (3.66), we see that for $\rho = 0$, $(\hat{s} \neq s)$

$$g_{11} = \frac{2}{|s-\hat{s}|}, \qquad g_{22} = g_{33} = \frac{1}{|s-\hat{s}|},$$

$$g_{ij} = 0 \quad \text{for} \quad i \neq j.$$

Thus, for $\rho = 0$, and $\hat{s} \to s$,

$$g_{1j}\left(\underline{R}-\underline{\hat{R}}\right)f_j(\hat{s}) - \frac{2f_1(s)}{|s-\hat{s}|} = \frac{2f_1(\hat{s})}{|s-\hat{s}|} - \frac{2f_1(s)}{|s-\hat{s}|} = 2f_1'(s)\,\mathrm{sgn}(s-\hat{s}),$$

$$g_{2j}\left(\underline{R}-\underline{\hat{R}}\right)f_j(\hat{s}) - \frac{f_2(s)}{|s-\hat{s}|} = \frac{f_2(\hat{s})}{|s-\hat{s}|} - \frac{f_2(s)}{|s-\hat{s}|} = f_2'(s)\,\mathrm{sgn}(s-\hat{s}),$$

$$g_{3j}\left(\underline{R}-\underline{\hat{R}}\right)f_j(\hat{s}) - \frac{f_3(s)}{|s-\hat{s}|} = f_3'(s)\,\mathrm{sgn}(s-\hat{s}).$$

Thus, the integrals in equations (3,88) are convergent as $\varepsilon \to 0$, so we may write

$$\left.\begin{aligned}
f_1(s)\left\{2\ln\left(\frac{\kappa\lambda}{2\sqrt{s(1-s)}}\right)+1\right\} &= -4\pi e_1 + \frac{1}{2}\int_0^1\left(g_{1j}\left(\underline{R}-\underline{\hat{R}}\right)f_j(\hat{s}) - \frac{2f_1(s)}{|s-\hat{s}|}\right)d\hat{s},\\
f_2(s)\left\{2\ln\left(\frac{\kappa\lambda}{2\sqrt{s(1-s)}}\right)-1\right\} &= -8\pi e_2 + \int_0^1\left(g_{2j}\left(\underline{R}-\underline{\hat{R}}\right)f_j(\hat{s}) - \frac{f_2(s)}{|s-\hat{s}|}\right)d\hat{s},\\
f_3(s)\left\{2\ln\left(\frac{\kappa\lambda}{2\sqrt{s(1-s)}}\right)-1\right\} &= -8\pi e_3 + \int_0^1\left(g_{3j}\left(\underline{R}-\underline{\hat{R}}\right)f_j(\hat{s}) - \frac{f_3(s)}{|s-\hat{s}|}\right)d\hat{s}.
\end{aligned}\right\} \qquad (3,89)$$

Letting $\underline{i}_1$, $\underline{i}_2$, and $\underline{i}_3$ be unit vectors along the 1, 2, and 3 directions, respectively, so that

$$\underline{i}_1 = \frac{d\underline{R}}{ds} = \underline{t}(s)\,,$$

then we can combine equations (3,89) as

$$\left[f_1(s)\underline{i}_1 + f_2(s)\underline{i}_2 + f_3(s)\underline{i}_3\right]\left[2\ln\left(\frac{\kappa\lambda}{2\sqrt{s(1-s)}}\right) - 1\right] + 2f_1(s)\underline{i}_1 = -8\pi\left[e_1\underline{i}_1 + e_2\underline{i}_2 + e_3\underline{i}_3\right] + 4\pi\, e_1\underline{i}_1$$
$$+ \int_0^1 \left\{\left[g_{1j}\left(\underline{R} - \hat{\underline{R}}\right)\underline{i}_1 + g_{2j}\left(\underline{R} - \hat{\underline{R}}\right)\underline{i}_2 + g_{3j}\left(\underline{R} - \hat{\underline{R}}\right)\underline{i}_3\right] f_j(\hat{s}) - \frac{\left[f_1(s)\underline{i}_1 + f_2(s)\underline{i}_2 + f_3(s)\underline{i}_3\right]}{|s-\hat{s}|}\right\} d\hat{s}$$
$$- \frac{1}{2}\int_0^1 g_{1j}\left(\underline{R} - \hat{\underline{R}}\right)\underline{i}_1 f_j(\hat{s})\, d\hat{s}$$

or

$$\underline{f}(s)\left[2\ln\left(\frac{\kappa\lambda}{2\sqrt{s(1-s)}}\right) - 1\right] + 2\underline{f}(s).\underline{t}(s)\underline{t}(s) = -8\pi\,\underline{e} + 4\pi\,\underline{e}.\underline{t}(s)\underline{t}(s)$$
$$+ \int_0^1 \left(\underline{\underline{g}}\left(\underline{R} - \hat{\underline{R}}\right).\underline{f}(\hat{s}) - \frac{\underline{f}(s)}{|s-\hat{s}|}\right) d\hat{s} - \frac{1}{2}\int_0^1 \underline{t}(s).\underline{\underline{g}}\left(\underline{R} - \hat{\underline{R}}\right).\underline{f}(\hat{s})\underline{t}(s)\, d\hat{s}$$

or

$$\underline{f}(s).\left[\left\{2\ln\left(\frac{\kappa\lambda}{2\sqrt{s(1-s)}}\right) - 1\right\}\underline{\underline{I}} + 2\underline{t}(s)\underline{t}(s)\right] = -8\pi\,\underline{e}.\left[\underline{\underline{I}} - \frac{1}{2}\underline{t}(s)\underline{t}(s)\right]$$
$$+ \int_0^1 \left(\left[\underline{\underline{I}} - \frac{1}{2}\underline{t}(s)\underline{t}(s)\right].\underline{\underline{g}}\left(\underline{R} - \hat{\underline{R}}\right).\underline{f}(\hat{s}) - \frac{\underline{f}(s)}{|s-\hat{s}|}\right) d\hat{s} \qquad (3,90)$$

Similarly, combining equations (3,87), one can write them as

$$\underline{f}(s).\left[\left\{2\ln\left(\frac{\kappa\lambda}{2\varepsilon}\right) - 1\right\}\underline{\underline{I}} + 2\underline{t}(s)\underline{t}(s)\right] = -8\pi\,\underline{e}.\left[\underline{\underline{I}} - \frac{1}{2}\underline{t}(s)\underline{t}(s)\right]$$
$$+ \left\{\int_0^{s-\varepsilon} + \int_{s+\varepsilon}^1\right\}\left(\underline{\underline{I}} - \frac{1}{2}\underline{t}(s)\underline{t}(s)\right).\underline{\underline{g}}\left(\underline{R} - \hat{\underline{R}}\right).\underline{f}(\hat{s})\, d\hat{s} \qquad (3,91)$$

where $\underline{R}$ is the value of r at the point under consideration, on the centreline; $\hat{\underline{R}}$ is the value of r at the point on the centreline with $s - \hat{s}$ (see figure 3.7), and the vector $\underline{t}$ is the tangent direction at s.

3.2.3.1 Some Points on the above Force Equation

- Since the above equation (3.91) for the hydrodynamic force per unit length acting on the body is of vectorial form, one may consider it relative to any arbitrary rectangular Cartesian coordinate system
- The value of ε appearing in the above force integral equation is arbitrary, satisfying only the inequality $0 < \varepsilon << 1$. Solution is independent of ε .
- The integral equation for $\underline{f}(s)$ is a Fredholm equation of the 3rd kind.
- The value of $\underline{f}(s)$ depends, in general, on the entire body shape $\alpha \le \hat{s} \le \beta$.

3.2.3.2 Value of the Tensor $\underline{\underline{g}}(\underline{r})$

Using equations (3.27) and (3.25), we are able to obtain the value of the tensor $\underline{\underline{g}}(\underline{r})$. Since

$$\psi(\underline{r}) = \frac{2}{Re}\int_0^{\frac{1}{2}Re(r-\underline{e}.\underline{r})} \frac{1-e^{-\alpha}}{\alpha} d\alpha ,$$

$$\psi_{,i} = \left\{\frac{1-e^{-1/2Re(r-\underline{e}.\underline{r})}}{\frac{1}{2}Re(r-\underline{e}.\underline{r})}\right\}\left(\frac{r_i}{r} - e_i\right),$$

$$\psi_{,ij} = \left\{\frac{1-e^{-1/2Re(r-\underline{e}.\underline{r})}}{\frac{1}{2}Re(r-\underline{e}.\underline{r})}\right\}\left(\frac{\delta_{ij}}{r} - \frac{r_i r_j}{r^3}\right)$$

$$+\left\{\frac{-1+\frac{1}{2}Re(r-\underline{e}.\underline{r})\,e^{-1/2Re(r-\underline{e}.\underline{r})}+e^{-1/2Re(r-\underline{e}.\underline{r})}}{\frac{1}{4}Re^2(r-\underline{e}.\underline{r})^2}\right\}\frac{1}{2}Re\left(\frac{r_j}{r} - e_j\right)\left(\frac{r_i}{r} - e_i\right),$$

$$\psi_{,kk} = \frac{2}{r} e^{-1/2Re(r - \underline{e}.\underline{r})}.$$

Thus, the equation (3,25) can be written as

$$g_{ij} = \psi_{,kk}\,\delta_{ij} - \psi_{,ij}, \quad \Rightarrow$$

$$g_{ij}(\underline{r}) = \frac{2\left\{1 - e^{-1/2Re(r - \underline{e}.\underline{r})}\right\}}{Re\,(r - \underline{e}.\underline{r})^2}\left\{\left(\frac{r_i}{r} - e_i\right)\left(\frac{r_j}{r} - e_j\right) - (r - \underline{e}.\underline{r})\left(\frac{\delta_{ij}}{r} - \frac{r_i r_j}{r^3}\right)\right\}$$
$$+ \frac{e^{-1/2Re(r - \underline{e}.\underline{r})}}{(r - \underline{e}.\underline{r})}\left\{\frac{2(r - \underline{e}.\underline{r})\delta_{ij}}{r} - \left(\frac{r_i}{r} - e_i\right)\left(\frac{r_j}{r} - e_j\right)\right\}. \qquad (3,92)$$

3.2.3.3 The limit of g_{ij} as $Re \to 0$

It is worth mentioning that if we take the limit of equation (3,92) as $Re \to 0$, we will have the following expression for creeping flow conditions

$$g_{ij}(\underline{r}) \sim \left(\frac{\delta_{ij}}{r} + \frac{r_i r_j}{r^3}\right) + O(Re),$$

therefore, as expected, we have R. E. Johnson's (1980) result.

The above equations (3,91) and (3,92) are basic equations for a general case. In the next section we use these essential equations to develop an expression for the force per unit length on a long cylinder. Then, we will apply the outcoming result to find out the flow field around such a cylinder. Having the flow field and force equations, we can develop the required expressions for the trajectory course of a small particle released far from the cylinder in a fluid with R <<1 (not zero).

3.3 THE MOTION OF FLUID AROUND AN INFINITE LONG CYLINDER

The special case of an infinitely long cylinder of circular cross-section with radius b is considered in the present section. The cylinder need not be mathematically infinite, but it is practically long enough to ignore the ends effects (e.g. a few miles). In order to find the flow field ($\underline{u}$, p) around the cylinder, we need to calculate the hydrodynamic forces per unit length acting on the cylinder; see equations (3,24) and (3,28) earlier in this chapter.

3.3.1 Driving Drag Forces per Unit Length of Cylinder

Since the cylinder is considered infinitely long, the force per unit length ($\mu\, U\underline{f}$) is independent of s, where $\underline{f}$ is the dimensionless force per unit length on cylinder. To solve the general equation of force per unit length on slender bodies, equation (3,91), for the case of cylinder, we need to calculate different elements of the tensor g_{ij}, as the first step. A set of Cartesian coordinate axes (1, 2, and 3) is defined (see figure 3. 10) so that the point P is located at the origin ($s = 0$).

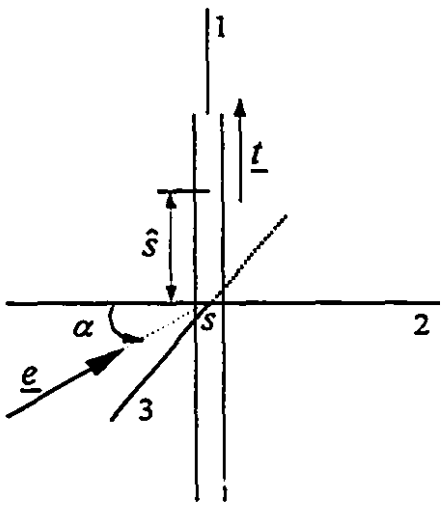

Figure 3.10 The Cartesian axes and the cylinder

Here, $\underline{t}$ is a unit vector along the cylinder axis and $\underline{e}$ is the unit vector of undisturbed velocity located in the surface of 1- and 2-axes. Because of symmetry, the

component of force per unit length in the direction of the cylinder axis (1-direction) is zero and the other components are constant and independent of $\hat{s}$. Thus

$$\underline{f}(\hat{s}) = (f_1, f_2, 0),$$

$$\underline{e} = (\sin\alpha, \cos\alpha, 0),$$

$$\underline{t} = (1, 0, 0),$$

and if we put $s = 0$, at the origin

$$\underline{r} = \underline{R} - \underline{\hat{R}} = \{(s - \hat{s}), 0, 0\} = \{-\hat{s}, 0, 0\},$$

$$(r - \underline{e}.\underline{r}) = |\hat{s} + \hat{s}\sin\alpha|,$$

$$\frac{\underline{r}}{r} = \left\{-\frac{\hat{s}}{|\hat{s}|}, 0, 0\right\} = \{-\operatorname{sgn}\hat{s}, 0, 0\},$$

$$\frac{(r - \underline{e}.\underline{r})}{r} = 1 + \frac{\hat{s}}{|\hat{s}|}\sin\alpha = 1 + (\operatorname{sgn}\hat{s})\sin\alpha.$$

Substituting the above quantities in equation (3,92)

$$g_{11} = \frac{2\left\{1 - e^{-1/2Re(|\hat{s}| + \hat{s}\sin\alpha)}\right\}}{Re(|\hat{s}| + \hat{s}\sin\alpha)^2}\left\{(-\operatorname{sgn}\hat{s} - \sin\alpha)^2 - (1 + (\operatorname{sgn}\hat{s})\sin\alpha)(1 - 1)\right\}$$
$$+ \frac{e^{-1/2Re(|\hat{s}| + \hat{s}\sin\alpha)}}{(|\hat{s}| + \hat{s}\sin\alpha)}\left\{2(1 + (\operatorname{sgn}\hat{s})\sin\alpha) - (-\operatorname{sgn}\hat{s} - \sin\alpha)^2\right\}$$

$$\Rightarrow$$

$$g_{11} = \frac{2\left\{1 - e^{-1/2Re(|\hat{s}| + \hat{s}\sin\alpha)}\right\}}{Re\,\hat{s}^2} + \frac{e^{-1/2Re(|\hat{s}| + \hat{s}\sin\alpha)}}{\hat{s}(\operatorname{sgn}\hat{s} + \sin\alpha)}\cos^2\alpha. \qquad (3,93)$$

Similarly, for g_{12}

$$g_{22} = \frac{2\left\{1 - e^{-1/2Re(|\hat{s}| + \hat{s}\sin\alpha)}\right\}}{Re(|\hat{s}| + \hat{s}\sin\alpha)^2}\left\{(-\cos\alpha)^2 - [1 + (\operatorname{sgn}\hat{s})\sin\alpha](1-0)\right\}$$
$$+ \frac{e^{-1/2Re(|\hat{s}| + \hat{s}\sin\alpha)}}{(|\hat{s}| + \hat{s}\sin\alpha)}\left\{2[1 + (\operatorname{sgn}\hat{s})\sin\alpha] - (-\cos\alpha)^2\right\}$$

$$\Rightarrow$$

$$g_{22} = -\frac{2\left\{1 - e^{-1/2Re(|\hat{s}| + \hat{s}\sin\alpha)}\right\}\sin\alpha}{Re\ \hat{s}^2(\operatorname{sgn}\hat{s} + \sin\alpha)} + \frac{e^{-1/2Re(|\hat{s}| + \hat{s}\sin\alpha)}(\operatorname{sgn}\hat{s} + \sin\alpha)}{\hat{s}}. \qquad (3,94)$$

Also

$$g_{33} = \frac{2\left\{1 - e^{-1/2Re(|\hat{s}| + \hat{s}\sin\alpha)}\right\}}{Re\ \hat{s}^2(\operatorname{sgn}\hat{s} + \sin\alpha)^2}\left\{-[1 + (\operatorname{sgn}\hat{s})\sin\alpha]\right\}$$
$$+ \frac{e^{-1/2Re(|\hat{s}| + \hat{s}\sin\alpha)}}{\hat{s}(\operatorname{sgn}\hat{s} + \sin\alpha)}\left\{2[1 + (\operatorname{sgn}\hat{s})\sin\alpha]\right\}$$

$$\Rightarrow$$

$$g_{33} = -\frac{2\left\{1 - e^{-1/2Re(|\hat{s}| + \hat{s}\sin\alpha)}\right\}\operatorname{sgn}\hat{s}}{Re\ \hat{s}^2(\operatorname{sgn}\hat{s} + \sin\alpha)} + \frac{2e^{-1/2Re(|\hat{s}| + \hat{s}\sin\alpha)}\operatorname{sgn}\hat{s}}{\hat{s}}. \qquad (3,95)$$

Also

$$g_{21} = g_{12} = \frac{2\left\{1 - e^{-1/2Re(|\hat{s}| + \hat{s}\sin\alpha)}\right\}}{Re\ \hat{s}^2(\operatorname{sgn}\hat{s} + \sin\alpha)^2}\left\{(-\operatorname{sgn}\hat{s} - \sin\alpha)(-\cos\alpha) - 0\right\}$$
$$+ \frac{e^{-1/2Re(|\hat{s}| + \hat{s}\sin\alpha)}}{\hat{s}(\operatorname{sgn}\hat{s} + \sin\alpha)}\left\{-(-\operatorname{sgn}\hat{s} - \sin\alpha)(-\cos\alpha)\right\},$$

$$= \frac{2\left\{1 - e^{-1/2Re(|\hat{s}| + \hat{s}\sin\alpha)}\right\}\cos\alpha}{Re\ \hat{s}^2(\operatorname{sgn}\hat{s} + \sin\alpha)} - \frac{e^{-1/2Re(|\hat{s}| + \hat{s}\sin\alpha)}\cos\alpha}{\hat{s}}. \qquad (3,96)$$

And similarly,

$$g_{23} = g_{32} = g_{13} = g_{31} = 0. \qquad (3,97)$$

Now, we may substitute the above quantities into equation (3,91). Thus

$$\left[(\underline{\underline{I}}-\frac{1}{2}\underline{tt}).\underline{\underline{g}}(\underline{R}-\hat{\underline{R}}).\underline{f}(\hat{s})\right]_1=(1-\frac{1}{2})\{g_{11}f_1+g_{12}f_2\}$$
$$=\frac{\{1-e^{-1/2Re(|\hat{s}|+\hat{s}\sin\alpha)}\}}{Re\,\hat{s}^2(\mathrm{sgn}\,\hat{s}+\sin\alpha)}\{(\mathrm{sgn}\,\hat{s}+\sin\alpha)f_1+\cos\alpha f_2\} \qquad (3,98)$$
$$+\frac{e^{-1/2Re(|\hat{s}|+\hat{s}\sin\alpha)}}{2\hat{s}(\mathrm{sgn}\,\hat{s}+\sin\alpha)}\{\cos^2\alpha f_1-(\mathrm{sgn}\,\hat{s}+\sin\alpha)\cos\alpha f_2\},$$

$$\left[(\underline{\underline{I}}-\frac{1}{2}\underline{tt}).\underline{\underline{g}}(\underline{R}-\hat{\underline{R}}).\underline{f}(\hat{s})\right]_2=\{g_{21}f_1+g_{22}f_2\}$$
$$=\frac{2\{1-e^{-1/2Re(|\hat{s}|+\hat{s}\sin\alpha)}\}}{Re\,\hat{s}^2(\mathrm{sgn}\,\hat{s}+\sin\alpha)}\{\cos\alpha f_1-\sin\alpha f_2\} \qquad (3,99)$$
$$+\frac{e^{-1/2Re(|\hat{s}|+\hat{s}\sin\alpha)}}{\hat{s}}\{-\cos\alpha f_1+(\mathrm{sgn}\,\hat{s}+\sin\alpha)f_2\},$$

and because of equations (3,97) we have

$$\left[(\underline{\underline{I}}-\frac{1}{2}\underline{tt}).\underline{\underline{g}}(\underline{R}-\hat{\underline{R}}).\underline{f}(\hat{s})\right]_2=\{g_{31}f_1+g_{32}f_2\}=0. \qquad (3,100)$$

It is noticeable that for an infinite rod the equation (3,91) must be replaced by

$$\underline{f}(s).\left[\left\{2\ln\left(\frac{\kappa\lambda}{2\varepsilon}\right)-1\right\}\underline{\underline{I}}+2\underline{tt}\right]=-8\pi\underline{e}.\left[\underline{\underline{I}}-\frac{1}{2}\underline{tt}\right]$$
$$+\left\{\int_{-\infty}^{-\varepsilon}+\int_{\varepsilon}^{\infty}\right\}(\underline{\underline{I}}-\frac{1}{2}\underline{tt}).\underline{\underline{g}}(-\hat{\underline{R}}).\underline{f}(\hat{s})d\hat{s}, \qquad (3,101)$$

where from equations (3,98) and (3,99) we see that the integrals are convergent at $\hat{s}=\pm\infty$ so long as

$$|\hat{s}|+\hat{s}\sin\alpha>0,$$

or $\quad 1+\mathrm{sgn}\,\hat{s}+\sin\alpha>0 \quad$ at both $\hat{s}=+\infty$ and $\hat{s}=-\infty$,

i.e. we require

$$1+\sin\alpha > 0 \quad \text{and} \quad 1-\sin\alpha > 0,$$

$$\Rightarrow \quad \alpha \neq \pm\frac{\pi}{2}. \tag{3,102}$$

Since the radius of the cylinder is the constant b, the non-dimensional width $\lambda = 1$. Thus the equation (3,101) may be written as

$$\begin{aligned} f_1\left[2\ln\left(\frac{\kappa}{2\varepsilon}\right)+1\right] &= -4\pi\sin\alpha + f_1\left\{\int_{-\infty}^{-\varepsilon}+\int_{\varepsilon}^{\infty}\right\}\left(\frac{\left\{1-e^{-1/2Re\hat{s}(\operatorname{sgn}\hat{s}+\sin\alpha)}\right\}}{Re\,\hat{s}^2}+\frac{e^{-1/2Re\hat{s}(\operatorname{sgn}\hat{s}+\sin\alpha)}\cos^2\alpha}{2\hat{s}(\operatorname{sgn}\hat{s}+\sin\alpha)}\right)d\hat{s} \\ &\quad + f_2\left\{\int_{-\infty}^{-\varepsilon}+\int_{\varepsilon}^{\infty}\right\}\left(\frac{\left\{1-e^{-1/2Re\hat{s}(\operatorname{sgn}\hat{s}+\sin\alpha)}\right\}\cos\alpha}{Re\,\hat{s}^2(\operatorname{sgn}\hat{s}+\sin\alpha)}-\frac{e^{-1/2Re\hat{s}(\operatorname{sgn}\hat{s}+\sin\alpha)}\cos\alpha}{2\hat{s}}\right)d\hat{s}, \end{aligned} \tag{3,103}$$

$$\begin{aligned} f_2\left[2\ln\left(\frac{\kappa}{2\varepsilon}\right)-1\right] &= -8\pi\cos\alpha + f_1\left\{\int_{-\infty}^{-\varepsilon}+\int_{\varepsilon}^{\infty}\right\}\left(\frac{\left\{1-e^{-1/2Re\hat{s}(\operatorname{sgn}\hat{s}+\sin\alpha)}\right\}2\cos\alpha}{Re\,\hat{s}^2(\operatorname{sgn}\hat{s}+\sin\alpha)}-\frac{e^{-1/2Re\hat{s}(\operatorname{sgn}\hat{s}+\sin\alpha)}\cos\alpha}{\hat{s}}\right)d\hat{s} \\ &\quad + f_2\left\{\int_{-\infty}^{-\varepsilon}+\int_{\varepsilon}^{\infty}\right\}\left(\frac{\left\{1-e^{-1/2Re\hat{s}(\operatorname{sgn}\hat{s}+\sin\alpha)}\right\}(-2\sin\alpha)}{Re\,\hat{s}^2(\operatorname{sgn}\hat{s}+\sin\alpha)}+\frac{e^{-1/2Re\hat{s}(\operatorname{sgn}\hat{s}+\sin\alpha)}(\operatorname{sgn}\hat{s}+\sin\alpha)}{\hat{s}}\right)d\hat{s} \end{aligned} \tag{3,104}$$

or we may write them as

$$\begin{aligned} \left[2\ln\left(\frac{\kappa}{2\varepsilon}\right)+1\right] &= -4\pi\sin\alpha + f_1\int_{\varepsilon}^{\infty}\left(\frac{\left\{1-e^{+1/2Re\hat{s}(-1+\sin\alpha)}\right\}}{Re\,\hat{s}^2}+\frac{e^{+1/2Re\hat{s}(-1+\sin\alpha)}\cos^2\alpha}{-2\hat{s}(-1+\sin\alpha)}\right)d\hat{s} \\ &\quad + f_1\int_{\varepsilon}^{\infty}\left(\frac{\left\{1-e^{-1/2Re\hat{s}(1+\sin\alpha)}\right\}}{Re\,\hat{s}^2}+\frac{e^{-1/2Re\hat{s}(1+\sin\alpha)}\cos^2\alpha}{2\hat{s}(1+\sin\alpha)}\right)d\hat{s} \\ &\quad + f_2\int_{\varepsilon}^{\infty}\left(\frac{\left\{1-e^{+1/2Re\hat{s}(-1+\sin\alpha)}\right\}\cos\alpha}{Re\,\hat{s}^2(-1+\sin\alpha)}-\frac{e^{+1/2Re\hat{s}(-1+\sin\alpha)}\cos\alpha}{-2\hat{s}}\right)d\hat{s} \\ &\quad + f_2\int_{\varepsilon}^{\infty}\left(\frac{\left\{1-e^{-1/2Re\hat{s}(1+\sin\alpha)}\right\}\cos\alpha}{Re\,\hat{s}^2(1+\sin\alpha)}-\frac{e^{-1/2Re\hat{s}(1+\sin\alpha)}\cos\alpha}{2\hat{s}}\right)d\hat{s}, \end{aligned} \tag{3,105}$$

and

$$f_2\left[2\ln\left(\frac{\kappa}{2\varepsilon}\right)-1\right]=-8\pi\cos\alpha+f_1\int_\varepsilon^{\infty}\left(\frac{\left\{1-e^{-1/2Re\hat{s}(-1+\sin\alpha)}\right\}2\cos\alpha}{Re\,\hat{s}^2(-1+\sin\alpha)}-\frac{e^{-1/2Re\hat{s}(-1+\sin\alpha)}\cos\alpha}{-\hat{s}}\right)d\hat{s}$$
$$+f_1\int_\varepsilon^{\infty}\left(\frac{\left\{1-e^{-1/2Re\hat{s}(1+\sin\alpha)}\right\}2\cos\alpha}{Re\,\hat{s}^2(1+\sin\alpha)}-\frac{e^{-1/2Re\hat{s}(1+\sin\alpha)}\cos\alpha}{\hat{s}}\right)d\hat{s}$$
$$+f_2\int_\varepsilon^{\infty}\left(\frac{\left\{1-e^{-1/2Re\hat{s}(-1+\sin\alpha)}\right\}(-2\sin\alpha)}{Re\,\hat{s}^2(-1+\sin\alpha)}+\frac{e^{-1/2Re\hat{s}(-1+\sin\alpha)}(-1+\sin\alpha)}{-\hat{s}}\right)d\hat{s} \qquad (3,106)$$
$$+f_2\int_\varepsilon^{\infty}\left(\frac{\left\{1-e^{-1/2Re\hat{s}(1+\sin\alpha)}\right\}(-2\sin\alpha)}{Re\,\hat{s}^2(1+\sin\alpha)}+\frac{e^{-1/2Re\hat{s}(1+\sin\alpha)}(1+\sin\alpha)}{\hat{s}}\right)d\hat{s}.$$

However, mathematically

$$\int_\varepsilon^{\infty}\frac{e^{-a\hat{s}}}{\hat{s}}d\hat{s}=\int_{a\varepsilon}^{\infty}\frac{e^{-t}}{t}dt=E_1(a\varepsilon)$$
$$\sim-\gamma-\ln(a\varepsilon)+O(\varepsilon)\qquad\text{as}\quad\varepsilon\to0,$$

where γ is Euler's constant. Then

$$\int_\varepsilon^{\infty}\frac{e^{-a\hat{s}}}{\hat{s}}d\hat{s}\sim(-\ln\varepsilon)+(-\gamma-\ln a)+O(\varepsilon). \qquad (3,107)$$

Also

$$\int_\varepsilon^{\infty}\frac{e^{-a\hat{s}}}{\hat{s}^2}d\hat{s}=\left[-\frac{e^{-as}}{s}\right]_\varepsilon^{\infty}+\int_\varepsilon^{\infty}\frac{(-a)e^{-as}}{s}ds$$
$$=\frac{e^{-a\varepsilon}}{\varepsilon}-a\int_\varepsilon^{\infty}\frac{e^{-as}}{s}ds=\frac{e^{-a\varepsilon}}{\varepsilon}-aE_1(a\varepsilon)$$
$$=\varepsilon^{-1}\left\{e^{-a\varepsilon}-a\varepsilon E_1(a\varepsilon)\right\}$$
$$\sim\varepsilon^{-1}\left\{1-a\varepsilon+\ldots-a\varepsilon(-\gamma-\ln a+\ldots)\right\}$$
$$\sim\varepsilon^{-1}-a+a\gamma+a\ln a+a\ln\varepsilon+O(\varepsilon)$$
$$\sim\varepsilon^{-1}+a\ln\varepsilon+a(\ln a+\gamma-1)$$

and

$$\int_\varepsilon^{\infty}\frac{d\hat{s}}{\hat{s}^2}=\left[-\frac{1}{s}\right]_\varepsilon^{\infty}=\frac{1}{\varepsilon},$$

thus,

$$\int_{\varepsilon}^{\infty} \frac{1-e^{-\alpha\hat{s}}}{\hat{s}^2} d\hat{s} \sim -\alpha \ln\varepsilon + \alpha(1-\gamma-\ln\alpha)+\ldots$$

Therefore, for $\varepsilon \to 0$, the equation (3,105) becomes

$$f_1\left[2\ln\left(\frac{\kappa}{2\varepsilon}\right)+1\right] = -4\pi\sin\alpha + f_1\left[\frac{1}{Re}\left\{-\frac{1}{2}Re(1-\sin\alpha)\ln\varepsilon \right.\right.$$
$$\left.+\frac{1}{2}Re(1-\sin\alpha)\left\{1-\gamma-\ln\left(\frac{1}{2}Re(1-\sin\alpha)\right)\right\}\right\}+\frac{\cos^2\alpha}{2(1-\sin\alpha)}\left\{-\ln\varepsilon-\gamma-\ln\left(\frac{1}{2}Re(1-\sin\alpha)\right)\right\}$$
$$+\frac{1}{Re}\left\{-\frac{1}{2}Re(1+\sin\alpha)\ln\varepsilon+\frac{1}{2}Re(1+\sin\alpha)\left\{1-\gamma-\ln\left(\frac{1}{2}Re(1+\sin\alpha)\right)\right\}\right\}$$
$$\left.+\frac{\cos^2\alpha}{2(1+\sin\alpha)}\left\{-\ln\varepsilon-\gamma-\ln\left(\frac{1}{2}Re(1+\sin\alpha)\right)\right\}\right]$$
$$+f_2\left[-\frac{\cos\alpha}{Re(1-\sin\alpha)}\left\{-\frac{1}{2}Re(1-\sin\alpha)\ln\varepsilon+\frac{1}{2}Re(1-\sin\alpha)\left\{1-\gamma-\ln\left(\frac{1}{2}Re(1-\sin\alpha)\right)\right\}\right\}\right.$$
$$+\frac{\cos\alpha}{2}\left\{-\ln\varepsilon-\gamma-\ln\left(\frac{1}{2}Re(1-\sin\alpha)\right)\right\}+\frac{\cos\alpha}{Re(1+\sin\alpha)}\left\{-\frac{1}{2}Re(1+\sin\alpha)\ln\varepsilon\right.$$
$$\left.\left.+\frac{1}{2}Re(1+\sin\alpha)\left\{1-\gamma-\ln\left(\frac{1}{2}Re(1+\sin\alpha)\right)\right\}\right\}-\frac{\cos\alpha}{2}\left\{-\ln\varepsilon-\gamma-\ln\left(\frac{1}{2}Re(1+\sin\alpha)\right)\right\}\right],$$

and after some algebraic operations

$$4\pi\sin\alpha = f_1\left[-2\ln\kappa+2\ln 2-2\gamma+2\ln 2-2\ln Re-2\ln(\cos\alpha)\right]+f_2[0],$$

where f_2 has a zero coefficient. The above equation gives

$$f_1 = \frac{2\pi\sin\alpha}{\ln\kappa^{-1}-\ln Re+2\ln 2-\gamma-\ln(\cos\alpha)}, \qquad (3,108)$$

or equivalently

$$f_1 = \frac{2\pi\sin\alpha}{\ln R^{-1}+2\ln 2-\gamma-\ln(\cos\alpha)}, \qquad (3,109)$$

where Reynolds number based on radius b is

$$R = \kappa Re = \frac{b}{l}\frac{lU}{\nu} = \frac{bU}{\nu}.$$

Thus, dimensional force per unit length in 1-direction is

$$f_1' = \frac{2\pi\,\mu U \sin\alpha}{\ln\left(\frac{bU}{\nu}\right)^{-1} + 2\ln 2 - \gamma - \ln(\cos\alpha)},$$

and it is noticeable that this force is independent of the length of cylinder l, as it should be.

Similarly as $\varepsilon \to 0$, we have the following for the equation (3,106)

$$8\pi\cos\alpha = f_2\left[1 - 2\ln\kappa + 2\ln 2 - 2\gamma + 2\ln 2 - 2\ln Re - 2\ln(\cos\alpha)\right] + f_1[0],$$

giving

$$f_2 = \frac{4\pi\cos\alpha}{\ln\kappa^{-1} - \ln Re + 2\ln 2 + \frac{1}{2} - \gamma - \ln(\cos\alpha)}, \qquad (3,110)$$

and equivalently

$$f_2 = \frac{4\pi\cos\alpha}{\ln R^{-1} + 2\ln 2 + \frac{1}{2} - \gamma - \ln(\cos\alpha)}, \qquad (3,111)$$

where $R = \kappa Re = \frac{bU}{\nu}$.

Therefore, dimensional force per unit length in the 2-direction is

$$f_2' = \frac{4\pi\,\mu U \sin\alpha}{\ln\left(\frac{bU}{\nu}\right)^{-1} + 2\ln 2 + \frac{1}{2} - \gamma - \ln(\cos\alpha)},$$

again, independent of l as it should be.

The errors in equations f_1 and f_2 are of order $\kappa f(Re) \sim \frac{b}{l} f\left(\frac{lU}{\nu}\right)$ and since this must be independent of l, it is of order $\frac{bU}{\nu}$ (i.e. of order R).

Let $\underline{t}$ be the unit vector along the cylinder axis and $\underline{e}$ be the unit vector along undisturbed flow direction (see figure 3.11).

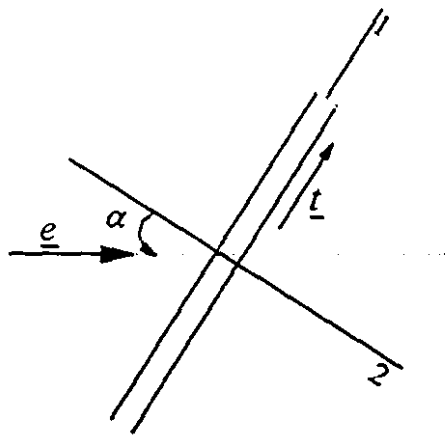

Figure 3.11 Unit vectors

Then,

$$\underline{t}\,.\,\underline{e} = \cos\left(\frac{\pi}{2} - \alpha\right) = \sin\alpha,$$

and the dimensionless force per unit length $\underline{f}$ on the cylinder is

$$\underline{f} = f_1\underline{i}_1 + f_2\underline{i}_2,$$

where $\underline{i}_1$ and $\underline{i}_2$ are unit vectors in the 1- and 2-directions, respectively.

Thus,

$$\underline{i}_1 = \underline{t},$$

$$\underline{i}_2 = \frac{\underline{e} - \underline{t}\,.\,\underline{e}\,\underline{t}}{\left|\underline{e} - \underline{t}\,.\,\underline{e}\,\underline{t}\right|} = \frac{\underline{e} - \underline{t}\,.\,\underline{e}\,\underline{t}}{\left\{\left(\underline{e} - \underline{t}\,.\,\underline{e}\,\underline{t}\right).\left(\underline{e} - \underline{t}\,.\,\underline{e}\,\underline{t}\right)\right\}^{1/2}}$$

$$= \frac{\underline{e} - \underline{t}\,.\,\underline{e}\,\underline{t}}{\left\{1 - \left(\underline{t}\,.\,\underline{e}\right)^2\right\}^{1/2}}.$$

Then,

$$\underline{f} = f_1\underline{t} + \frac{f_2\left(\underline{e} - \underline{t}\,.\,\underline{e}\,\underline{t}\right)}{\left\{1 - \left(\underline{t}\,.\,\underline{e}\right)^2\right\}^{1/2}}.$$

Since $\underline{t} \cdot \underline{e} = \sin\alpha$ and $\cos\alpha = \left\{1-(\underline{t}\cdot\underline{e})^2\right\}$, we will have

$$\underline{f} = \frac{2\pi(\underline{t}\cdot\underline{e})\underline{t}}{\ln R^{-1} + 2\ln 2 - \gamma - \ln(\cos\alpha)} + \frac{4\pi(\underline{e} - \underline{t}\cdot\underline{e}\,\underline{t})}{\ln R^{-1} + 2\ln 2 + \frac{1}{2} - \gamma - \ln(\cos\alpha)},$$

or

$$\frac{\underline{f}}{2\pi} = \frac{(\underline{t}\cdot\underline{e})\underline{t}}{\ln R^{-1} + 2\ln 2 - \gamma - \frac{1}{2}\ln(1-(\underline{t}\cdot\underline{e})^2)} + \frac{2(\underline{e} - \underline{t}\cdot\underline{e}\,\underline{t})}{\ln R^{-1} + 2\ln 2 + \frac{1}{2} - \gamma - \frac{1}{2}\ln(1-(\underline{t}\cdot\underline{e})^2)}. \quad (3,112)$$

3.3.1.1 Noticeable Points on the above Equation of Force on Cylinder

- As was mentioned earlier, the dimensionless force per unit length on the cylinder $\underline{f}$ is independent of the length of cylinder l and the error associated with equation (3,112) is of order R, where $R \ll 1$.
- $\underline{f} \to \underline{0}$ as $R \to 0$, in other words, there is no solution for viscous flow, $R = 0$ (Stokes paradox).
- The equation (3,112) is valid so long as $\underline{t}\cdot\underline{e} \neq \pm 1$ (i.e. $\alpha \neq \pm\frac{\pi}{2}$) otherwise we get the term $\ln 0 = -\infty$ in the denominator of the fraction. This means that if the undisturbed velocity is in the direction of cylinder axis, the above equation will not help. However, when $-\frac{\pi}{2} < \alpha < \frac{\pi}{2}$, the equation is still correct and applicable.

Since the concentration of this research, in this regard, is on $\alpha = 0$ (undisturbed velocity is perpendicular to the cylinder axis), we have $\underline{t}\cdot\underline{e} = 0$ from now on. Thus the equation (3,112) becomes

$$\frac{f}{2\pi} = \frac{2}{\ln R^{-1} + 2\ln 2 + \frac{1}{2} - \gamma} + O(R), \quad (3,113)$$

which agrees with the result obtained by Khayat & Cox (1989). In this equation $R = \kappa Re = \frac{bU}{\nu}$, and the unit vector of velocity $\underline{e}$ does not appear in this equation. This is because $\underline{e}$ = (0, 1, 0), then the only non-zero component of force is in the2-direction. Therefore, the dimensionless force per unit length on the cylinder f in the equation (3.113) is automatically in the 2-direction.

Having obtained the force equation, we are now able to calculate the flow field ($\underline{u}$, p) around the cylinder. The universal solution valid everywhere is obtained by matching two different solutions for the outer and inner regions. Therefore, we first expand a solution for the outer region as follows.

3.3.2 Outer Region Solution for Flow Perpendicular to an Infinite Rod

In the outer region the dimensionless flow velocity $\underline{u}$ and the pressure p, based on the expansion over the parameter κ are generally the summation of uniform flow terms ($\underline{e}$, 0) and the terms related to the presence of cylinder in such a flow.

$$\left.\begin{aligned} \underline{u} &= \underline{e} + \underline{u}_1(\kappa) + \ldots, \\ p &= 0 + p_1(\kappa) + \ldots. \end{aligned}\right\} \tag{3.114}$$

where for the case of an infinite cylinder, the terms related to disturbance can be written as follows (see equations (3,24) and (3,28)).

$$\left.\begin{aligned} (u_1)_i &= \frac{1}{8\pi}\int_{-\infty}^{\infty} g_{ij}\left(\underline{r} - \underline{R}(\hat{s})\right) f_j^*(\hat{s})\, d\hat{s}, \\ p_1 &= \frac{1}{8\pi}\int_{-\infty}^{\infty} g_{ij}\frac{\left(r_j - R_j(\hat{s})\right)}{\left|\underline{r} - \underline{R}(\hat{s})\right|^3} f_j^*(\hat{s})\, d\hat{s}. \end{aligned}\right\} \tag{3.115}$$

Considering figure 3.12, we may define a unit vector along the undisturbed velocity $\underline{e}$, a unit vector along the cylinder axis $\underline{t}$, and a position vector in the outer region $\underline{r}$ as

$$\underline{e} = (0, 1, 0),$$
$$\underline{t} = (1, 0, 0),$$

$$\underline{r} = (0, \rho\cos\phi, \rho\sin\phi), \quad \text{and} \quad |\underline{r}| = \rho.$$

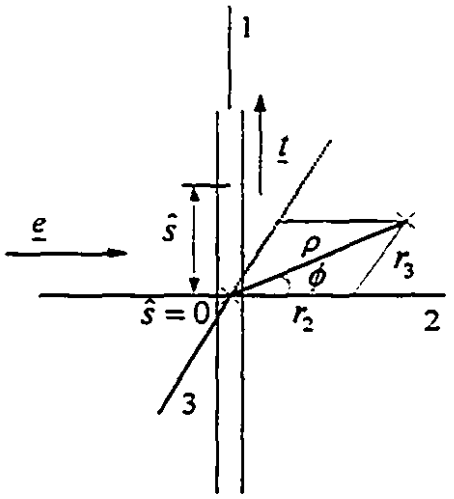

Figure 3.12 Cylinder and outer region variables

By symmetry, the only component of force per unit length on the cylinder $\underline{f}$, is in the 2-direction. Thus, we show it as f

$$\underline{f} = (0, f, 0),$$

and

$$\underline{R}(\hat{s}) = (\hat{s}, 0, 0),$$

then,

$$\underline{r} - \underline{R}(\hat{s}) = (-\hat{s}, \rho\cos\phi, \rho\sin\phi), \qquad |\underline{r} - \underline{R}(\hat{s})| = \sqrt{\rho^2 + \hat{s}^2},$$

$$\underline{e}.(\underline{r} - \underline{R}(\hat{s})) = \rho\cos\phi .$$

Thus,

$$\left\{|\underline{r} - \underline{R}(\hat{s})| - \underline{e}.(\underline{r} - \underline{R}(\hat{s}))\right\} = \sqrt{\rho^2 + \hat{s}^2} - \rho\cos\phi ,$$

$$\frac{\left(r_j - R_j(\hat{s})\right)}{\left|\underline{r} - \underline{R}(\hat{s})\right|^3} = \frac{1}{\sqrt{\rho^2 + \hat{s}^2}}\left(-\hat{s},\, \rho\cos\phi,\, \rho\sin\phi\right).$$

By symmetry, $(u_1)_1 = 0$, however

$$\left.\begin{aligned} (u_1)_2 &= -\frac{f}{8\pi}\int_{-\infty}^{\infty} g_{22}\left(\underline{r} - \underline{R}(\hat{s})\right) d\hat{s}, \\ (u_1)_3 &= -\frac{f}{8\pi}\int_{-\infty}^{\infty} g_{32}\left(\underline{r} - \underline{R}(\hat{s})\right) d\hat{s}, \\ p_1 &= -\frac{f}{8\pi}\int_{-\infty}^{\infty} \frac{\left(r_2 - R_2(\hat{s})\right)}{\left|\underline{r} - \underline{R}(\hat{s})\right|^3} d\hat{s}, \end{aligned}\right\} \qquad (3,116)$$

where in $(u_1)_i$, the first subscript corresponds to the first term of disturbance in equation (3,114), and the second subscript represents the direction of velocity. Since $f_1 = f_2 = 0$, we have only the component of $j = 2$ in equations (3,116).

For pressure p_1

$$p_1 = -\frac{f}{8\pi}\int_{-\infty}^{\infty} \frac{\rho\cos\phi}{\left(\rho^2 + \hat{s}^2\right)^{3/2}} d\hat{s}.$$

Letting $\hat{s} = \rho\tan\theta$,

$$p_1 = -\frac{f}{8\pi}\int_{-\pi/2}^{\pi/2} \frac{\rho\cos\phi \cdot \rho\sec^2\theta}{\rho^3\sec^3\theta}\, d\theta = -\frac{f}{8\pi}\frac{\cos\phi}{\rho}\int_{-\pi/2}^{\pi/2}\cos\theta\, d\theta,$$

gives us the pressure field for the outer region as

$$p_1 = -\frac{f}{4\pi}\rho^{-1}\cos\phi\,. \qquad (3,117)$$

For the velocity component $(u_1)_2$

$$(u_1)_2 = -\frac{f}{8\pi}\int_{-\infty}^{\infty} g_{22}\left(\underline{r} - \underline{R}(\hat{s})\right) d\hat{s},$$

where, by equation (3,92), g_{22} can be written as

$$g_{22}=\frac{2\left\{1-e^{1/2Re(\sqrt{\rho^2+\hat{s}^2}-\rho\cos\phi)}\right\}}{Re(\sqrt{\rho^2+\hat{s}^2}-\rho\cos\phi)^2}\left\{\left(\frac{\rho\cos\phi}{\sqrt{\rho^2+\hat{s}^2}}-1\right)^2-(\sqrt{\rho^2+\hat{s}^2}-\rho\cos\phi)\left(\frac{1}{\sqrt{\rho^2+\hat{s}^2}}-\frac{\rho^2\cos^2\phi}{(\rho^2+\hat{s}^2)^{3/2}}\right)\right\}$$

$$+\frac{e^{1/2Re(\sqrt{\rho^2+\hat{s}^2}-\rho\cos\phi)}}{(\sqrt{\rho^2+\hat{s}^2}-\rho\cos\phi)}\left\{\frac{2}{\sqrt{\rho^2+\hat{s}^2}}(\sqrt{\rho^2+\hat{s}^2}-\rho\cos\phi)-\left(\frac{\rho\cos\phi}{\sqrt{\rho^2+\hat{s}^2}}-1\right)^2\right\},$$

$$\Rightarrow$$

$$g_{22}=\frac{2\rho\cos\phi}{Re(\rho^2+\hat{s}^2)^{3/2}}+\left\{\frac{1}{\sqrt{\rho^2+\hat{s}^2}}+\frac{\rho\cos\phi}{(\rho^2+\hat{s}^2)}+\frac{2\rho\cos\phi}{Re(\rho^2+\hat{s}^2)^{3/2}}\right\}e^{1/2Re(\rho\cos\phi)}e^{-1/2Re(\sqrt{\rho^2+\hat{s}^2})}$$

Thus,

$$(u_1)_2=-\frac{f}{8\pi}\left[-\frac{2\rho\cos\phi}{Re}\int_{-\infty}^{\infty}\frac{d\hat{s}}{(\rho^2+\hat{s}^2)^{3/2}}+e^{1/2Re\rho\cos\phi}\int_{-\infty}^{\infty}\left\{\frac{1}{\sqrt{\rho^2+\hat{s}^2}}+\frac{\rho\cos\phi}{(\rho^2+\hat{s}^2)}+\frac{2\rho\cos\phi}{Re(\rho^2+\hat{s}^2)^{3/2}}\right\}e^{-1/2Re\sqrt{\rho^2+\hat{s}^2}}d\hat{s}\right].$$

By writing

$$\hat{s}=\rho\sinh t,\qquad d\hat{s}=\rho\cosh t\,dt,\qquad \sqrt{\rho^2+\hat{s}^2}=\rho\cosh t,$$

we have

$$\int_{-\infty}^{\infty}\frac{d\hat{s}}{(\rho^2+\hat{s}^2)^{3/2}}=\int_{-\infty}^{\infty}\frac{\rho\cosh t\,dt}{\rho^3\cosh^3 t}=\rho^{-2}\left[\tanh t\right]_{-\infty}^{\infty}=2\rho^{-2},$$

and

$$\int_{-\infty}^{\infty}\frac{e^{-1/2Re\sqrt{\rho^2+\hat{s}^2}}}{\sqrt{\rho^2+\hat{s}^2}}d\hat{s}=\int_{-\infty}^{\infty}\frac{e^{-1/2Re\rho\cosh t}\rho\cosh t\,dt}{\rho\cosh t}=\int_{-\infty}^{\infty}e^{-1/2Re\rho\cosh t}dt,$$

$$\int_{-\infty}^{\infty}\frac{e^{-1/2Re\sqrt{\rho^2+\hat{s}^2}}}{(\rho^2+\hat{s}^2)}d\hat{s}=\int_{-\infty}^{\infty}\frac{e^{-1/2Re\rho\cosh t}\rho\cosh t\,dt}{\rho^2\cosh^2 t}=\rho^{-1}\int_{-\infty}^{\infty}\frac{e^{-1/2Re\rho\cosh t}}{\cosh t}dt,$$

$$\int_{-\infty}^{\infty}\frac{e^{-1/2Re\sqrt{\rho^2+\hat{s}^2}}}{(\rho^2+\hat{s}^2)^{3/2}}d\hat{s}=\rho^{-2}\int_{-\infty}^{\infty}\frac{e^{-1/2Re\rho\cosh t}}{\cosh^2 t}dt.$$

Thus,

$$(u_1)_2 = -\frac{f}{8\pi}\left[-\frac{4\cos\phi}{Re\rho} + e^{1/2Re\rho\cos\phi}\int_{-\infty}^{\infty} e^{-1/2Re\rho\cosh t}\left\{1+\frac{\cos\phi}{\cosh t}+\frac{2\cos\phi}{Re\rho\cosh^2 t}\right\}dt\right].$$

But

$$\int_{-\infty}^{\infty}\frac{e^{-1/2Re\rho\cosh t}}{\cosh^2 t}dt = \int_{-\infty}^{\infty} e^{-1/2Re\rho\cosh t}\,\mathrm{sech}^2 t\,dt$$
$$= \frac{Re\rho}{2}\int_{-\infty}^{\infty} e^{-1/2Re\rho\cosh t}(\cosh t - \frac{1}{\cosh t})dt.$$

Substituting the above quantity into $(u_1)_2$ and simplifying, we will get

$$(u_1)_2 = \frac{f}{8\pi}\left[\frac{4\cos\phi}{Re\rho} - e^{1/2Re\rho\cos\phi}\int_{-\infty}^{\infty} e^{-1/2Re\rho\cosh t}\left(1+\cos\phi\cosh t\right)dt\right]. \qquad (3,118)$$

For the velocity component $(u_1)_3$

$$(u_1)_3 = -\frac{f}{8\pi}\int_{-\infty}^{\infty} g_{32}(\underline{r} - \underline{R}(\hat{s}))\,d\hat{s},$$

similarly, we can use the equation (3,92) to find g_{32}, and substitute it into the above equation. After simplifying,

$$g_{32} = -\frac{2\rho\sin\phi}{Re\left(\rho^2+\hat{s}^2\right)^{3/2}} + \left\{\frac{1}{\sqrt{\rho^2+\hat{s}^2}} + \frac{\rho\sin\phi}{\left(\rho^2+\hat{s}^2\right)} + \frac{2\rho\sin\phi}{Re\left(\rho^2+\hat{s}^2\right)^{3/2}}\right\}e^{1/2Re(\rho\cos\phi)}e^{-1/2Re\left(\sqrt{\rho^2+\hat{s}^2}\right)},$$

and $(u_1)_3$ becomes

$$(u_1)_3 = \frac{f}{8\pi}\left[\frac{4\sin\phi}{Re\rho} - e^{1/2Re\rho\cos\phi}\sin\phi\int_{-\infty}^{\infty} e^{-1/2Re\rho\cosh t}\cosh t\,dt\right]. \qquad (3,119)$$

To write these velocity components in polar components, we have

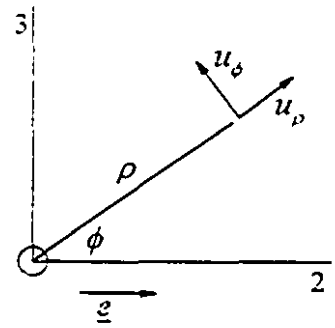

Figure 3.13 Outer region polar components of velocity

$$(u_1)_\rho = (u_1)_2 \cos\phi + (u_1)_3 \sin\phi$$
$$= \frac{f}{8\pi}\left\{\frac{4}{Re\,\rho} - e^{1/2Re\rho\cos\phi}\int_{-\infty}^{\infty}(\cos\phi + \cosh t)\,e^{-1/2Re\rho\cosh t}dt\right\}, \qquad (3,120)$$

and

$$(u_1)_\phi = -(u_1)_2 \sin\phi + (u_1)_3 \cos\phi$$
$$= \frac{f}{8\pi}\left\{\sin\phi\, e^{1/2Re\rho\cos\phi}\int_{-\infty}^{\infty} e^{-1/2Re\rho\cosh t}dt\right\}. \qquad (3,121)$$

However, the $K_\circ(z)$ modified Bessel function is

$$K_\circ(z) = \int_0^\infty e^{-z\cosh t}dt,$$

differentiating with respect to z

$$K_\circ'(z) = \int_0^\infty -\cosh t\, e^{-z\cosh t}dt,$$

thus,

$$\int_0^\infty \cosh t\, e^{-z\cosh t}dt = -K_\circ'(z) = +K_1'(z).$$

Therefore,

$$\int_{-\infty}^{\infty} e^{-z\cosh t}dt = 2\int_0^\infty e^{-z\cosh t}dt = 2K_\circ(z),$$

$$\int_{-\infty}^{\infty} \cosh t \, e^{z\cosh t} dt = 2\int_{0}^{\infty} \cosh t \, e^{z\cosh t} dt = 2K_1(z).$$

Thus,

$$\left.\begin{aligned}(u_1)_2 &= \frac{f}{8\pi}\left\{\frac{4\cos\phi}{Re\,\rho} - 2e^{1/2Re\rho\cos\phi}\left[K_0\left(\frac{1}{2}Re\,\rho\right) + \cos\phi\, K_1\left(\frac{1}{2}Re\,\rho\right)\right]\right\},\\ (u_1)_3 &= \frac{f}{8\pi}\left\{\frac{4\sin\phi}{Re\,\rho} - 2e^{1/2Re\rho\cos\phi}\sin\phi\, K_1\left(\frac{1}{2}Re\,\rho\right)\right\}.\end{aligned}\right\} \qquad (3,122)$$

or in polar components

$$\left.\begin{aligned}(u_1)_\rho &= \frac{f}{8\pi}\left\{\frac{4}{Re\,\rho} - 2e^{1/2Re\rho\cos\phi}\left[\cos\phi\, K_0\left(\frac{1}{2}Re\,\rho\right) + K_1\left(\frac{1}{2}Re\,\rho\right)\right]\right\},\\ (u_1)_\phi &= \frac{f}{8\pi}\left\{2\sin\phi\, e^{1/2Re\rho\cos\phi} K_0\left(\frac{1}{2}Re\,\rho\right)\right\}.\end{aligned}\right\} \qquad (3,123)$$

Thus, the complete dimensionless velocity in the outer region, in a Cartesian system, with polar variables (see equations (3,114)) is

$$\left.\begin{aligned}(u)_2 &= 1 + \frac{f}{8\pi}\left\{\frac{4\cos\phi}{Re\,\rho} - 2e^{1/2Re\rho\cos\phi}\left[K_0\left(\frac{1}{2}Re\,\rho\right) + \cos\phi\, K_1\left(\frac{1}{2}Re\,\rho\right)\right]\right\},\\ (u)_3 &= \frac{f}{8\pi}\left\{\frac{4\sin\phi}{Re\,\rho} - 2e^{1/2Re\rho\cos\phi}\sin\phi\, K_1\left(\frac{1}{2}Re\,\rho\right)\right\}.\end{aligned}\right\} \qquad (3,124)$$

Obviously, there is no velocity in the 1-direction. Now, we need to write the outer solution in terms of inner variables. We recall that $R = \frac{bU}{\nu} = \kappa\, Re << 1$. Since $\bar{\rho} = \kappa^{-1}\rho$, then,

$$Re\,\rho = Re\,\kappa\bar{\rho} = R\bar{\rho}, \quad \Rightarrow$$

$$\left.\begin{aligned}(u)_2 &= 1+\frac{f}{8\pi}\left\{\frac{4\cos\phi}{R\bar{\rho}}-2e^{1/2R\bar{\rho}\cos\phi}\left[K_0\left(\frac{1}{2}R\bar{\rho}\right)+\cos\phi\,K_1\left(\frac{1}{2}R\bar{\rho}\right)\right]\right\},\\ (u)_3 &= \frac{f}{8\pi}\left\{\frac{4\sin\phi}{R\bar{\rho}}-2e^{1/2R\bar{\rho}\cos\phi}\sin\phi\,K_1\left(\frac{1}{2}R\bar{\rho}\right)\right\}.\end{aligned}\right\} \tag{3,125}$$

Since the asymptotic expansion of modified Bessel functions are

$$\left.\begin{aligned}K_0(z) &\sim -\ln\left(\frac{1}{2}z\right)-\gamma+O(z^2\ln z),\\ K_1(z) &\sim z^{-1}+O(z\ln z),\end{aligned}\right\}$$

this value for $\bar{\rho}=O(1)$ with $R\to 0$ has the form

$$(u)_2 = 1+\frac{f}{8\pi}\left\{\frac{4\cos\phi}{R\bar{\rho}}-2\left(1+\frac{1}{2}R\bar{\rho}\cos\phi+\frac{1}{8}(R\bar{\rho}\cos\phi)^2+\ldots\right)\left[\left(-\ln\frac{1}{4}R\bar{\rho}-\gamma+\ldots\right)\cos\phi\left(\frac{2}{R\bar{\rho}}+\ldots\right)\right]\right\},$$

$$(u)_3 = \frac{f}{8\pi}\left\{\frac{4\sin\phi}{R\bar{\rho}}-2\left(1+\frac{1}{2}R\bar{\rho}\cos\phi+\frac{1}{8}(R\bar{\rho}\cos\phi)^2+\ldots\right)\sin\phi\left(\frac{2}{R\bar{\rho}}+\ldots\right)\right\}.$$

Thus,

$$\left.\begin{aligned}u_2 &\sim 1+\frac{f}{8\pi}\left\{+2\ln\frac{1}{4}R\bar{\rho}+2\gamma-2\cos^2\phi\right\}+\ldots,\\ u_3 &\sim \frac{f}{8\pi}\left\{-2\sin\phi\cos\phi\right\}+\ldots,\end{aligned}\right\} \tag{3,126}$$

or, in polar coordinates

$$u_r = u_z \cos\phi + u_s \sin\phi$$
$$= \cos\phi \left\{ 1 + \frac{f}{4\pi}\left[\ln R\bar{\rho} - 2\ln 2 + \gamma - 1\right]\right\} + \ldots,$$

and

$$u_\phi = -u_z \sin\phi + u_s \cos\phi$$
$$= \sin\phi \left\{ -1 + \frac{f}{4\pi}\left[-\ln R\bar{\rho} + 2\ln 2 - \gamma \right]\right\} + \ldots.$$

Applying equation (3,113) into the above equations,

$$\frac{f}{2\pi} = \frac{2}{\ln R^{-1} + 2\ln 2 + \frac{1}{2} - \gamma} + O(R),$$

$$u_\rho = \cos\phi \left[1 + \frac{\left(\ln R - 2\ln 2 + \gamma - 1\right) + \ln\bar{\rho}}{\left(-\ln R + 2\ln 2 - \gamma + 1/2\right)} \right] + \ldots$$
$$= \cos\phi \left[\frac{-1/2 + \ln\bar{\rho}}{\left(-\ln R + 2\ln 2 - \gamma + 1/2\right)} \right] + \ldots$$

$$\Rightarrow \quad u_\rho = \frac{f}{4\pi}\cos\phi \left(\ln\bar{\rho} - 1/2\right) + \ldots, \tag{3,127}$$

and similarly

$$u_\phi = \frac{f}{4\pi}\sin\phi \left(-\ln\bar{\rho} - 1/2\right) + \ldots. \tag{3,128}$$

3.3.3 Inner Region Solution for Flow Perpendicular to an Infinite Rod

We calculated outer region solutions, so far, both the actual outer solution (using outer variables) and the outer solution with inner variables. Now, in order to compare the outer solution with inner variables with the inner solution, we need to have the inner region solution too. By equation (3,74), we may write

$$\left.\begin{aligned} C(\kappa) &= \frac{1}{8\pi} f_2^* = -\frac{1}{8\pi} f_2 = -\frac{1}{8\pi} f \\ D(\kappa) &= \frac{1}{8\pi} f_1^* = -\frac{1}{8\pi} f_1 = 0 \\ E(\kappa) &= \frac{1}{8\pi} f_1^* = -\frac{1}{8\pi} f_1 = 0 \end{aligned}\right\}$$

So that the equations (3,15), taking $\lambda = 1$ for length scale = b, gives values of inner region solution as

$$\bar{u}_\rho = -\frac{f}{8\pi}\cos\phi\left(1-\bar{\rho}^{-2}-2\ln\bar{\rho}\right),$$

$$\bar{u}_\phi = -\frac{f}{8\pi}\sin\phi\left(1-\bar{\rho}^{-2}+2\ln\bar{\rho}\right),$$

or

$$\left.\begin{aligned} \bar{u}_\rho &= \frac{f}{4\pi}\cos\phi\left(\ln\bar{\rho}-1/2+1/2\,\bar{\rho}^{-2}\right), \\ \bar{u}_\phi &= \frac{f}{4\pi}\sin\phi\left(-\ln\bar{\rho}-1/2+1/2\,\bar{\rho}^{-2}\right). \end{aligned}\right\} \qquad (3,129)$$

3.3.4 Matching Inner and Outer Region Solutions

Comparing the inner region solution (3,129) with the outer region solution in inner variables (3,127) and (3,128), we see that the latter has terms $\frac{f}{4\pi}\cos\phi\left(1/2\,\bar{\rho}^{-2}\right)$ in $\bar{u}_\rho$ and $\frac{f}{4\pi}\sin\phi\left(1/2\,\bar{\rho}^{-2}\right)$ in u_ϕ missing. Thus the universal solution valid everywhere is obtained by adding these terms onto the outer region solution (these terms are proportional to $\bar{\rho}^{-2} = \kappa^2\rho^{-2}$ and are thus of order κ^2, so negligible, in the outer region). Since the complete outer region solution, using equation (3,124), in polar coordinates is

$$\left.\begin{aligned} u_\rho &= \cos\phi - \frac{f}{8\pi}\left\{\frac{4}{Re\,\rho} - 2e^{1/2Re\,\rho\cos\phi}\left[\cos\phi\,K_0\left(\frac{1}{2}Re\,\rho\right) + K_1\left(\frac{1}{2}Re\,\rho\right)\right]\right\}, \\ u_\phi &= -\sin\phi + \frac{f}{8\pi}\left\{2\sin\phi\, e^{1/2Re\,\rho\cos\phi}K_0\left(\frac{1}{2}Re\,\rho\right)\right\}, \end{aligned}\right\}$$

or in terms of inner variables

$$\left.\begin{aligned} u_\rho &= \cos\phi + \frac{f}{8\pi}\left\{\frac{4}{R\bar{\rho}} - 2e^{1/2R\bar{\rho}\cos\phi}\left[\cos\phi\,K_0\left(\frac{1}{2}R\bar{\rho}\right) + K_1\left(\frac{1}{2}R\bar{\rho}\right)\right]\right\}, \\ u_\phi &= -\sin\phi + \frac{f}{8\pi}\left\{2\sin\phi\, e^{1/2R\bar{\rho}\cos\phi}K_0\left(\frac{1}{2}R\bar{\rho}\right)\right\}, \end{aligned}\right\}$$

the universal solution, valid everywhere, in polar coordinates is

$$\left.\begin{aligned} u_\rho &= \cos\phi + \frac{f}{8\pi}\left\{\frac{4}{R\bar{\rho}} - 2e^{1/2R\bar{\rho}\cos\phi}\left[\cos\phi\,K_0\left(\frac{1}{2}R\bar{\rho}\right) + K_1\left(\frac{1}{2}R\bar{\rho}\right)\right] + \bar{\rho}^{-2}\cos\phi\right\}, \\ u_\phi &= -\sin\phi + \frac{f}{8\pi}\left\{2\sin\phi\, e^{1/2R\bar{\rho}\cos\phi}K_0\left(\frac{1}{2}R\bar{\rho}\right) + \bar{\rho}^{-2}\sin\phi\right\}, \end{aligned}\right\}$$

or

$$\left.\begin{aligned} u_\rho &= \cos\phi\left\{1 + \frac{f}{8\pi}\left[\bar{\rho}^{-2} - 2e^{1/2R\bar{\rho}\cos\phi}\,K_0\left(\frac{1}{2}R\bar{\rho}\right)\right]\right\} \\ &\quad + \frac{f}{8\pi}\left[\frac{4}{R\bar{\rho}} - 2e^{1/2R\bar{\rho}\cos\phi}K_1\left(\frac{1}{2}R\bar{\rho}\right)\right], \\ u_\phi &= \sin\phi\left\{-1 + \frac{f}{8\pi}\left[\bar{\rho}^{-2} + 2\,e^{1/2R\bar{\rho}\cos\phi}K_0\left(\frac{1}{2}R\bar{\rho}\right)\right]\right\}. \end{aligned}\right\}$$

In Cartesian coordinates, this is

$$u_2 = u_\rho\cos\phi - u_\phi\sin\phi$$

$$u_2 = 1 - \frac{f}{4\pi} e^{1/2R\bar{\rho}\cos\phi} K_0\left(\frac{1}{2}R\bar{\rho}\right) + \frac{f}{8\pi}\bar{\rho}^{-2}(\cos^2\phi - \sin^2\phi)$$
$$+ \cos\phi \frac{f}{4\pi}\left[\frac{2}{R\bar{\rho}} - e^{1/2R\bar{\rho}\cos\phi} K_1\left(\frac{1}{2}R\bar{\rho}\right)\right],$$

and

$$u_3 = u_\rho \sin\phi + u_\phi \cos\phi,$$

$$u_3 = \sin\phi\cos\phi \frac{f}{4\pi}\bar{\rho}^{-2} + \sin\phi \frac{f}{4\pi}\left[\frac{2}{R\bar{\rho}} - e^{1/2R\bar{\rho}\cos\phi} K_1\left(\frac{1}{2}R\bar{\rho}\right)\right].$$

Thus, the universal flow field in Cartesian coordinates is

$$\left.\begin{aligned} u_2 &= 1 - \frac{f}{4\pi} e^{1/2R\bar{\rho}\cos\phi} K_0\left(\frac{1}{2}R\bar{\rho}\right) + \frac{f}{8\pi}\bar{\rho}^{-2}(\cos 2\phi) \\ &\quad + \cos\phi \frac{f}{4\pi}\left[\frac{2}{R\bar{\rho}} - e^{1/2R\bar{\rho}\cos\phi} K_1\left(\frac{1}{2}R\bar{\rho}\right)\right], \\ u_3 &= \frac{f}{8\pi}\bar{\rho}^{-2}\sin 2\phi + \sin\phi \frac{f}{4\pi}\left[\frac{2}{R\bar{\rho}} - e^{1/2R\bar{\rho}\cos\phi} K_1\left(\frac{1}{2}R\bar{\rho}\right)\right]. \end{aligned}\right\} \quad (3,130)$$

In inner region the above equation (3,130) takes the form of equation (3,129) or

$$\bar{u}_2 = \bar{u}_\rho \cos\phi - \bar{u}_\phi \sin\phi = \frac{f}{4\pi}\ln\bar{\rho} + \frac{f}{4\pi}(-1/2 + 1/2\bar{\rho}^{-2})\cos 2\phi,$$
$$\bar{u}_3 = \bar{u}_\rho \sin\phi + \bar{u}_\phi \cos\phi = \frac{f}{8\pi}\sin 2\phi\,(-1 + \bar{\rho}^{-2}),$$

or the universal flow field can be also expressed as

$$\left.\begin{aligned} \bar{u}_2 &= \frac{f}{4\pi}\ln\bar{\rho} + \frac{f}{8\pi}(\bar{\rho}^{-2} - 1)\cos 2\phi, \\ \bar{u}_3 &= \frac{f}{8\pi}(\bar{\rho}^{-2} - 1)\sin 2\phi. \end{aligned}\right\} \quad (3,131)$$

We can write equation (3.130) in *dimensional form*, by multiplying it by uniform velocity field in infinity, U' (dimensional), and using $\bar{\rho} = \frac{\rho'}{b}$. Thus, the *dimensional* universal flow in Cartesian coordinates is

$$\left.\begin{aligned} u_2 &= U\left\{1 - \frac{f}{4\pi} e^{1/2R(\frac{\rho'}{b})\cos\phi} K_0\left(\frac{1}{2}R(\frac{\rho'}{b})\right) + \frac{f}{8\pi}(\frac{\rho'}{b})^{-2}(\cos 2\phi)\right. \\ &\quad \left. + \cos\phi \frac{f}{4\pi}\left[\frac{2}{R(\frac{\rho'}{b})} - e^{1/2R(\frac{\rho'}{b})\cos\phi} K_1\left(\frac{1}{2}R(\frac{\rho'}{b})\right)\right]\right\}, \\ u_3 &= U\left\{\frac{f}{8\pi}(\frac{\rho'}{b})^{-2}\sin 2\phi + \sin\phi \frac{f}{4\pi}\left[\frac{2}{R(\frac{\rho'}{b})} - e^{1/2R(\frac{\rho'}{b})\cos\phi} K_1\left(\frac{1}{2}R(\frac{\rho'}{b})\right)\right]\right\}. \end{aligned}\right\} \quad (3.132)$$

where

$$\frac{f}{2\pi} = \frac{2}{\ln R^{-1} + 2\ln 2 + \frac{1}{2} - \gamma} + O(R),$$

$$\gamma \cong 0.57722,$$

$$R = \kappa\, Re = \frac{bU}{\nu} << 1.$$

3.4 THE MOTION OF A TINY PARTICLE IN THE FLOW

Assume that we release a very small solid pollutant particle far from the cylinder, where $x_1' \cong -\infty$, (see figure 3.14) in a fluid flow with the velocity fields expressed by equations (3,132). In order to find collision efficiency of this particle onto the cylinder, we need to develop the governing equations on motion of such a particle. Let radius of particle be a and density of particle be ρ_p. Thus the mass of particle will be

$$m = (\frac{4}{3}\pi\ a^3\rho_p).$$

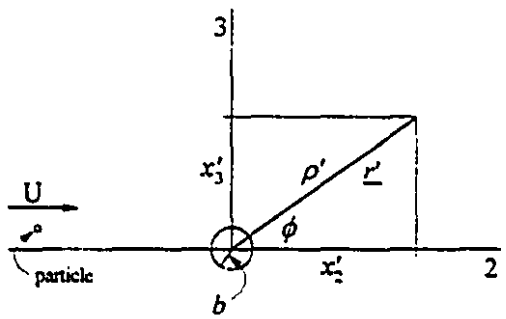

Figure 3.14 Motion of particle toward the cylinder

According to the Newton's second law of motion and by using the result of Stokes' problem

$$(\frac{4}{3}\pi\ a^3\rho_p)\ddot{\underline{r}}' = 6\pi\mu a\left(-\dot{\underline{r}}' + \underline{u}'(\underline{r}')\right),$$

or

$$(\frac{2}{9}a^2\frac{\rho_p}{\mu})\ddot{\underline{r}}' = -\dot{\underline{r}}' + \underline{u}'(\underline{r}'),$$

where $\ddot{\underline{r}}'$ is the second derivative of position vector $\underline{r}'$ in respect to time and $\underline{u}'(\underline{r}')$ is dimensional velocity field of fluid relative to the cylinder. Therefore, the term $\left(-\dot{\underline{r}}' + \underline{u}'(\underline{r}')\right)$ indicates the velocity of the fluid relative to the particle.

This is a vectorial equation and we can decompose it into its 2- and 3-components. We also can write the motion of particle in Cartesian coordinates, using velocity field obtained earlier, equations (3.132), and

$$\left|\underline{r'}\right| = \rho, \qquad \rho = \sqrt{x_2'^2 + x_3'^2},$$

$$\rho\cos\phi = x_2', \qquad \rho\sin\phi = x_3',$$
$$\cos 2\phi = \cos^2\phi - \sin^2\phi,$$
$$\sin 2\phi = 2\sin\phi\cos\phi.$$

Thus, taking x_2' and x_3' as the components of position vector $\underline{r'}$, we have for the 2-direction

$$\left(\frac{2}{9}a^2\frac{\rho_p}{\mu}\right)\ddot{x}_2' = -\dot{x}_2' + U\left[1 - \frac{f}{4\pi}e^{1/2R\frac{x_3'}{b}}K_0\left(\frac{1}{2}R\frac{\sqrt{x_2'^2 + x_3'^2}}{b}\right) + \frac{f}{8\pi}\frac{b^2}{\left(x_2'^2 + x_3'^2\right)^2}\left(x_2'^2 - x_3'^2\right)\right.$$
$$\left. + \frac{f}{4\pi}\frac{x_2'}{\sqrt{x_2'^2 + x_3'^2}}\left\{\frac{2b}{R\sqrt{x_2'^2 + x_3'^2}} - e^{1/2R\frac{x_3'}{b}}K_1\left(\frac{1}{2}R\frac{\sqrt{x_2'^2 + x_3'^2}}{b}\right)\right\}\right],$$

and for the 3-direction

$$\left(\frac{2}{9}a^2\frac{\rho_p}{\mu}\right)\ddot{x}_3' = -\dot{x}_3' + U\left[\frac{f}{4\pi}\frac{b^2 x_2' x_3'}{\left(x_2'^2 + x_3'^2\right)^2}\right.$$
$$\left. + \frac{f}{4\pi}\frac{x_3'}{\sqrt{x_2'^2 + x_3'^2}}\left\{\frac{2b}{R\sqrt{x_2'^2 + x_3'^2}} - e^{1/2R\frac{x_3'}{b}}K_1\left(\frac{1}{2}R\frac{\sqrt{x_2'^2 + x_3'^2}}{b}\right)\right\}\right].$$

Using dimensional values b and U, we can non-dimensionalize the above two equations, so that

$$x_2 = \frac{x_2'}{b}, \qquad x_3 = \frac{x_3'}{b},$$

and the dimensionless parameter t related to time

$$t = \frac{t'}{b/U} = \frac{U}{b}t',$$

thus, the universal non-dimensionalized equations of motion of particle toward the cylinder is expressed as

$$\left.\begin{aligned}
\mathrm{p}\frac{d^2x_2}{dt^2} &= -\frac{dx_2}{dt} + \left[1 - \frac{f}{4\pi}e^{1/2Rx_2}K_0\left(\frac{1}{2}R\sqrt{x_2^2+x_3^2}\right) + \frac{f}{8\pi}\frac{\left(x_2^2-x_3^2\right)}{\left(x_2^2+x_3^2\right)^2}\right.\\
&\qquad \left. + \frac{f}{4\pi}\frac{x_2}{\sqrt{x_2^2+x_3^2}}\left\{\frac{2}{R\sqrt{x_2^2+x_3^2}} - e^{1/2Rx_2}K_1\left(\frac{1}{2}R\sqrt{x_2^2+x_3^2}\right)\right\}\right],\\
\mathrm{p}\frac{d^2x_3}{dt^2} &= -\frac{dx_3}{dt} + \left[\frac{f}{4\pi}\frac{x_2x_3}{\left(x_2^2+x_3^2\right)^2}\right.\\
&\qquad \left. + \frac{f}{4\pi}\frac{x_3}{\sqrt{x_2^2+x_3^2}}\left\{\frac{2}{R\sqrt{x_2^2+x_3^2}} - e^{1/2Rx_2}K_1\left(\frac{1}{2}R\sqrt{x_2^2+x_3^2}\right)\right\}\right],
\end{aligned}\right\} \qquad (3,133)$$

where K_0 and K_1 are modified Bessel functions and p is dimensionless particle parameter and being defined as

$$\mathrm{p} = \frac{2a^2\rho_p U}{9\mu b}, \qquad (3,134)$$

and, as we have already had, Reynolds number and dimensionless force per unit length on cylinder are, respectively

$$R = \frac{bU}{\nu} << 1 \quad \text{and} \quad \frac{f}{2\pi} = \frac{2}{\ln R^{-1} + 2\ln 2 + \frac{1}{2} - \gamma}.$$

Finally, we obtained a pair of simultaneous non-linear, second-order ordinary differential equations (3,133), governing the motion of a tiny pollutant particle moving

toward an isolated cylinder with the trajectory direction initially perpendicular to the cylinder ($\alpha = 0$). The collision efficiency of a particle on the cylinder is to be calculated by simultaneously solving the equations (3.133), numerically. It is described in chapter 4.

3.5 EFFECTS NOT INCLUDED IN THIS THEORY

(a) Effect of finite (non-zero) size of particle. Nevertheless, to compensate, we may add the value of particles radius to the collision efficiency E presented in chapter five.

(b) When a particle gets close to the cylinder surface the hydrodynamic interaction of the particle with the cylinder surface will result in a change of trajectory [actually including (a) and (b) would result in $E = 0$].

(c) Intermolecular (van der Waals) forces and electrostatic forces between a particle and the cylinder or other colloidal forces. this is especially true for particle parameter $p \leq 0.05$.

(d) Possibility of different cases in impact of particle and cylinder. The particle may

1) bounce - no capture or

2) be captured at the surface.

(e) Effect of gravity on particle.

(f) Brownian motion of the particle (diffusion portion of motion). Diffusion may dominate over convection with very small particles.

(g) Shape of particle will modify many of the above effects.

Chapter 4

NUMERICAL SOLUTION

The collision efficiency E is to be calculated in the present research. The main part of the numerical calculations to obtain the collision efficiency is to find out the impact point of a particle on the cylinder for each pair of Reynolds number R and particle parameter p, if we release the particle far from the cylinder in the outer region. In this chapter we concentrate on the numerical method to solve the equations of motion of a particle to find the impact point for any pair of R and p. By definition, E is the area $(X_\infty' \times 1)$ divided by the area $(b \times 1)$, where 1 is the unit length in the direction of cylinder axis.

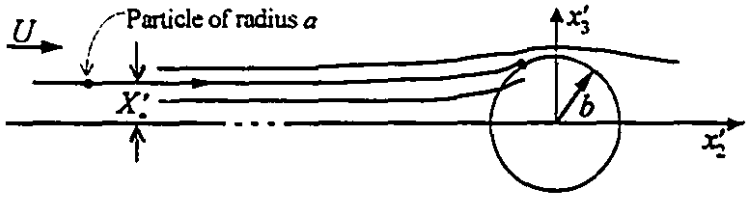

Figure 4.1 Cross-section of problem

In other words, the collision efficiency E, for each unit length of the cylinder, is the ratio of the largest amount of initial x_3' (shown as X_∞' in figure 4.1) over b so that if we release the particle at X_∞', it will cause an impact on the surface of the cylinder. Thus, for any particular R and p

$$E = \frac{X_\infty'}{b}, \quad \Rightarrow \quad E = X_\infty, \tag{4,1}$$

where X_∞ is the dimensionless initial x_3' (we recall that *unprimed* variables are dimensionless).

As was explained in chapter 3, equations (4,2) describe the motion of a particle with a trajectory direction perpendicular to the cylinder at infinity toward the cylinder. The equations (4,2) are a pair of simultaneous non-linear, second-order ordinary differential equations.

$$\left.\begin{aligned}
\mathrm{p}\frac{d^2x_2}{dt^2} &= -\frac{dx_2}{dt} + \left[1 - \frac{f}{4\pi}e^{1/2Rx_2}K_0\left(\frac{1}{2}R\sqrt{x_2^2+x_3^2}\right) + \frac{f}{8\pi}\frac{\left(x_2^2-x_3^2\right)}{\left(x_2^2+x_3^2\right)^2}\right.\\
&\qquad \left. + \frac{f}{4\pi}\frac{x_2}{\sqrt{x_2^2+x_3^2}}\left\{\frac{2}{R\sqrt{x_2^2+x_3^2}} - e^{1/2Rx_2}K_1\left(\frac{1}{2}R\sqrt{x_2^2+x_3^2}\right)\right\}\right],\\
\mathrm{p}\frac{d^2x_3}{dt^2} &= -\frac{dx_3}{dt} + \left[\frac{f}{4\pi}\frac{x_2x_3}{\left(x_2^2+x_3^2\right)^2}\right.\\
&\qquad \left. + \frac{f}{4\pi}\frac{x_3}{\sqrt{x_2^2+x_3^2}}\left\{\frac{2}{R\sqrt{x_2^2+x_3^2}} - e^{1/2Rx_2}K_1\left(\frac{1}{2}R\sqrt{x_2^2+x_3^2}\right)\right\}\right],
\end{aligned}\right\} \qquad (4,2)$$

where, as described earlier, K_0 and K_1 are modified Bessel functions and p is a dimensionless particle parameter, being defined as

$$\mathrm{p} = \frac{2a^2\rho_p U}{9\mu b}, \qquad (4,3)$$

also, Reynolds number and dimensionless force per unit length on cylinder are, respectively

$$R = \frac{bU}{\nu} << 1 \quad \text{and} \quad \frac{f}{2\pi} = \frac{2}{\ln R^{-1} + 2\ln 2 + \frac{1}{2} - \gamma}.$$

4.1 INITIAL VALUE PROBLEM

Since all variables are known at $x_2 = -\infty$, equations (4,2) are a kind of initial value problem and need to be solved numerically for more than three thousand times to create the desired results in the form of different graphs. In order to solve them we change this pair of simultaneous non-linear, second-order ordinary differential equations into four first-

order differential equations. Thus, we will have new variables as

DESCRIPTION	OLD VARIABLE	NEW VARIABLE
Dimensionless time (independent variable)	t	x
Dimensionless distance in 2-direction	x_2	y_2
Dimensionless distance in 3-direction	x_3	y_3
Dimensionless velocity in 2-direction	$\frac{dx_2}{dt}$	y_1
Dimensionless velocity in 3-direction	$\frac{dx_3}{dt}$	y_4

Table 4.1 Changing variables

Therefore, equations (4,2) become

$$\left.\begin{aligned}
\frac{dy_1}{dx} &= \left\{-y_1 + \left[1 - \frac{f}{4\pi} e^{1/2R y_2} K_0\left(\frac{1}{2}R\sqrt{y_2^2 + y_3^2}\right) + \frac{f}{8\pi}\frac{\left(y_2^2 - y_3^2\right)}{\left(y_2^2 + y_3^2\right)^2}\right.\right. \\
&\quad \left.\left. + \frac{f}{4\pi}\frac{y_2}{\sqrt{y_2^2 + y_3^2}}\left\{\frac{2}{R\sqrt{y_2^2 + y_3^2}} - e^{1/2R y_2} K_1\left(\frac{1}{2}R\sqrt{y_2^2 + y_3^2}\right)\right\}\right]\right\} / \mathrm{p}, \\
\frac{dy_2}{dx} &= y_1, \\
\frac{dy_3}{dx} &= y_4, \\
\frac{dy_4}{dx} &= \left\{-y_4 + \left[\frac{f}{4\pi}\frac{y_2 y_3}{\left(y_2^2 + y_3^2\right)^2}\right.\right. \\
&\quad \left.\left. + \frac{f}{4\pi}\frac{y_3}{\sqrt{y_2^2 + y_3^2}}\left\{\frac{2}{R\sqrt{y_2^2 + y_3^2}} - e^{1/2R y_2} K_1\left(\frac{1}{2}R\sqrt{y_2^2 + y_3^2}\right)\right\}\right]\right\} / \mathrm{p}.
\end{aligned}\right\} \qquad (4,4)$$

Now, we have a set of four simultaneous non-linear, first-order ordinary differential equations (4.4). As soon as we set up the initial values for this set of differential equations, we will be able to solve them.

Some of the initial values to be taken in the numerical solution are either given or can be arbitrarily chosen from a valid range. However, there are some values, like initial velocities in 2- and 3-dorections, which need more attention. In each trial, the above mentioned equations are solved by taking $0 <$ (*initial* y_3) <1, and *initial* y_2 as a negative large number (large enough to be considered quite in outer region). The Reynolds number based on radius b, R, and the particle parameter p are also chosen so that for every particular pair of R and p, we should find the corresponding *initial* y_3 at which if we release the particle in the outer region, it will finally collide with the cylinder. In other words, by trial and error, we should find a particular *initial* y_3 (for each pair of R and p) at which if we release the particle, the impact is guaranteed.

The important point here is that the impact point is not necessarily the top point of the cylinder where $x_3' = b$ (see figure 4.1), but it can be everywhere in $-b < x_3' \leq 0$ and $0 < x_3' \leq b$, otherwise it would be easier (no trial and error) to cover the distance vice versa (from right to left in figure 4.1).

In addition, since we can not start the program right from $x_2 = -\infty$ (where initial particle velocities are known), two initial velocities must be determined. It can be done by different methods discussed in the next section.

4.1.1 Calculation of Initial Particle Velocity

Even if the value to be taken for the initial particle velocity is not correct, it does not matter since the effect of is velocity is only local, affecting the particle motion only over distances of order $\frac{mU}{\mu a}$, m being the mass of the particle, U the uniform flow

velocity, a the radius of the particle, and μ the viscosity. However as we see in figure 4.2, if the velocity is not correct, the *initial* value of y_3 will not be correct either.

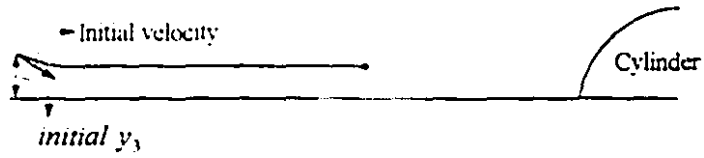

Figure 4.2 Initial velocity

To avoid this initial transient effect, one should take the initial particle velocity at infinity to be the fluid velocity at infinity. That is

$$\left(\frac{dy_2}{dt}, \frac{dy_3}{dt}\right) \to (1, 0) \quad \text{as } \textit{initial}\, x_2 \to -\infty.$$

For the numerical solution, however, one must take x_2 as finite. In this case one has three options.

1. Take the particle initial velocity as the fluid velocity at infinity.

$$\left(\frac{dy_2}{dt}, \frac{dy_3}{dt}\right) = (1, 0).$$

2. Take the particle velocity as the fluid velocity at the particle's initial position.
3. Take the position and velocity of the particle initially to be that calculated from the particle's motion from infinity to the distance *initial* x_2.

The other way to solve this initial transient effect problem is to use the results of a few steps after initial step in numerical solution where we get a smooth trajectory for the particle course. But we do not consider it as an option because we need to have control over E (or *initial* y_3). In any case, of these three possibilities, the third one would be the best. Thus, we follow this option.

The equations (3,125) can be used to describe the velocity field in the *outer region* with inner variables. We use inner variables only because $\overline{\rho}$ was non-dimensicnalized in

the same manner as x_2 and x_3 (by b). Dimensionalizing, by multiplying the velocity equations by U

$$\left.\begin{aligned}(u)_2 &= U\left[1+\frac{f}{8\pi}\left\{\frac{4\cos\phi}{R\bar{\rho}}-2e^{1/2R\bar{\rho}\cos\phi}\left[K_0\left(\frac{1}{2}R\bar{\rho}\right)+\cos\phi\,K_1\left(\frac{1}{2}R\bar{\rho}\right)\right]\right\}\right],\\ (u)_3 &= U\left[\frac{f}{8\pi}\left\{\frac{4\sin\phi}{R\bar{\rho}}-2e^{1/2R\bar{\rho}\cos\phi}\sin\phi\,K_1\left(\frac{1}{2}R\bar{\rho}\right)\right\}\right].\end{aligned}\right\} \quad (4.5)$$

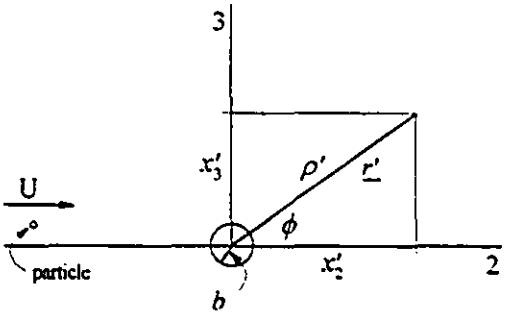

Figure 4.3 Dimensional variables

Since *initial* x_2 is a large negative number, $\phi \cong \pi$ and $\cos\phi \cong -1$, making the term $e^{1/2R\bar{\rho}\cos\phi} \cong 0$. Considering mass times acceleration for the particle in the outer region

$$(\frac{4}{3}\pi\, a^3\rho_p)\ddot{\underline{r}}' = 6\pi\,\mu\, a\left(-\dot{\underline{r}}' + \underline{u}'(\underline{r}')\right),$$

or

$$(\frac{2}{9}a^2\frac{\rho_p}{\mu})\ddot{\underline{r}}' = -\dot{\underline{r}}' + \underline{u}'(\underline{r}'), \quad (4,6)$$

where $\ddot{\underline{r}}'$ is the second derivative of position vector $\underline{r}'$ with respect to time and $\underline{u}'(\underline{r}')$ is the dimensional velocity field of fluid in the outer region relative to the cylinder. Therefore, the term $\left(-\dot{\underline{r}}' + \underline{u}'(\underline{r}')\right)$ indicates the velocity of fluid relative to the particle. Applying Cartesian variables in the outer region velocity equations and inserting them in equation (4,6),

$$\rho'\cos\phi = x_2', \qquad \rho'\sin\phi = x_3',$$

$$\overline{\rho} = \frac{\rho'}{b}, \quad \rho' = \left|\underline{r}'\right|, \quad \rho' = \sqrt{x_2'^2 + x_3'^2},$$

we will have

$$\left.\begin{aligned} \mathrm{p}'\,\ddot{x}_2' &= -\dot{x}_2' + U\left[1 + \frac{f}{2\pi}\frac{b\,x_2'}{R\left(x_2'^2 + x_3'^2\right)}\right], \\ \mathrm{p}'\,\ddot{x}_3' &= -\dot{x}_3' + U\left[\frac{f}{2\pi}\frac{b\,x_3'}{R\left(x_2'^2 + x_3'^2\right)}\right], \end{aligned}\right\} \tag{4.7}$$

where p′ is a dimensional particle parameter related to p by

$$\mathrm{p}' = \frac{2a^2\rho_p}{9\mu} = \mathrm{p}\,\frac{b}{U}.$$

Using dimensional values b and U, we can non-dimensionalize the above two equations, so that

$$x_2 = \frac{x_2'}{b}, \qquad x_3 = \frac{x_3'}{b},$$

and the dimensionless parameter t related to time

$$t = \frac{t'}{b/U} = \frac{U}{b}t',$$

using the chain rule, we have

$$\left.\begin{aligned} \mathrm{p}'\left(\frac{U^2}{b}\frac{d^2x_2}{dt^2}\right) &= -\frac{dx_2}{dt} + U\left[1 + \frac{f}{2\pi}\left(\frac{b^2\,x_2}{Rb^2\left(x_2^2 + x_3^2\right)}\right)\right], \\ \mathrm{p}'\left(\frac{U^2}{b}\frac{d^2x_3}{dt^2}\right) &= -\frac{dx_3}{dt} + U\left[\frac{f}{2\pi}\left(\frac{b^2\,x_3}{Rb^2\left(x_2^2 + x_3^2\right)}\right)\right], \end{aligned}\right\}$$

and finally considering

$$R x_3^2 << 1. \tag{4,8}$$

one can write the dimensionless particle's equations of motion in outer region as

$$\left.\begin{aligned} \mathrm{p}\left(\frac{d^2x_2}{dt^2}\right) &= -\frac{dx_2}{dt} + \left[1 + \frac{f}{2\pi R}\left(\frac{1}{x_2}\right)\right], \\ \mathrm{p}\left(\frac{d^2x_3}{dt^2}\right) &= -\frac{dx_3}{dt} + \left[\frac{f}{2\pi R}\left(\frac{x_3}{x_2^2}\right)\right]. \end{aligned}\right\} \tag{4,9}$$

On the other hand, we know that far enough in the outer region, where we need to find the initial velocities, the second derivatives in (4,9) can be taken zero (a linear expression for velocities). This is true for distances for which

$$R x_2 >> 1, \tag{4,10}$$

thus, dimensionless initial velocities, quite far in outer region, can be written as

$$\left.\begin{aligned} \frac{dx_2}{dt} &= 1 + \frac{f}{2\pi R}\left(\frac{1}{x_2}\right), \\ \frac{dx_3}{dt} &= \frac{f}{2\pi R}\left(\frac{x_3}{x_2^2}\right), \end{aligned}\right\} \tag{4,11}$$

where

$$R = \frac{bU}{\nu} << 1 \quad \text{and} \quad \frac{f}{2\pi} = \frac{2}{\ln R^{-1} + 2\ln 2 + \frac{1}{2} - \gamma}.$$

In 1994, using another analytical method, Professor R. G. Cox obtained the same results for initial velocities but in different directions. Those results have been applied in numerical calculations.

4.2 NUMERICAL METHOD

It is the nature of the boundary conditions and the behavior of the equations that determines which numerical methods will be feasible. Based on the needed accuracy, efficiency, and existing facilities one may choose a suitable method for the problem on hand. There are many different practical methods to solve a set of ODEs numerically. Neglecting conceptual methods like Euler's and Modified Euler's method and Taylor Series method, some popular and practical methods are briefly discussed here.

1. *Runge-Kutta* methods, named after two German mathematicians, Runge and Kutta, are very popular because they virtually always succeed. Instead of computing higher derivatives for the truncated Taylor series, they basically propagate a solution over an interval by combining the information from several Euler style steps and using the information obtained to match a Taylor Series expansion up to some higher order. Although these methods improved the efficiency of Taylor Series and Euler's methods considerably, they are usually good when moderate accuracy is required. Higher orders (the most popular Runge-Kutta are fourth and fifth-order while Euler's method is a special case of a second-order Runge-Kutta) and even adaptive stepsize control for Runge-Kutta are available. However, these single-step methods are used when (1) we have a trivial problem where computational efficiency is of no concern, or (2) we do not know any better, or (3) we have a problem where better methods are failing.

2. *Predictor-corrector* methods are a particular subcategory of multistep and multivalue methods. They store the solution along the way, and use the results to extrapolate the solution one step advanced; they then correct the extrapolation using derivative information at the new point. As a result, they need adequate memory space to run. These methods are good when a high precision solution is needed for very smooth functions with a very complicated right-hand side. The most popular predictor-corrector methods are probably the Adams-Bashforth-Moulton schemes which have very good stability properties.

3. *Richardson extrapolation* uses the powerful idea of extrapolating a computed result to the value that *would* have been obtained if the stepsize had been very much smaller than what it actually was. The first practical ODE integrator that implemented this idea was developed by Bulirsch and Stoer, and so extrapolation methods are often called Bulirsch-Stoer methods.

For high-precision applications or where evaluations of the right-hand sides are not expensive, Bulirsch-Stoer methods dominate. For convenience, or for low-precision, adaptive-stepsize Runge-Kutta dominates. Predictor-corrector methods are in the middle. They are suitable for the exceptional case of very smooth equations and very complicated right-hand sides when high-precision is needed. The trajectory course of a particle is very smooth as far as the particle is not close to the cylinder. But when the particle gets close to the cylinder, which is the most important part of our calculations, one can not guaranty that the equations remain as smooth as before. On the other hand, we need more accuracy than what we may get from Runge-kutta methods. This is because (1) the final results depend on the accuracy of the method *directly* and (2) *initial* y_2 is a very large negative number that means we have to calculate a very long course with numerous steps up until $y_2 = 0$ (the end of the course). That may cause an accumulation of truncation errors.

As a result, the use of the Bulirsch-Stoer method is preferred. In the next section, the basic theories behind this method are explained briefly.

4.2.1 Richardson Extrapolation and the Bulirsch-Stoer Method

The Bulirsch-Stoer method discussed in this section is at least one of the best known ways (if not the only one) to obtain high accuracy solutions to ordinary differential equations with minimal computational effort. Three ideas are put together in this method.

The first idea is a very general idea called *Richardson's deferred approach to the limit*: perform some numerical algorithm for various values of a parameter h, and then extrapolate the result to the continuum limit $h = 0$. In other words, the idea is to consider

the final answer of the numerical calculation as itself being an analytic function of an adjustable parameter like the substep-size h. Performing the calculation with various values of h, the analytic function, then, can be evaluated. The point is that none of the values of h needs to be small enough to yield the accuracy that we desire. Gathering information about the function through different numbers of substeps, we *fit* it to some analytic form and then evaluate it at the optimal point $h = 0$. As shown in figure 4.4, a large stepsize H is divided into different sequences of finer and finer substeps. Their results are extrapolated to an answer that is supposed to correspond to infinitely fine substeps.

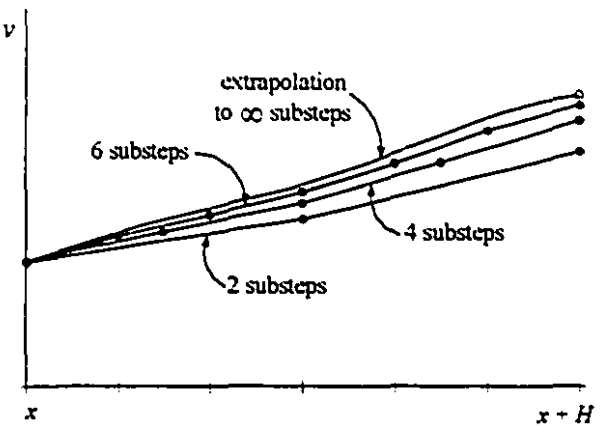

Figure 4.4 Richardson extrapolation

The second issue is that what kind of fitting function is used. Bulirsch and Stoer first recognized the strength of *rational function extrapolation* in Richardson type applications. But more recent experience suggests that for smooth problems straightforward *polynomial extrapolation*, using Neville's algorithm[1] (not Lagrange's classical formula) that gives error estimate as well, is slightly more efficient than rational function extrapolation. Neville's algorithm generates a tableau form of P's (the value at x of the unique polynomials of various degrees) to derive the corrections that make the extrapolation one order higher.

[1] A complete explanation of Neville's method can be found in many books in the field of Applied Numerical Analysis.

In fact, Neville's algorithm is a recursive way of filling in the numbers in the tableau a column at a time. Keeping track of the small differences between elements of each column and the next column of the tableau, at each level m (for m = 1,2,...,N-1 and N being the number of points) one can compute the corrections due to higher order extrapolations and repeat it until no further considerable gain is obtained with regard to roundoff errors. The final answer $P_{1\ N}$ (or y), is the sum of any y_i (an arbitrary element of the first column of the tableau) plus a set of corrections that form a path to the rightmost element. We will accordingly use polynomial extrapolation as a fitting function in our program. The corresponding routine is called `pzextr` (see Appendix A).

The third idea is to use a method which error function is strictly even, allowing the polynomial extrapolation to be in terms of the variable h^2 instead of just h. For this purpose, the *modified midpoint method* is used to advance a vector of dependent variables $y(x)$ from a point x to a point $x + H$ by a sequence of n substeps each of size h.

$$h = \frac{H}{n}.$$

Basically, the modified midpoint method is itself an ODE integrator. In practice, the method finds its most important application as a part of the more powerful Bulirsch-Stoer technique. The number of right-hand side evaluations required by the modified midpoint method is $n + 1$. The relationships are

$$\begin{aligned} z_0 &\equiv y(x) \\ z_1 &= z_0 + h f(x, z_0) \\ z_{m+1} &= z_{m-1} + 2h f(x + mh, z_m) \quad \text{for} \quad m = 1, 2, \ldots, n-1, \end{aligned}$$

and

$$y(x + H) \approx y_n \equiv \frac{1}{2}\left[z_n + z_{n-1} + h f(x + H, z_n)\right], \tag{4,12}$$

where z's are intermediate approximations which march along in substeps of h, and y_n is the final approximation to $y(x + H)$. The method is basically a "centered difference" or "midpoint" method, except at the first and last points which give the qualifier "modified".

The modified midpoint method is a second-order method but with the advantage of requiring (asymptotically for large n) only one derivative evaluation per substep h instead of the two required by the second-order Runge-Kutta method, for instance.

The usefulness of the modified midpoint method to the Bulirsch-Stoer technique derives from a result about equation (4.12). It turns out that the error of this equation, expressed as a power series in h, contains only *even* powers of h,

$$y_n - y(x+H) = \sum_{i=1}^{\infty} \alpha_i h^{2i},$$

where H is taken as a constant but h changes by varying n in $h = H/n$. Obtaining an even power series is important because one can combine substeps to eliminate higher-order error terms. For example, suppose n is even and let $y_{n/2}$ denote the result of (4,12) with half as many substeps ($n \to n/2$). Then the estimate

$$y(x+H) \approx \frac{4y_n - y_{n/2}}{3} \tag{4.13}$$

is fourth-order accurate, the same as fourth-order Runge-Kutta, but requires only about 1.5 derivative evaluations per substep h instead of Runge-Kutta's four evaluations. Nevertheless, the result of one full step H is considerably improved by using the Richardson extrapolation. Thus, a single Bulirsch-Stoer step takes us from x (any dimensionless time point) to $x + H$, where H is supposed to be quite a large number. That single step is a grand leap consisting of many (dozens to hundreds) substeps of the modified midpoint method, which are then extrapolated to zero stepsize. This is very useful when we have, for instance, for $R = 10^{-4}$, *initial* y_2 = -500,000. Otherwise we need much more time to get the results of the computations. We recall that, for initial values, we should keep $R\,x_2 >> 1$, or in new variables *initial* $y_2 >> R^{-1}$. A value of -50 R^{-1} is used for *initial* y_2 when R is from 10^{-6} to 10^{-3} and -100 R^{-1} is used in the case of larger R's to make sure the starting point is far in the outer region.

The sequence of separate attempts to cross the interval H is made with increasing values of n, the number of substeps. Bulirsch and Stoer originally proposed the sequence

$$n = 2,4,6,8,12,16,24,32,48,64,96,\ldots,[n_j = 2n_{j-2}],\ldots$$

Then the sequence was improved to the more efficient one as

$$n = 2,4,6,8,10,12,14,16,\ldots,[n_j = 2j],\ldots \qquad (4,14)$$

We do not know, in advance, for each step how far up this sequence we will go. After each successive n is tried, a polynomial extrapolation is attempted. That extrapolation returns both extrapolated values and error estimates. If the errors are not satisfactory, a higher n is chosen. When they are satisfactory, the next step is started with a new $n = 2$.

There must be some upper limit, beyond which we conclude that there is some obstacle in our path in the interval H, so that we should reduce H rather than just subdivide it more finely. The maximum number of n's to be tried is taken equal to 8; the 8^{th} value of the sequence (4,14) is 16, so this is the maximum number of subdivision H that is used. This is because, generally, there is very little further gain in efficiency whereas roundoff can become a problem.

Error control is enforced by monitoring internal consistency, and adapting the stepsize to match a bound on the local truncation error. Each new result from the sequence of a modified midpoint integration (a new y for a new n) allows a tableau like the Neville's algorithm tableau to be extended by one additional set of diagonals. The size of the new correction added at each stage (dy) is taken as the (conservative) error estimate. This error estimate is used to adjust the stepsize. Moreover, by implementation of different ε's (values of the required tolerance for each step) and comparing the final results of programs we made sure that the accuracy control is met. It is discussed in the next chapter.

Chapter 5

IMPLEMENTATION, RESULTS, AND DISCUSSION

Applying a computer program, written based on Bulirsch-Stoer method, to solve the set of four simultaneous non-linear, first-order ordinary differential equations (4.4), obtained in chapter 4, presenting the results, and discussing them are the issues under consideration in this chapter. The purpose of the numerical calculation is to obtain the *collision efficiency* of a particle onto the cylinder for various Reynolds numbers R and particle parameters p.

We recall that the motion of particle toward the cylinder is described by

$$\left.\begin{aligned}
\frac{dy_1}{dx} &= \left\{ -y_1 + \left[1 - \frac{f}{4\pi} e^{1/2R y_2} K_0\left(\frac{1}{2}R\sqrt{y_2^2+y_3^2}\right) + \frac{f}{8\pi}\frac{(y_2^2-y_3^2)}{(y_2^2+y_3^2)^2} \right.\right. \\
&\qquad \left.\left. + \frac{f}{4\pi}\frac{y_2}{\sqrt{y_2^2+y_3^2}}\left\{ \frac{2}{R\sqrt{y_2^2+y_3^2}} - e^{1/2R y_2} K_1\left(\frac{1}{2}R\sqrt{y_2^2+y_3^2}\right)\right\}\right]\right\} / \mathrm{p}, \\
\frac{dy_2}{dx} &= y_1, \\
\frac{dy_3}{dx} &= y_4, \\
\frac{dy_4}{dx} &= \left\{ -y_4 + \left[\frac{f}{4\pi}\frac{y_2 y_3}{(y_2^2+y_3^2)^2} \right.\right. \\
&\qquad \left.\left. + \frac{f}{4\pi}\frac{y_3}{\sqrt{y_2^2+y_3^2}}\left\{ \frac{2}{R\sqrt{y_2^2+y_3^2}} - e^{1/2R y_2} K_1\left(\frac{1}{2}R\sqrt{y_2^2+y_3^2}\right)\right\}\right]\right\} / \mathrm{p}.
\end{aligned}\right\} \qquad (5.1)$$

In this set of differential equations, y_2 and y_3 are dimensionless initial velocities in 2- and 3-directions, respectively. Using new variables from table 4.1, we get these velocities, from equations (4.11), as

$$\left.\begin{aligned} \frac{dy_2}{dx} &= 1 + \frac{f}{2\pi R}\left(\frac{1}{y_2}\right), \\ \frac{dy_3}{dx} &= \frac{f}{2\pi R}\left(\frac{y_3}{y_2^3}\right), \end{aligned}\right\} \tag{5.2}$$

where

$$R = \frac{bU}{\nu} << 1 \quad \text{and} \quad \frac{f}{2\pi} = \frac{2}{\ln R^{-1} + 2\ln 2 + \frac{1}{2} - \gamma},$$

and under the conditions

$$R\,x_2 >> 1, \quad \text{or in new variables} \quad \textit{initial}\ y_2 >> R^{-1}, \tag{5.3}$$

and

$$0 < \textit{initial}\ y_3 < 1. \tag{5.4}$$

It is important to notice that, in the development of the equations of motion of the particle (3.133), the cylinder was considered as a line force so that the disturbance effects due to the presence of the cylinder in the flow field were taken into account without considering its physical appearance. This approach is necessary to solve the problem in an easier way.

5.1 NUMERICAL SOLUTION CONCEPTS

In order to get a clear idea of what has been done in regard with the numerical solution, the procedure of numerical calculations and the ideas behind them is discussed here conceptually. The collision efficiency E based on equation (4,1),in new variables, is

$$E = Y_*, \tag{5.5}$$

where Y_* is the largest value of *initial* y_3 which can cause an impact of the particle onto the cylinder (see figure 5.1)

In the case that the height of the initial position of the particle from the equatorial plane (*initial* y_3) is greater than Y_*, the particle will miss the cylinder. If it is less than Y_*, the particle passes through the cylinder (certainly has an impact if the presence of the cylinder is considered) and if *initial* y_3 is equal to some Y_*, the particle just and only just touches the surface of the cylinder. Thus, $E = Y_*$ is the point we are interested in and can be found by trial and error.

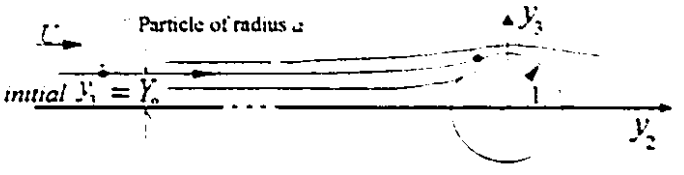

Figure 5.1 Particle's trajectory and new variables

Consider the case of Reynolds number $R = 10^{-3}$, particle parameter $p = 10^3$, and (far enough in the outer region) *initial* $y_3 = -50000$. In order to find the collision efficiency E for these given conditions, the first trial for Y_* is assumed to be *initial* $y_3 = 0.65$. In the region where $y_2 \leq 1$, for each step of the program, the radial distance of the particle from origin is calculated and the minimum amount of these radial distances in all steps of this trial is kept in a memory (the stepsize of the program is controlled so that we have about 850 steps for the distance $0 \leq y_2 \leq 1$).

If the minimum radial distance is less than one, the *initial* y_3 must be increased and if it is greater than one the *initial* y_3 must be decreased. The calculation of the trajectory course must be repeated with a new *initial* y_3 until the minimum radial distance is close enough to one (in the implemented program only minimum radial distances ≥ 0.9996 that are ≤ 1.00039 are accepted). The result is Y_* (collision efficiency E) for the above

mentioned given conditions and represents only one point on a curve you will see later in this chapter

Changing the particle parameter p and finding another E, by trial and error, for these new conditions, another point of a curve is found. Therefore, each curve corresponds to only one Reynolds number R and many different p's. We continue this process with a new Reynolds number R and various p's to get enough results to draw the corresponding curve and the like for another R...

5.2 OPTIMIZING THE SOLUTION

The computer run time required to finish only one point on a curve (one R and one p) varies between about one minute for the best conditions (when p is a large number, like 100 or higher, or R is not too small, like 10^{-4} or higher) and about ten hours for the worst conditions (when p is less than 100 and R is less than 10^{-4})[1]. If we consider an average of two hours for each point to be calculated, having more than 150 points for seven curves to be investigated, we need more than 300 hours of pure run time to calculate all points. This is excluding the time needed to check out and debug the program and subroutines and rerun the program with a different error tolerance ε in order to compare the output to get a reliable result which is usually much more time consuming.

In other words, if we use a computer 10 hours a day (not normally available), we need more than a month of just calculating the final results. That is why optimizing is a matter of concern. We used different levels of optimization. On the first level, a suitable numerical method for the problem in hand must be chosen. Richardson extrapolation with Bulirsch-Stoer method is a quite powerful and efficient method for our purpose. The second level, is to optimize the FORTRAN language commands throughout the program

---

[1] These results are mainly from a PC 486DX2/66. Sun System's results can not be compared directly to theses results because Sun uses a standard multitasking (multiprogramming) environment in which tasks share the CPU by switching processing between the tasks very rapidly. However, the overall results on Sun System was not only somewhat faster, but also the accuracy and the ability to deal with very small numbers (underflow errors) was considerably better.

and also to write special commands to stop the program when something unexpected or wrong occurs. The third level, is to minimize the numbers of trial and errors by choosing a proper method and a start point for *initial* y_3.

When we have absolutely no idea about the position of Y, the Bisection method is the best one to use. However, when we know that, for instance, Y must be greater or less than Y of the last calculated point, the Goldensection method is preferable.[2] Therefore, a good start and a proper method can save a great deal of time.

5.3 ERROR CONTROL

There are several sources of error in a numerical calculation in addition to the truncation error. Here, we discuss different sources of error very briefly.

1. *Original Data Errors* are due to initial conditions. When initial conditions are not known exactly, the solution will be effected to a greater or lesser degree, depending on the sensitivity of the equations. To reduce this kind of error, we calculate the initial velocities analytically in chapter 4. This is actually the best we could do. However, since there have been some assumptions and simplifications in this analytical probe, the result is not perfect.

2. *Round-Off Errors* are related to the finite number of decimal places in computations. No matter whether we round or chop off, there is always error dealing with real quantities. Carrying more decimal places in the intermediate calculations than we require in the final answer is the normal practice to minimize this, but in lengthy calculation this is a source of error that is extremely difficult to analyze and control. Furthermore, in a computer program, if we use double precision, we require a longer execution time and also more storage to hold the more precise values. This type of

---

[2] In Goldensection method the dividing proportions are 0.618 and 0.382 (instead of 1.0 and 0.5 in Bisection method).

error is especially acute when two nearly equal quantities are subtracted. This was actually the case for very small Reynolds numbers with small particle parameters. *Underflow* and *divided by zero* were the most common errors in such cases. To avoid these errors, double precision on a Sun System was used. Moreover, reducing the volume of computations by controlling the stepsize is one of the best ways to reduce round-off errors. Since this was discussed at the end of chapter 4, we do not repeat it here.

3. *Truncation Errors of the Method* are due to the use of truncated series for approximation in our work. In other words, the truncation error is because of the approximate nature of the numerical method. The best control is the choice of method. Richardson extrapolation and Bulirsch-Stoer method, explained in chapter 4, were the answer to this problem.

Despite all these discussions, one needs a sort of reliable and understandable way to trust the outcome of numerical calculations. Since there is not experimental nor analytical data to compare our results, the best way is to vary the local truncation error ε and check the solutions and accept only the solutions exhibiting a relative difference less than some desirable value. Although we can only show the values of collision efficiency on our graphs up to two decimal points, we accept only the solutions with a relative difference less than 10^{-3} for the worst conditions. This corresponds to a local truncation error $\varepsilon = 10^{-5}$ and guarantees even a higher accuracy for other most cases.

5.4 NUMERICAL RESULTS

Presenting the results of numerical calculations is done in two forms—tables and graphs. Each table which is the output of computer calculations, corresponds to only one Reynolds number but several particle parameters. At the beginning of each table the relevant conditions are introduced and then a summary of the important values of the results is printed out.

THIS IS THE RESULT OF THE PROGRAM MAIN7: ONE "R",
FOR THE FOLLOWING CONDITIONS:

R= 1.00000E-06
EPS= 1.00000E-05
Initial Y(2) = YSTART(2) = -5.00000E-07

THE RESULTS

dY(2)/dt = Y(1) = YSTART(1) = 0.997365

I	Trial(J)	Min.Hyptns.	Prtclp.	E=Yo	Ln(Prtclp)
1	2	0.99989	30000000.0	0.99618	17.2167
2	5	0.99997	22000000.0	0.98387	16.9065
3	11	0.99993	10000000.0	0.96205	16.1181
4	9	0.99999	2000000.0	0.89543	14.5087
5	9	0.99971	300000.0	0.76573	12.6115
6	9	0.99962	60000.0	0.64431	11.0021
7	5	1.00026	20000.0	0.56236	9.90349
8	13	0.99999	15000.0	0.54062	9.61581
9	11	0.99965	10000.0	0.51001	9.21034
10	14	0.99995	6000.0	0.47173	8.69951
11	11	0.99966	3000.0	0.41910	8.00637
12	12	1.00038	1500.0	0.36620	7.31322
13	7	0.99966	1000.0	0.33441	6.90776
14	11	0.99966	800.0	0.31696	6.68461
15	11	0.99990	500.0	0.27987	6.21461
16	12	1.00006	350.0	0.25136	5.85793
17	14	0.99978	220.0	0.21346	5.39363
18	13	0.99967	120.0	0.16355	4.78749
19	12	0.99988	80.0	0.12984	4.38203
20	12	0.99985	50.0	0.09082	3.91202
21	11	0.99963	30.0	0.04998	3.40120
22	8	0.99982	20.0	0.01763	2.99573
23	14	1.00012	15.0	0.00001	2.70805
24	2	1.00104	10.0	0.00000	2.30259

Table 5.1 Results for Reynolds number $R = 10^{-6}$

The first column of each table (I) is a counter, indicating the number of rows that is the number of points on the related graph. The second column (Trial(J)) is the number of trials to find Y_* for the corresponding particle parameter (Prtclp), in column four. The third column (Min.Hyptns) shows the minimum hypotenuse (radial distance from origin) of the last trial of the row. This number must be close enough to *one* (the dimensionless size of the cylinder radius) in order to accept the collision efficiency (E=Y_o)[3],

[3] Or X_* in old variables

in column five. The last column (Ln. Prtclp) is the natural logarithm of column four.

The number of computed steps in some trials like for $R = 10^{-1}$ and p = 10, is about one million while for cases like $R = 10^{-2}$ and p = 20,000 it is about 350 steps (it does not include the substeps in the Richardson extrapolation). This is because of the role of p in our differential equations and also the smaller R the larger the absolute value of *initial* y_2.

```
THIS IS THE RESULT OF THE PROGRAM MAIN7: ONE "R",
          FOR THE FOLLOWING CONDITIONS:

                R=    1.000000E-02
              EPS=    1.000000E-05
   Initial Y(2) = YSTART(2) =  -10000.000000

                      THE  RESULTS
-------------------------------------------------------

      dY(2)/dt = Y(1) = YSTART(1) =  0.9966183

 I Trial(J) Min.Hyptns.    Prtclp.    E=Yo     Ln(Prtclp)
-------------------------------------------------------
 1     18      0.99716      50000.0   0.99999   10.81978
 2     11      0.99970      20000.0   0.98877    9.90349
 3     13      1.00025      15000.0   0.98567    9.61581
 4     11      0.99967      10000.0   0.97991    9.21034
 5     12      1.00016       6000.0   0.97251    8.69951
 6     11      1.00007       3000.0   0.95552    8.00637
 7      9      1.00039       1500.0   0.92611    7.31322
 8     12      1.00036       1000.0   0.90054    6.90776
 9      9      1.00039        800.0   0.88355    6.68461
10     12      1.00012        500.0   0.83980    6.21461
11     10      0.99973        350.0   0.79887    5.85793
12     10      0.99992        220.0   0.73575    5.39363
13     12      1.00001        120.0   0.63581    4.78749
14     10      1.00034         80.0   0.55925    4.38203
15     10      0.99970         50.0   0.46213    3.91202
16     10      0.99969         30.0   0.35067    3.40120
17     10      0.99984         22.0   0.28179    3.09104
18     11      1.00015         14.0   0.18303    2.63906
19     11      0.99978          9.0   0.09285    2.19722
20      8      0.99965          7.0   0.04678    1.94591
21     14      0.99964          5.0   0.01331    1.60944
22     16      1.00027          3.0   0.00463    1.09861
23     15      0.99992          2.7   0.00409    1.00001
24     16      1.00004          1.5   0.00243    0.40547
25     16      0.99998          1.0   0.00196    0.00000
26     17      0.99965          0.5   0.00157   -0.69315
```

Table 5.2 Results for Reynolds number $R = 10^{-2}$

Here, we only show the tables for three Reynolds numbers ($R = 10^{6}$, 10^{2}, and $R = 1.0$), the others are presented in Appendix A.

Although $R = 1.0$ is not a valid case, based on our assumptions $R \gg 1$, to investigate the behavior of the solution, we present the related results here and discuss it later.

```
THIS IS THE RESULT OF THE PROGRAM MAIN7: ONE "R",
          FOR THE FOLLOWING CONDITIONS:

                    R=     1.00000
                 EPS=     1.00000E-05
      Initial Y(2) = YSTART(2) =    -5000.00

                      THE  RESULTS
 ------------------------------------------------------

      dY(2)/dt = Y(1) = YSTART(1) =  0.999694
```

I	Trial(J)	Min.Hyptns.	Prtclp.	E=Yo	Ln(Prtclp)
1	15	0.99979	20000.0	0.99927	9.90349
2	14	0.99981	15000.0	0.99881	9.61581
3	13	0.99977	10000.0	0.99808	9.21034
4	14	0.99990	6000.0	0.99735	8.69951
5	13	0.99985	3000.0	0.99571	8.00637
6	12	1.00006	1500.0	0.99306	7.31322
7	12	0.99975	1000.0	0.98996	6.90776
8	13	0.99987	800.0	0.98804	6.68461
9	12	1.00020	500.0	0.98256	6.21461
10	13	0.99985	350.0	0.97607	5.85793
11	14	0.99968	220.0	0.96484	5.39363
12	13	0.99978	120.0	0.94310	4.78749
13	13	1.00007	80.0	0.92228	4.38203
14	7	0.99961	50.0	0.88857	3.91202
15	11	1.00022	30.0	0.83906	3.40120
16	9	0.99961	22.0	0.79960	3.09104
17	6	0.99967	14.0	0.72954	2.63906
18	10	0.99979	9.0	0.64484	2.19722
19	8	0.99980	5.0	0.50973	1.60944
20	13	1.00018	2.7	0.35835	1.00001
21	11	1.00014	1.5	0.23419	0.40547
22	14	0.99989	1.0	0.17947	0.00000
23	12	1.00022	0.5	0.13204	-0.69315
24	9	1.00002	0.2	0.10838	-1.60944
25	13	1.00010	0.1	0.10126	-2.30259
26	11	1.00015	0.05	0.09779	-2.99573

Table 5.3 Results for Reynolds number $R = 1.0$

Using the data from the tables in semi-logarithmic graphs, the results can be presented as the following figures. Only columns four and five are used to draw the graphs

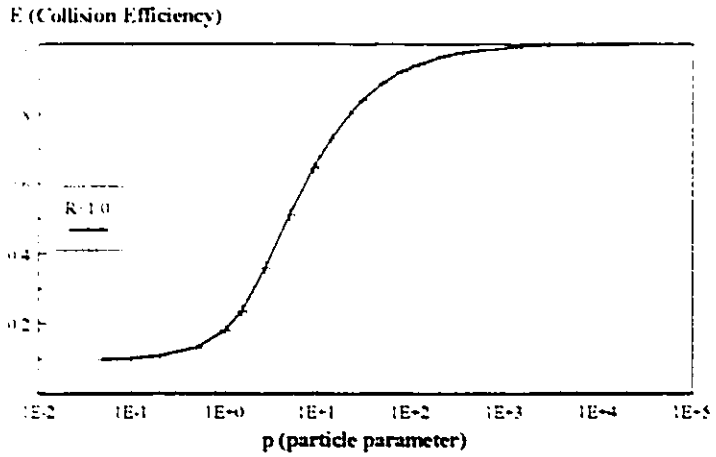

Figure 5.2 Collision efficiency for Reynolds number $R = 1.0$

As shown in figure 5.2, we use a logarithmic scale for the values of particle parameter p (for its large changes) and a linear scale for the collision efficiency $E = Y_c$.

If the data related to the Reynolds number $R = 0.1$ is used, the outcome is the following graph.

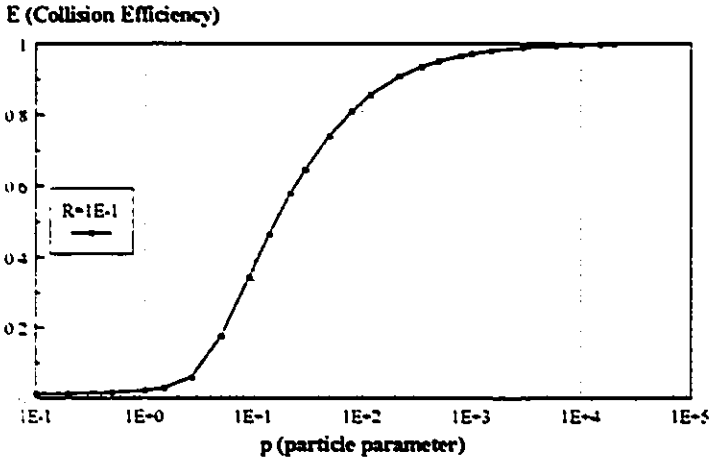

Figure 5.3 Collision efficiency for Reynolds number $R = 0.1$

The graph below corresponds to the data from the table of results for $R = 0.01$

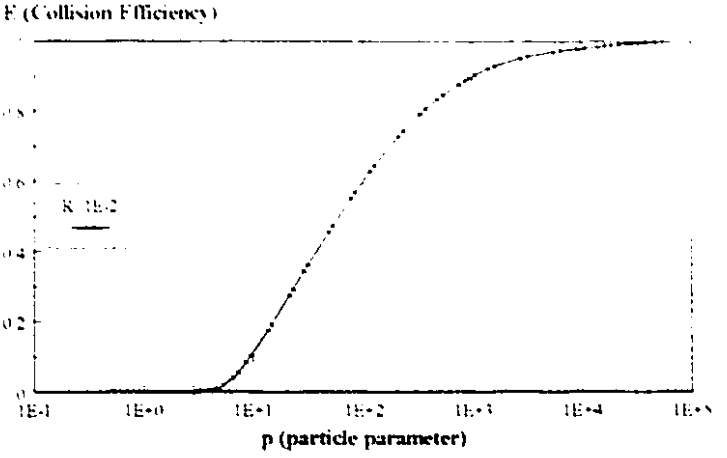

Figure 5.4 Collision fficiency for Reynolds number $R = 0.01$

Similarly, for the Reynolds number $R = 10^{-3}$, we have

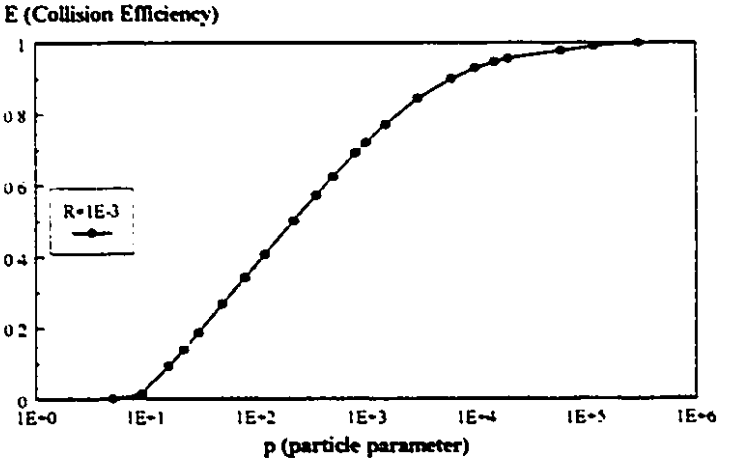

Figure 5.5 Collision efficiency for Reynolds number $R = 10^{-3}$

and for the Reynolds number $R = 10^{-4}$.

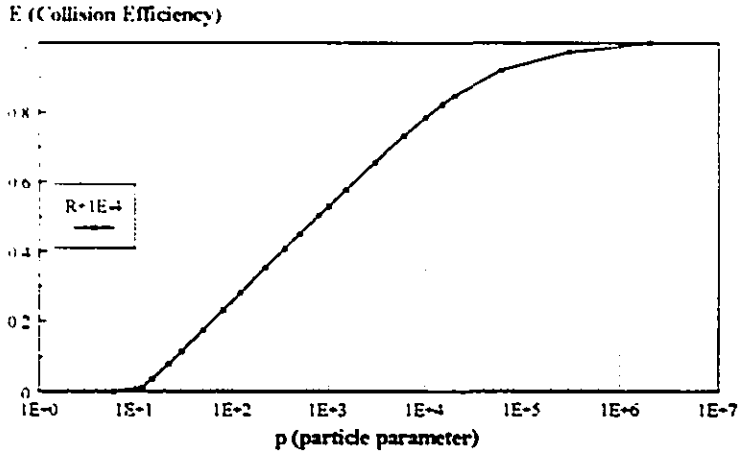

Figure 5.6 Collision efficiency for Reynolds number $R = 10^{-4}$

The results in the table for the Reynolds number $R = 10^{-5}$ are presented in the following graph.

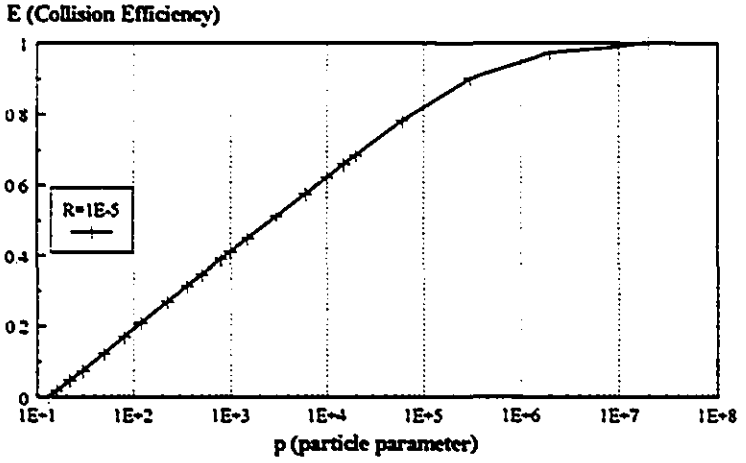

Figure 5.7 Collision efficiency for Reynolds number $R = 10^{-5}$

The graph below presents the results related to Reynolds number $R = 10^{-6}$.

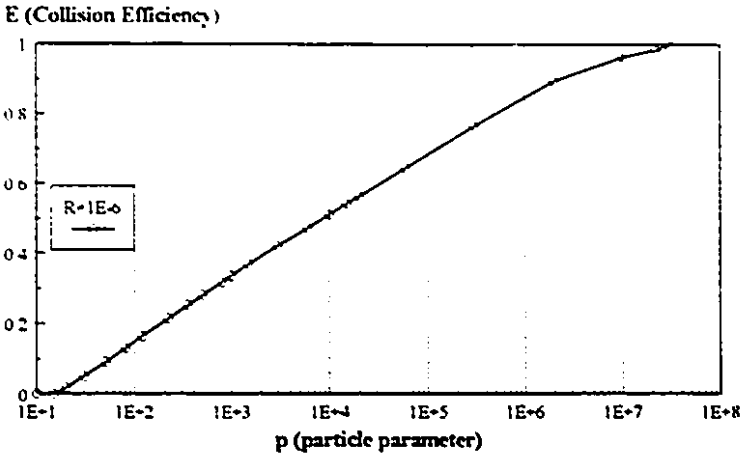

Figure 5.8 Collision efficiency for Reynolds number $R = 10^{-6}$

5.4.1 Why to Non-Dimensionalize

During our work, we kept trying to deal with dimensionless variables. Now that we got the results, the advantage of non-dimensionalizing is more clear. In the original problem, in dimensional form, the involved quantities are particle radius, particle density, cylinder radius, fluid viscosity, fluid density, and fluid velocity. Thus, the answer was going to depend upon six quantities. If we want to solve the problem in dimensional form, we will have six variables to change. If we just choose for each variable 10 values, we get 10^6 problems to solve. While in dimensionless form, we only get two variables, the Reynolds number and the particle parameter, and about 150 cases to solve (6 R's times 25 p's).

Moreover, on each graph, instead of having six, we get only two variables R and p and all the information is put on a single graph. Therefore, for all possible combinations of the values of dimensional variables in R and p, one can easily calculate the values of these two dimensionless quantities, select the appropriate curve and p, and just read off the collision efficiency E.

5.5 DISCUSSION ABOUT THE RESULTS

As we recall, the restrictions and effects not included in our theory and its implementation are as follows.

(a) The particle parameter p is a positive quantity (zero to infinity).

(b) Reynolds number R, based on radius of the cylinder b, is very small ($R << 1$). It is questionable whether the theory can apply to $R = 10^{-2}$.

(c) Effect of finite (non-zero) size of the particle. However, we can compensate it by adding the value of particles radius to the collision efficiency E presented in chapter five, after reading E from a table or a graph. This is true, considering in our problem $E = Y_*$, for relatively small particles.

(d) When a particle gets close to the cylinder surface the hydrodynamic interaction of the particle with the cylinder surface will result in a change of trajectory [actually including (c) would result in $E = 0$].

(e) Intermolecular (van der Waals) forces and electrostatic forces (or other colloidal forces) between the particle and the cylinder. This is especially true for the particle parameter $p \leq 0.05$ which is not included in this research.

(f) Possibility of different cases in impact of the particle and the cylinder. The particle may

1) bounce - no capture or

2) be captured at the surface.

(g) Effect of gravity on the particle.

(h) Brownian motion of the particle (diffusion portion of motion). Diffusion may dominate over convection with very small particles.

(i) Shape of the particle will modify many of the above effects.

(j) The particle parameter p can be written as

$$p = \frac{2a^2 \rho_p U}{9\mu b} = \frac{2}{9}\left(\frac{a}{b}\right)^2 \frac{\rho_p}{\rho} \kappa Re,$$

where ρ is fluid density. Since $\kappa Re = R << 1$, p<<1 (except when $a >> b$). Thus, deposition of the particle due to inertia impact is negligible.

Considering the above restrictions, the results are discussed in this section. Putting the graphs together, we have a better view to see the changes. The first three graphs for Reynolds numbers R = 1, 0.1, and 0.01 are presented as the following graph.

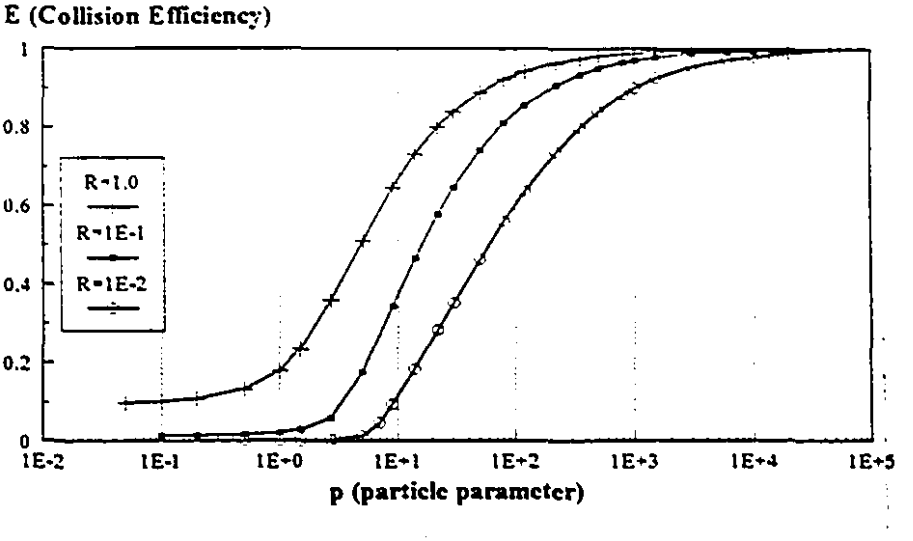

Figure 5.9 Collision efficiency for Reynolds numbers R = 1, 0.1, and 0.01

At collision efficiency E = 0, there is no impact at all (when the largest value of *initial* y_2 which can cause an impact is zero, no impact can be expected any more). The other extreme is E = 1 at which particle goes in straight line even in inner region and quite close to cylinder. The extreme E = 1 is not of particular interest, however, for every Reynolds number R, the points at which $E \equiv 0$ are important. Such points shows the minimum values of particle parameter that can be expected to cause an impact. The other noticeable point is that as $p \rightarrow 0$, the equations of particle trajectory become streamline equations, resulting in no impact (E = 0) again.

Since the Reynolds number R = 1.0 is not in the range of our assumptions (R << 1), its curve can not be valid and behaves differently in figure 5.9. The next Reynolds

number $R = 0.1$ is still questionable. While in large p's its curve shows an acceptable situation, in small values of p is not quite reliable. The other curves have reasonable characteristics

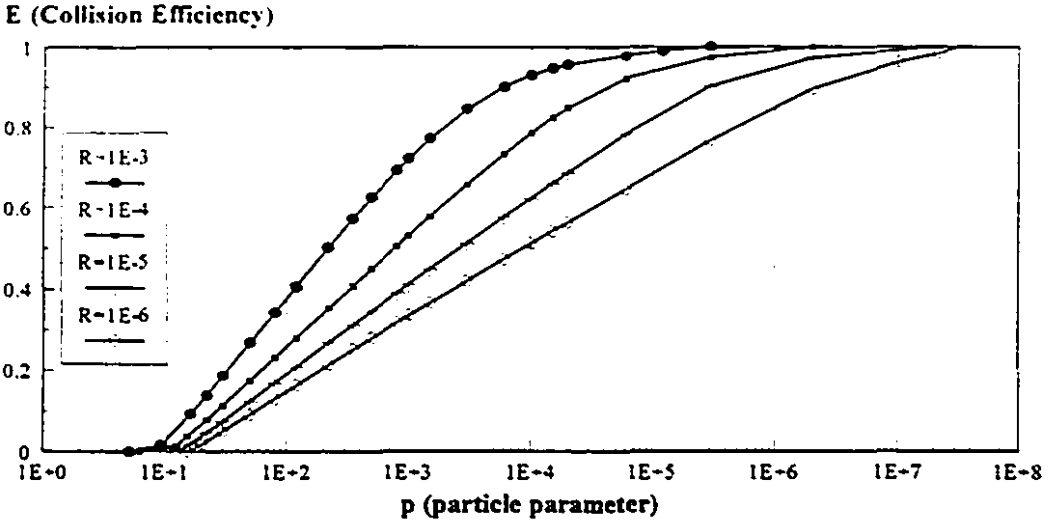

Figure 5.10 Collision efficiency for Reynolds numbers $R = 10^{-3}$ to 10^{-6}

From the beginning, it was a question that as $R \rightarrow 0$, what may happen to the curves? Whether they move to the right and go to infinity or whether they move toward a certain curve. It was known that for smaller Reynolds numbers R's, the collision efficiency E goes down (considering one p, for instance, p = 1000, one may see it on figure 5.10 too), but how the curves behave was a matter of interest. Figure 5.10 shows, explicitly, the tendency of the curves as R becomes smaller. Now, it can be concluded that as $R \rightarrow 0$ the corresponding curves act more like a straight line. The characteristics of that line is not so important to us because, based on our theory, when the Reynolds number $R \rightarrow 0$ (i.e. 10^{-8} or less) it needs a cylinder longer than 10^{10} times (or 10^{9} times) of its radius (no physical meaning).

In the Reynolds number $R = 0$, there is no physical flow around the circular cylinder. This is actually the Stokes' paradox and there is no solution for two dimensional flow around the cylinder in $R = 0$. Thus, $R = 0$ is meaningless.

As it is already mentioned, the points at which $E \equiv 0$ are important. This is because these points shows the minimum values of particle parameter (p_m) that can be expected to cause an impact. In other words, they are the boundaries of impact onto the cylinder (collector). If for a certain Reynolds number the corresponding p varies ten times, it means that we may change, for example, the mass of particle ten times greater or smaller to assure an impact. The values for p_m, can be extracted from the results tables. Because we have calculated no $E = 0$, we only accepted the values of p corresponding to $E \equiv 0$ (at least $E < 0.005$). Since the data is already a numerical approximation, more accuracy is meaningless.

R	p_m
1.E-6	15
1.E-5	13
1.E-4	6
1.E-3	5
1.E-2	1

Table 5.4 Values of p for which $E < 0.005$

In the Reynolds number $R = 0.1$, we have $p_m << 0.05$ (see figure 5.9) which is not in range of our theory, besides, our calculation is not quite valid for such a case. When particle parameter and Reynolds number are very small ($p<5$ and $R<10^{-5}$) the solution may face a stiffness problem. If one likes to concentrate on such a region, a semi-implicit extrapolation method like Bader and Deuflhard Method[4] can be used.

[4] Numerical Recipes in FORTRAN (1992),Cambridge Univ. press.

Chapter 6

CONCLUSION AND FUTURE WORK

6.1 CONCLUSION

Throughout this thesis, we obtained various analytical and numerical results that are reflected in the previous chapters. In this chapter, we put all those results together and then bring up some useful ideas that can be worked on in future studies.

The first step in any study related to the design of a filter involves obtaining a detailed knowledge of the fluid dynamics of the flow around (single) filter fibers. As the analytical basis for development of flow field around the cylinder, long slender body theory was used and the hydrodynamic force per unit length of an isolated slender body, considering inertia effects and correct to the order of κ^{-1}, as an *integral equation* was obtained analytically in chapter three. The result was equation (3,91) as

$$\begin{aligned}\underline{f}(s).\left[\left\{2\ln\left(\frac{\kappa\lambda}{2\varepsilon}\right)-1\right\}\underline{\underline{I}}+2\underline{t}(s)\underline{t}(s)\right]&=-8\pi\,\underline{e}.\left[\underline{\underline{I}}-\frac{1}{2}\underline{t}(s)\underline{t}(s)\right]\\&+\left\{\int_0^{s-\epsilon}+\int_{s+\epsilon}^{1}\right\}\left(\underline{\underline{I}}-\frac{1}{2}\underline{t}(s)\underline{t}(s)\right).\underline{\underline{g}}\left(\underline{R}-\underline{\hat{R}}\right).\underline{f}(\hat{s})\,d\hat{s}\end{aligned}\qquad(6,1)$$

and the value of the tensor $\underline{\underline{g}}(\underline{r})$ is

$$\begin{aligned}g_{ij}(\underline{r})=&\frac{2\left\{1-e^{-1/2Re(r-\underline{e}.\underline{r})}\right\}}{Re\,(r-\underline{e}.\underline{r})^2}\left\{\left(\frac{r_i}{r}-e_i\right)\left(\frac{r_j}{r}-e_j\right)-(r-\underline{e}.\underline{r})\left(\frac{\delta_{ij}}{r}-\frac{r_i\,r_j}{r^3}\right)\right\}\\&+\frac{e^{-1/2Re(r-\underline{e}.\underline{r})}}{(r-\underline{e}.\underline{r})}\left\{\frac{2(r-\underline{e}.\underline{r})\delta_{ij}}{r}-\left(\frac{r_i}{r}-e_i\right)\left(\frac{r_j}{r}-e_j\right)\right\}.\end{aligned}\qquad(6,2)$$

If we take the limit of equation (6.2) as $Re \to 0$, we will have the following expression for creeping flow conditions

$$g_{ij}(\underline{r}) \sim \left(\frac{\delta_{ij}}{r} + \frac{r_i r_j}{r^3}\right) + O(Re),$$

therefore, as it should be, we have R. E. Johnson's (1980) result.

The next result, in analytical development, was the forces on the cylinder, by modifying what we obtained for a long slender body. The result, for a general flow direction and correct to the order of R ($R << 1$), expressed as equation (3.112),

$$\frac{f}{2\pi} = \frac{(\underline{t}.\underline{e})\underline{t}}{\ln R^{-1} + 2\ln 2 - \gamma - \frac{1}{2}\ln(1-(\underline{t}.\underline{e})^2)} + \frac{2(\underline{e} - \underline{t}.\underline{e}\,\underline{t})}{\ln R^{-1} + 2\ln 2 + \frac{1}{2} - \gamma - \frac{1}{2}\ln(1-(\underline{t}.\underline{e})^2)}. \quad (6,3)$$

Writing this equation for flow perpendicular to the cylinder axis, we got equation (3,113) as

$$\frac{f}{2\pi} = \frac{2}{\ln R^{-1} + 2\ln 2 + \frac{1}{2} - \gamma} + O(R), \quad (6,4)$$

which agrees with the result obtained from a power series by Khayat & Cox (1989) .

The flow field universal solution, valid everywhere, around the cylinder was obtained by matching two different solutions for the outer and inner regions. The results was expressed as equation (3,130), in dimensionless form

$$\left.\begin{aligned} u_2 &= 1-\frac{f}{4\pi}e^{\frac{1}{2}R\bar{\rho}\cos\phi}K_0\left(\frac{1}{2}R\bar{\rho}\right)-\frac{f}{8\pi}\bar{\rho}^{-2}(\cos 2\phi) \\ &\quad -\cos\phi\,\frac{f}{4\pi}\left[\frac{2}{R\bar{\rho}}-e^{\frac{1}{2}R\bar{\rho}\cos\phi}K_1\left(\frac{1}{2}R\bar{\rho}\right)\right], \\ u_3 &= \frac{f}{8\pi}\bar{\rho}^{-2}\sin 2\phi+\sin\phi\,\frac{f}{4\pi}\left[\frac{2}{R\bar{\rho}}-e^{\frac{1}{2}R\bar{\rho}\cos\phi}K_1\left(\frac{1}{2}R\bar{\rho}\right)\right]. \end{aligned}\right\} \tag{6,5}$$

Our next results was equations (3,133) governing the motion of particle as a pair of simultaneous non-linear, second-order ordinary differential equations.

$$\left.\begin{aligned} \mathrm{p}\frac{d^2x_2}{dt^2} &= -\frac{dx_2}{dt}+\left[1-\frac{f}{4\pi}e^{\frac{1}{2}Rx_2}K_0\left(\frac{1}{2}R\sqrt{x_2^2+x_3^2}\right)+\frac{f}{8\pi}\frac{\left(x_2^2-x_3^2\right)}{\left(x_2^2+x_3^2\right)^2}\right. \\ &\quad \left.+\frac{f}{4\pi}\frac{x_2}{\sqrt{x_2^2+x_3^2}}\left\{\frac{2}{R\sqrt{x_2^2+x_3^2}}-e^{\frac{1}{2}Rx_2}K_1\left(\frac{1}{2}R\sqrt{x_2^2+x_3^2}\right)\right\}\right], \\ \mathrm{p}\frac{d^2x_3}{dt^2} &= -\frac{dx_3}{dt}+\left[\frac{f}{4\pi}\frac{x_2x_3}{\left(x_2^2+x_3^2\right)^2}\right. \\ &\quad \left.+\frac{f}{4\pi}\frac{x_3}{\sqrt{x_2^2+x_3^2}}\left\{\frac{2}{R\sqrt{x_2^2+x_3^2}}-e^{\frac{1}{2}Rx_2}K_1\left(\frac{1}{2}R\sqrt{x_2^2+x_3^2}\right)\right\}\right], \end{aligned}\right\} \tag{6,6}$$

where K_0 and K_1 are modified Bessel functions and p is a dimensionless particle parameter defined as

$$\mathrm{p}=\frac{2a^2\rho_p U}{9\mu b}, \tag{6,7}$$

and, as we have already had, the Reynolds number and the dimensionless force per unit length on cylinder are, respectively

$$R=\frac{bU}{\nu}\ll 1 \quad \text{and} \quad \frac{f}{2\pi}=\frac{2}{\ln R^{-1}+2\ln 2+\frac{1}{2}-\gamma}.$$

We also got dimensionless initial velocities in the 2- and 3-directions, equations (4,11), as

$$\frac{dx_2}{dt} = 1 - \frac{f}{2\pi R}\left(\frac{1}{x_2}\right),$$
$$\frac{dx_3}{dt} = \frac{f}{2\pi R}\left(\frac{x_3}{x_2^2}\right). \qquad (6.8)$$

Solving the particle equations of motion, numerically, we calculated the collision efficiency of the particle onto the cylinder. The results were plotted into different graphs for Reynolds numbers R (from 10^{-6} to 1) and various particle parameters p.

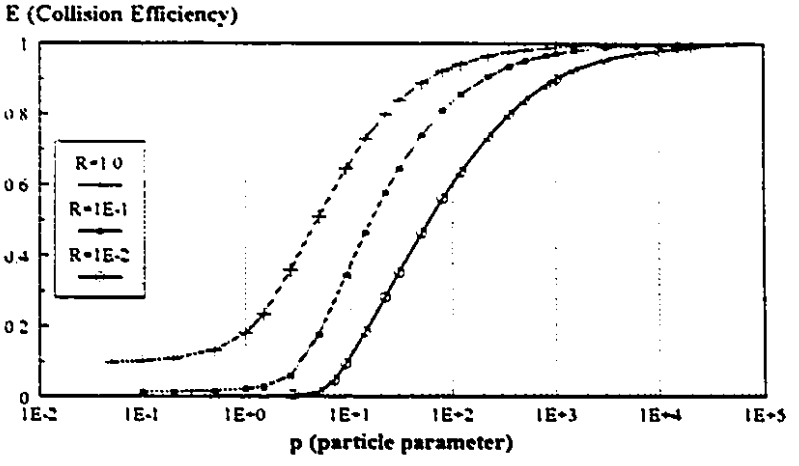

Figure 6.1 Collision efficiency for Reynolds numbers R = 1, 0.1, and 0.01

We recall that, based on our assumptions, the Reynolds number R = 1.0 is not in the range of our assumptions ($R \ll 1$), its curve can not be valid and shows a different behavior in figure 6.1. The next Reynolds number R = 0.1 is questionable. While in large p's its curve shows an acceptable situation, in small values of p is not quite reliable. The other curves have reasonable characteristics.

It was also shown that the inertial impact is not important when $Re = O(1)$ and also $R \ll 1$. Taking van der Waals forces into account is the most recommendable work to do.

Finally, considering all results, we could answer the question about the behavior of curves as $R \to 0$.

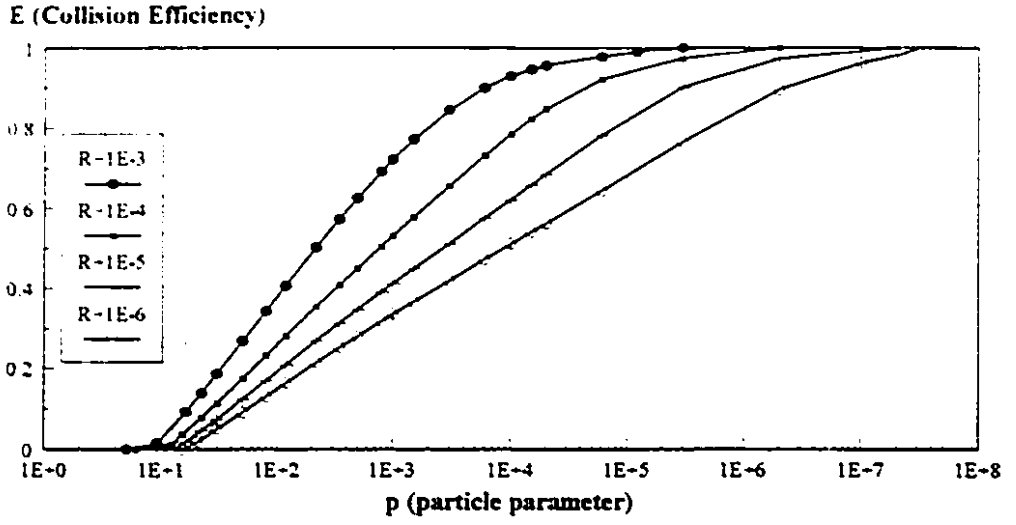

Figure 6.2 Collision efficiency for Reynolds numbers $R = 10^{-3}$ to 10^{-6}

The question was that, as $R \rightarrow 0$, do the corresponding curves move to right to a certain curve or go to infinity or become a straight-line? It was concluded that they finally act more like a straight line for $R \rightarrow 0$. The characteristics of that line are not so important to us because, based on our theory, when the Reynolds number $R \rightarrow 0$ (i.e. 10^{-8} or less) it needs a cylinder longer than 10^{10} times (or 10^{9} times) of its radius (no physical meaning).

The other question was that what the maximum value of p (p_m) is for $E \cong 0$. This value tells us, for each R, the minimum amount of p we should keep in order to have an impact with the lowest efficiency. The values for p_m was extracted from the results tables. Because we have calculated no $E = 0$, we only accept the values of p corresponding to $E \cong 0$ ($E < 0.005$). Since the data points are already numerical approximations, these results are inexact, yet, provide us with a good estimate of the lowest efficiency.

R	p_m
1.E-6	15
1.E-5	13
1.E-4	6
1.E-3	5
1.E-2	1

Table 6.1 Values of p for which $E < 0.005$

6.2 SUGGESTIONS FOR FUTURE STUDIES

As any other research study, this work was limited by the available time and facilities. For future work the following ideas, related directly to the problem on hand, can be suggested.

1) The study of collision efficiency of a particle onto a cylinder when the uniform flow in infinity is in a general direction (not restricted to the direction perpendicular to the cylinder axis). Equation (6,3) states the drag force per unit length of the cylinder exerted by the fluid for such a general condition. We can develop the flow field around the cylinder and, applying Newton's second law of motion, find the particle trajectory course for this case. A numerical calculation will be needed to obtain the collision efficiency.
2) The next step can be the study of a cylinder with finite length. Because of the ends effects, development of force per unit length is much more difficult in such a case. A bent infinite cylinder is another alternative.
3) Instead of working on a single cylinder, study can be done on a row of cylinders and several particles. This case can be studied both for an infinitely long cylinder and a cylinder with a finite length.
4) High Reynolds number flow is another perspective for almost the same kind of approach as that of this research.
5) Effects of van der Waals attractions can be added to the velocity terms in a region close enough to the cylinder. This is useful especially when we have $E \equiv 0$ as $p \rightarrow 0$ and can be readily incorporated with the present theory.

References

Adamczyk, Z. & van de Ven, T. G. M. (1981) *Deposition of Brownian Particles onto Cylindrical Collectors.* J Colloid Interface Sci. **84:2**, pp. 497-518.

Batchelor, G. K. (1967) *An Introduction to Fluid Dynamics.* Cambridge, At the Univ. Press.

Berg, O. T. G., Gaukler, T. A. & Vaughan U. (1970) *Collision Efficiency in Washout.* J Atmospheric Sci. **27**, 1074.

Borse, G. J. (1991) *FORTRAN 77 and Numerical Methods for Engineers, 2nd ed.* PWS-Kent Pub. Co., Boston.

Churchill, S. W. (1988) *Viscous Flows, The Practical Use of Theory.* Butterworths.

Cox, R. G. (1970) *The motion of long slender bodies in a viscous fluid, part 1. General Theory.* J. Fluid Mech. **44:4**, pp. 791-810.

Cox, R. G. (1971) *The motion of long slender bodies in a viscous fluid, part 2. Shear flow.* J. Fluid Mech. **45:4**, pp. 625-657.

Etter, D. M. (1992) *FORTRAN 77 with Numerical Methods for Engineers and Scientists.*

Gerald, C. F. & Wheatly, P. O. (1994) *Applied Numerical Analysis, 5th ed.* Addison-Wesley Pub. Co.

Happle, J. & Brenner, H. (1965) *Low Reynolds Number Hydrodynamics.* Prentice-Hall.

Ingham, D. B. & Hildyard, M. L. (1989) *The Particle Collection Efficiency of a Cascade of Cylinders.* Can. J. Chem. Eng. **67**, pp. 545-553.

Ingham, D. B., Hildyard, M. L. & Heggs, P. J. (1991) *The Particle Collection of an array of Cylinders Using the Boundary element Method.* Eng. Analysis Boundary Elements. **8:1**, 36.

Johnson, R. E. (1980) *An improved slender body theory for Stokes flow.* J. Fluid Mech. **99:2**, pp. 411-431.

Khayat, R. E. & Cox, R. G. (1989) *Inertia effects on the motion of long slender bodies.* J. Fluid Mech. **209**, pp. 435-462.

Kreyszig, E. (1979) *Advanced Engineering Mathematics, 4th ed.* John Wiley & Sons, New York.

Lamb, H. (1945) *Hydrodynamics.* Cambridge Univ. Press.

Langlois, W. E. (1964) *Slow Viscous Flow.* The Macmillan Co. New York.

McLaughlin, C., McComber, P. & Gakwaya, A. (1986) *Numerical Calculation of Particle Collection by a Row of Cylinders in a Viscous Fluid.* Can. J. Chem. Eng. **64**, 205.

Pachner, J. (1984) *Handbook of Numerical Analysis Applications.* McGraw-Hill.

Press, W. H., Teukolsky, S. A., Vetterling, W. T., & Flannery, B. P. (1992) *Numerical Recipes in FORTRAN.* Cambridge Univ. Press.

Schofield, C. F. (1989) *Optimizing FORTRAN programs.*

Shampine, L. F. & Gordon M. K. (1975) *Computer solution of ordinary differential equations, The initial value problem.* W. H. Freeman & Co., San Francisco.

Van Dyke, M. D. (1964) *Perturbation methods in fluid Mechanics.* Academic Press.

White, F. M. (1991) *Viscous Fluid Flow.* McGraw-Hill.

Zill, D. G. & Cullen, M. R. (1992) *Advanced engineering mathematics.* PWS-Kent, Boston.

Appendix A

SOURCE PROGRAM AND OUTPUTS

A.1 SOURCE PROGRAM

In our numerical calculations, we used the following routines which are all in FORTRAN. In addition to the source programs, their input variables and output tables are explained in this appendix.

This program (PROGRAM MAIN7) solves up to a maximum of 19 trials to find the collision efficiency E (or Y_o) for only one Reynolds number R and maximum 20 p's (to plot a complete curve or a part of it). Each trial means covering a distance from *initial* y_2 to the point where $y_2 = 0$. We can mathematically prove that the maximum of 19 trials is for the worst conditions and we will not need more than that.

```
                                PROGRAM MAIN7

 PARAMETER(R=1.0E-5,YSTRT2=-5.E6,PI=3.14159265358979300,EPS=
+1.0E-5,NVAR=4,NMAX=5)
 COMMON /PATH/KMAX,NSTP,HYPTNM
 COMMON /PATH8/HDONE,DYY2,YP(NMAX),XP
 COMMON /LBL1/PRTCLP,RD2,FD4PI
 DIMENSION YSTART(NVAR),P(2)
 DATA P/10.,6./


 KMAX=0
 X1=0.0
 RD2=R/2.
 FD4PI=1./(-LOG(R)+1.309078696222)

 YSTART(2)=YSTRT2
 YSTART(1)=1.+(FD4PI/RD2/YSTART(2))
 HMIN=1.E-5

 OPEN(50,FILE='       ',STATUS='NEW')

 WRITE(50,*)'    THIS IS THE RESULT OF THE PROGRAM MAIN7: ONE "R",'
 WRITE(50,*)'            FOR THE FOLLOWING CONDITIONS:'
 WRITE(50,*)' '
 WRITE(50,*) 'R=',R
```

```
      WRITE(50,*) 'EPS=',EPS
      WRITE(50,*) 'Initial Y(2) = YSTART(2) =',YSTART(2)
      WRITE(50,10)
10    FORMAT (' ' [illegible],T33,'THE RESULTS'/' ',T11,[illegible])
      WRITE(50,*)'dy(2)/dt = Y(1) = YSTART(1) =',YSTART(1)
      WRITE(50,* ' '
      WRITE(50,30)
30    FORMAT(' I  Trial(J)  Min.Hyptnm.   Prtclp.    E=Ys    Ln(Prtclp)'
     +   KHMIN')
      WRITE(50,35)
35    FORMAT(1X,79('='))

      CLOSE(50)


      E=0.018
      DO I=1, 2
         PRTCLP=P(I)
         UP=E
         DWN=0.0
         YS=DWN+0.382*(UP-DWN)
         DO J=1, 19
            YSTART(3)=YS
            YSTART(4)=FD4PI*YSTART(3)/(RD2*YSTART(2)**2)
            H1=1.0

            CALL ODEINT(YSTART,NVAR,X1,EPS,H1,HMIN,NOK,NBAD,KHMIN)
            OPEN(50,FILE='        ',STATUS='OLD',ACCESS='APPEND')
            WRITE(50,40) I,J,HYPTNM,PRTCLP,YSTART(3),LOG(PRTCLP),KHMIN
            CLOSE (50)

             IF(HYPTNM.GE.0.9996.AND.HYPTNM.LE.1.00039) THEN
               E=YSTART(3)
               GOTO 5
            ELSE IF(HYPTNM.GT.1.0) THEN
               UP=YS
            ELSE
               DWN=YS
            ENDIF
            YS=DWN+0.382*(UP-DWN)
         ENDDO
5        WRITE(50,40) I,J,HYPTNM,PRTCLP,YSTART(3),LOG(PRTCLP),KHMIN
40       FORMAT(' ',I2,3X,I3,5X,F8.5,5X,F10.1,2X,F8.5,2X,F8.5,1X,I8)
      ENDDO
      PRINT*,' '
      PRINT*,'Total comp. steps for the last trial of the last PRTCLP ='
     +   ,NSTP

      END



      SUBROUTINE ODEINT(YSTART,NVAR,X1,EPS,H1,HMIN,NOK,NBAD,KHMIN)
      PARAMETER (MAXSTP=5E8,NMAX=5,TINY=1.E-30)
      REAL H,HDID,HNEXT,X
      COMMON /PATH/KMAX,NSTP,HYPTNM
      COMMON /PATH8/HDONE,DYY2,YP(NMAX),XP
      DIMENSION YSTART(NVAR),YSCAL(NMAX),Y(NMAX),DYDX(NMAX)

      X=X1
      H=H1
      NOK=0
      NBAD=0
      DY2=0.0
      HYPTNM=99.99
      KHMIN=0
      K=0
      KOUNT=0
      DO I=1,NVAR
        Y(I)=YSTART(I)
      ENDDO

      DO  NSTP=1,MAXSTP
        CALL DERIVS(Y,DYDX)
        DO  I=1,NVAR
```

```
            YSCAL(I)=ABS(Y(I))+ABS(H*DYDX(I))+TINY
          ENDDO


          CALL BSSTEP(Y,DYDX,NVAR,X,H,EPS,YSCAL,HDID,DYD,HNEXT)
          IF(HDID.EQ.H)THEN
            NOK=NOK+1
          ELSE
            NBAD=NBAD+1
          ENDIF
          IF(Y(2).GE.-1.)THEN
            HYPTNS=SQRT(Y(1)*Y(2)+Y(3)*Y(3))
            HYPTNM=MIN(HYPTNS,HYPTNM)
          ENDIF

          IF(Y(2)+DYD*H.GE.0.0)THEN
            IF(NMAX.EQ.1)THEN
              XP=X
              HDONE=HDID
              DYD=DYD
              DO I=1,NVAR
                YP(I)=Y(I)
              ENDDO
            ENDIF
            RETURN
          ENDIF

          IF(ABS(HNEXT).LT.HMIN) NMIN=NMIN+1
          HNEXT=MAX(HMIN,HNEXT)
          H=HNEXT
        ENDDO
        PAUSE 'Too many steps in odeint.'
        RETURN
        END


        SUBROUTINE BSSTEP(Y,DYDX,NV,X,HTRY,EPS,YSCAL,HDID,DYD,HNEXT)
        PARAMETER (NMAX=5,KMAXX=8,IMAX=KMAXX+1,SAFE1=.25,SAFE2=.7,
       +    REDMAX=1.E-5,REDMIN=.7,TINY=1.E-30,SCALMX=.1)
C       INTEGER NV,NMAX,KMAXX,IMAX
        INTEGER I,IQ,K,KK,KM,KMAX,KOPT,NSEQ(IMAX)
C       REAL EPS,HDID,HNEXT,HTRY,X,DYDX(NV),Y(NV),YSCAL(NV),SAFE1,
C    +     SAFE2,REDMAX,REDMIN,TINY,SCALMX
        REAL EPS1,EPSOLD,ERRMAX,FACT,H,RED,SCALE,WORK,WRKMIN,XEST,
       +     XNEW,A(IMAX),ALF(KMAXX,KMAXX),ERR(KMAXX),YERR(NMAX),
       +     YSAV(NMAX),YSEQ(NMAX)
        LOGICAL FIRST,REDUCT
        DIMENSION DYDX(NV),Y(NV),YSCAL(NV)
        SAVE A,ALF,EPSOLD,FIRST,KMAX,KOPT,NSEQ,XNEW
        DATA FIRST/.TRUE./,EPSOLD/-1./
        DATA NSEQ /2,4,6,8,10,12,14,16,18/

        IF(EPS.NE.EPSOLD)THEN
          HNEXT=-1.E29
          XNEW=-1.E29
          EPS1=SAFE1*EPS
          A(1)=NSEQ(1)+1
          DO K=1, KMAXX
            A(K+1)=A(K)+NSEQ(K+1)
          ENDDO
          DO IQ=2, KMAXX
            DO K=1, IQ-1
              ALF(K,IQ)=EPS1**((A(K+1)-A(IQ+1))/
       +          ((A(IQ+1)-A(1)+1.)*(2*K+1)))
            ENDDO
          ENDDO
          EPSOLD=EPS
          DO KOPT=2, KMAXX-1
            IF(A(KOPT+1).GT.A(KOPT)*ALF(KOPT-1,KOPT))GOTO 1
          ENDDO
1         KMAX=KOPT
        ENDIF
        H=HTRY
        DO I=1, NV
          YSAV(I)=Y(I)
```

```
      ENDDO
      IF(H.NE.HNEXT..AND.K.NE.KMAX)THEN
          FIRST=.TRUE.
          KOPT=KAMAX
      ENDIF
      REDUCT=.FALSE.
2     DO K=1, KAMAX
        KNEW=K+H
3       IF(KNEW.EQ.K)PAUSE 'STEP SIZE UNDERFLOW IN RSSTEP'
        CALL MMID(YSAV,DYDX,NV,X,H,NSEQ(K),YSEQ)
        XEST=(H/NSEQ(K))**2
        CALL RZEXTR(K,XEST,YSEQ,Y,YERR,NV)
        IF(K.NE.1)THEN
            ERRMAX=TINY
            DO I=1, NV
              ERRMAX=MAX(ERRMAX,ABS(YERR(I)/YSCAL(I)))
            ENDDO
            ERRMAX=ERRMAX/EPS
            KM=K-1
            ERR(KM)=(ERRMAX/SAFE1)**(1./(2*KM+1))
        ENDIF
        IF(K.NE.1.AND..K.GE.KOPT-1.OR.FIRST))THEN
            IF(ERRMAX.LT.1.)GOTO 4
            IF(K.EQ.KAMAX.OR.K.EQ.KOPT+1)THEN
                RED=SAFE2/ERR(KM)
                GOTO 3
            ELSE IF(K.EQ.KOPT)THEN
                IF(ALF(KOPT-1,KOPT).LT.ERR(KM))THEN
                    RED=1./ERR(KM)
                    GOTO 3
                ENDIF
            ELSE IF(KOPT.EQ.KAMAX)THEN
                IF(ALF(KM,KAMAX-1).LT.ERR(KM))THEN
                    RED=ALF(KM,KAMAX-1)*SAFE2/ERR(KM)
                    GOTO 3
                ENDIF
            ELSE IF(ALF(KM,KOPT).LT.ERR(KM))THEN
                RED=ALF(KM,KOPT-1)/ERR(KM)
                GOTO 3
            ENDIF
        ENDIF
      ENDDO
3     RED=MIN(RED,REDMIN)
      RED=MAX(RED,REDMAX)
      H=H*RED
      REDUCT=.TRUE.
      GOTO 2
4     X=XNEW
      HDID=H
      FIRST=.FALSE.
      WRKMIN=1.E35
      DO KK=1, KM
          FACT=MAX(ERR(KK),SCALMX)
          WORK=FACT*A(KK+1)
          IF(WORK.LT.WRKMIN)THEN
              SCALE=FACT
              WRKMIN=WORK
              KOPT=KK+1
          ENDIF
      ENDDO
      HNEXT=H/SCALE
      IF(KOPT.GE.K.AND.KOPT.NE.KAMAX.AND..NOT.REDUCT)THEN
          FACT=MAX(SCALE/ALF(KOPT-1,KOPT),SCALMX)
          IF(A(KOPT+1)*FACT.LE.WRKMIN)THEN
              HNEXT=H/FACT
              KOPT=KOPT+1
          ENDIF
      ENDIF

      DY2=ABS(YSAV(2)-Y(2))
      IF (DY2.EQ.0.0) DY2=TINY
          IF(Y(2).GE.-2000.)THEN
                  IF(Y(2)+DY2.GE.0.0)GOTO 10
              IF(Y(2).LE.-2000.)THEN
                  HNEXT=MIN(HNEXT,990./DY2*HDID)
```

```
            ELSE IF(Y(2).LE.-[illegible])THEN
               HNEXT=MIN(HNEXT,[illegible]/DY2*HDID)
            ELSE IF(Y(2).LE.-[illegible])THEN
               HNEXT=MIN(HNEXT,3.[illegible]/DY2*HDID)
            ELSE IF(Y(2).LE.-[illegible])THEN
               HNEXT=MIN(HNEXT,1.5/DY2*HDID)
            ELSE IF(Y(2).LE.-1.5)THEN
               HNEXT=MIN(HNEXT,[illegible]/DY2*HDID)
            ELSE IF(Y(2).LE.-1.0)THEN
              HNEXT=MIN(HNEXT,[illegible].5E-[illegible]/DY2*HDID)
            ELSE IF(Y(2).LE.[illegible])THEN
              HNEXT=[illegible]1.E-[illegible]/DY2*HDID)
            ENDIF
        ENDIF

10    RETURN
      END


      SUBROUTINE MMID(Y,DYDX,NVAR,XS,HTOT,NSTEP,YOUT)
      PARAMETER (NMAX=5)
      DIMENSION Y(NVAR),DYDX(NVAR),YOUT(NVAR),YM(NMAX),YN(NMAX)
      H=HTOT/NSTEP
      DO I=1,NVAR
        YM(I)=Y(I)
        YN(I)=Y(I)+H*DYDX(I)
      ENDDO
      X=XS+H
      CALL DERIVS(YN,YOUT)
      H2=2.*H
      DO N=2,NSTEP
        DO I=1,NVAR
          SWAP=YM(I)+H2*YOUT(I)
          YM(I)=YN(I)
          YN(I)=SWAP
        ENDDO
        X=X+H
        CALL DERIVS(YN,YOUT)
      ENDDO
      DO I=1,NVAR
        YOUT(I)=0.5*(YM(I)+YN(I)+H*YOUT(I))
      ENDDO
      RETURN
      END


      SUBROUTINE PZEXTR(IEST,XEST,YEST,YZ,DY,NV)
      PARAMETER (IMAX=13,NMAX=5)
      DIMENSION X(IMAX),YEST(NV),YZ(NV),DY(NV),QCOL(NMAX,IMAX),D(NMAX)
      SAVE QCOL,X
      X(IEST)=XEST
      DO J=1,NV
        DY(J)=YEST(J)
        YZ(J)=YEST(J)
      ENDDO
      IF(IEST.EQ.1) THEN
        DO J=1,NV
          QCOL(J,1)=YEST(J)
        ENDDO
      ELSE
        DO J=1,NV
          D(J)=YEST(J)
        ENDDO
        DO K1=1,IEST-1
          DELTA=1./(X(IEST-K1)-XEST)
          F1=XEST*DELTA
          F2=X(IEST-K1)*DELTA
          DO J=1,NV
            Q=QCOL(J,K1)
            QCOL(J,K1)=DY(J)
            DELTA=D(J)-Q
            DY(J)=F1*DELTA
            D(J)=F2*DELTA
            YZ(J)=YZ(J)+DY(J)
          ENDDO
```

```
      ENDDO
      DO J=1,NV
        QSOL(J,ISET)=Y(J)
      ENDDO
    ENDIF
    RETURN
    END


    SUBROUTINE DERIVS(Y,DYDX)
    DOUBLE PRECISION PART
    COMMON/LBLI PRTCLP,RD2,FD4PI
    DIMENSION Y(4),DYDX(4)

    SQ=SQRT(Y(2)**2+Y(3)**2)
C       if(y(2).ge.-1.) then
C       print*, ' y(2)      rd2*(-5E-4)*y(2)       -exp(-
C       print*,y(2),rd2*y(2),-exp(rd2*y(2))
C       endif
    PART=1.0/(RD2*SQ)-EXP(RD2*Y(2))*BESSK1(RD2*SQ)
    DYDX(1)=(-Y(2)+(1.0-FD4PI*EXP(RD2*Y(2))*BESSK0(RD2*SQ)+
   +        FD4PI*2.*(Y(2)*Y(2)-Y(3)*Y(3))/(SQ**4.0)+
   +        FD4PI*Y(2)/SQ*PART))/PRTCLP
    DYDX(2)=Y(2)
    DYDX(3)=Y(4)
    DYDX(4)=(-Y(4)+(FD4PI*Y(2)*Y(3)/(SQ**4.0)+
   +        FD4PI*Y(3)/SQ*PART))/PRTCLP

    RETURN
    END


    FUNCTION BESSK0(X)
    DOUBLE PRECISION Y,P1,P2,P3,P4,P5,P6,P7,
   +    Q1,Q2,Q3,Q4,Q5,Q6,Q7
    DATA P1,P2,P3,P4,P5,P6,P7/-0.57721566D0,0.42278420D0,0.23069756D0,
   +    0.3488590D-1,0.262698D-2,0.10750D-3,0.74D-5/
    DATA Q1,Q2,Q3,Q4,Q5,Q6,Q7/1.25331414D0,-0.7832358D-1,0.2189568D-1,
   +    -0.1062446D-1,0.587872D-2,-0.251540D-2,0.53208D-3/

C       IF(X.LE.0.) PRINT*, 'X=0. DOES NOT MAKE SENSE IN BESSK0'
      IF(X.LE.2.) THEN
        Y=X*X/4.
        BESSK0=(-LOG(X/2.0)*BESSI0(X))+(P1+Y*(P2+Y*(P3+
   +            Y*(P4+Y*(P5+Y*(P6+Y*P7))))))
      ELSE
        Y=(2.0/X)
        BESSK0=(EXP(-X)/SQRT(X))*(Q1+Y*(Q2+Y*(Q3+
   +         Y*(Q4+Y*(Q5+Y*(Q6+Y*Q7))))))
      ENDIF
    RETURN
    END

    FUNCTION BESSI0(X)
    DOUBLE PRECISION Y,P1,P2,P3,P4,P5,P6,P7,
   +    Q1,Q2,Q3,Q4,Q5,Q6,Q7,Q8,Q9
    DATA P1,P2,P3,P4,P5,P6,P7/1.0D0,3.5156229D0,3.0899424D0,1.2067492D
   +0,
   +    0.2659732D0,0.360768D-1,0.45813D-2/
    DATA Q1,Q2,Q3,Q4,Q5,Q6,Q7,Q8,Q9/0.39894228D0,0.1328592D-1,
   +    0.2253192D-2,-0.157565D-2,0.916281D-2,-0.2057706D-1,
   +    0.2635537D-1,-0.1647633D-1,0.392377D-2/
    AX=ABS(X)
    IF (AX.LT.3.75) THEN
      Y=(X/3.75)**2
      BESSI0=P1+Y*(P2+Y*(P3+Y*(P4+Y*(P5+Y*(P6+Y*P7)))))
    ELSE
      Y=3.75/AX
      BESSI0=(EXP(AX)/SQRT(AX))*(Q1+Y*(Q2+Y*(Q3+Y*(Q4
   +      +Y*(Q5+Y*(Q6+Y*(Q7+Y*(Q8+Y*Q9)))))))
    ENDIF
    RETURN
    END
```

```
      FUNCTION BESSK1(X)
      DOUBLE PRECISION Y,P1,P2,P3,P4,P5,P6,P7,
     *    Q1,Q2,Q3,Q4,Q5,Q6,Q7,Q8,Q9
      DATA P1,P2,P3,P4,P5,P6,P7/0.5D0,0.87890594D0,0.51498869D0,
     *    0.15084934D0,0.2658733D-1,0.301532D-2,0.32411D-3/
      DATA Q1,Q2,Q3,Q4,Q5,Q6,Q7,Q8,Q9/0.39894228D0,-0.3988024D-1,
     *    -0.362018D-2,0.163801D-2,-0.1031555D-1,0.2282967D-1,
     *    -0.2895312D-1,0.1787654D-1,-0.420059D-2/
      AX=ABS(X)
      IF (AX.LT.3.75) THEN
        Y=(X/3.75)**2
        BESSI1=X*(P1+Y*(P2+Y*(P3+Y*(P4+Y*(P5+Y*(P6+Y*P7))))))
      ELSE
        Y=3.75/AX
        BESSI1=(EXP(AX)/SQRT(AX))*(Q1+Y*(Q2+Y*(Q3+Y*(Q4+
     *      Y*(Q5+Y*(Q6+Y*(Q7+Y*(Q8+Y*Q9))))))))
      ENDIF
      RETURN
      END
```

A.2 INPUT VARIABLES

The first input variables are in the first line of the program.

```
      PARAMETER(R=1.0E-5,YSTRT2=-5.E6,PI=3.14159265358979 3D0,EPS=
     +1.0E-5,NVAR=4,NMAX=5)
```

The value for Reynolds number R must be entered as in `R=1.0E-5`. The second variable is *initial* y_2 which is always a negative number and entered for `YSTRT2`. If you like, you may change the value for local accuracy `EPS`. The third variable is particle parameter which is entered as an array of maximum 20 values in the command `DATA P/10.,6./`. You may enter less than 20 values for p, in that case, the number of p's must be entered in the command `DIMENSION YSTART(NVAR),P(2)`. This number must be also entered in the first `DO` command in the program as in `DO I=1, 2`. This loop is the main loop of trial and error and values in `E, UP,` and `DWN` can be entered based on

golden-section method and or in respect with the previous results (if any).

A.3 PROGRAM OUTPUTS

In this section, the output of the program for different Reynolds numbers R_e is presented. At the beginning of each table the relevant conditions are introduced and then a summary of the important values of the results is printed out. The first column of each table (I) is a counter, indicating the number of rows that is the number of points on the related graph. The second column (Trial(J)) is the number of trials to find Y_o for the corresponding particle parameter (Prtclp), in column four. The third column (Min.Hyptns) shows minimum hypotenuse of the last trial of the row. This number must be close enough to *one* (the dimensionless size of cylinder radius) in order to accept collision efficiency (E=Y_o)[1], in column five. The last column (Ln(Prtclp)) is the natural logarithm of column four. It might be needed in drawing the graphs.

THIS IS THE RESULT OF THE PROGRAM MAIN7: ONE "5",
FOR THE FOLLOWING CONDITIONS:
R= 1.00000E+00
EPS= 1.00000E-05
Initial Y(2) = YSTART 2) = -5.00000E+07

THE RESULTS

dY(2)/dt = Y(1) - YSTART(1) = 0.997355

I	Trial J)	Min.Hyptns.	Prtclp.	E=Yo	Ln.Prtclp)
1	-	0.99989	3000.300.0	0.99618	17.2167
-	-	0.99997	2000.100.0	0.98587	14.9065
3	11	0.99993	1000.000.0	0.96205	13.8181
4	9	0.99999	2.00300.0	0.89543	12.6987
5	9	0.99971	300000.0	0.76573	12.6115
6	9	0.99962	50000.0	0.64431	10.8021
7	8	1.00026	20000.0	0.56236	9.90349
8	13	0.99999	15000.0	0.54062	9.61581
9	11	0.99965	10000.0	0.51001	9.21034
10	14	0.99995	5000.0	0.47173	8.69951
11	11	0.99966	3000.0	0.41910	8.00637
12	12	1.00038	1500.0	0.36620	7.31322
13	7	0.99966	1000.0	0.33441	6.90776
14	11	0.99966	600.0	0.31696	6.68461
15	11	0.99990	500.0	0.27987	6.21461
16	11	1.00006	350.0	0.25136	5.85793
17	14	0.99978	220.0	0.21346	5.39363
18	13	0.99967	120.0	0.16355	4.78749
19	12	0.99988	80.0	0.12984	4.38203
20	11	0.99985	50.0	0.09082	3.91202
21	11	0.99963	30.0	0.04998	3.40120
22	7	0.99982	20.0	0.01763	2.99573
23	14	1.00012	15.0	0.00001	2.70805
24	1	1.00104	10.0	0.00000	2.30259

[1] Or X_o in old variables

[illegible]

THE RESULTS

[illegible]

I	Trial J	Min.Hyptns.	Prtclp.	E-Yo	Ln Prtclp)
1	14	[illegible]	[illegible]	[illegible]	[illegible]
2	11	[illegible]	[illegible]	[illegible]	[illegible]
3	4	1.00010	2000000.0	0.97214	14.50387
4	9	1.00003	300000.0	0.90165	12.61115
5	8	1.00030	60000.0	0.78285	11.00021
6	11	1.00022	20000.0	0.68505	9.90349
7	11	1.00019	15000.0	0.65873	9.61581
8	11	0.99965	10000.0	0.62146	9.21034
9	12	0.99992	6000.0	0.57506	8.69351
10	14	0.99983	3000.0	0.51183	8.00637
11	12	1.00020	1500.0	0.44852	7.31322
12	14	0.99990	1000.0	0.41097	6.90776
13	11	1.00024	600.0	0.35041	6.39461
14	14	1.00010	500.0	0.34638	6.21461
15	12	1.00020	350.0	0.31267	5.85793
16	14	1.00006	220.0	0.26818	5.39363
17	12	0.99993	120.0	0.20917	4.78749
18	11	1.00015	80.0	0.16931	4.38203
19	13	1.00029	50.0	0.12317	3.91202
20	11	0.99998	30.0	0.07438	3.40120
21	16	1.00010	22.0	0.04638	3.13104
22	9	1.00009	16.0	0.01869	2.77259
23	11	1.00026	13.0	0.00013	2.56495

THIS IS THE RESULT OF THE PROGRAM MAIN7: ONE "R",
FOR THE FOLLOWING CONDITIONS:

R= 1.00000E-04
EPS= 1.00000E-05
Initial Y(2) = YSTART(2) = -500000.

THE RESULTS

dY(1)/dt = Y(1) - YSTART(1) = 0.996198

I	Trial J	Min.Hyptns.	Prtclp.	E-Yo	Ln Prtclp)
1	13	0.99968	2000000.0	0.99971	14.5087
2	9	0.99960	300000.0	0.97347	12.6115
3	8	0.99973	60000.0	0.92206	11.0021
4	11	0.99979	20000.0	0.84793	9.90349
5	11	0.99963	15000.0	0.82308	9.61581
6	11	0.99961	10000.0	0.78453	9.21034
7	11	0.99964	6000.0	0.73191	8.69351
8	8	0.99973	3000.0	0.65563	8.00637
9	11	1.00006	1500.0	0.57670	7.31322
10	8	1.00003	1000.0	0.52983	6.90776
11	11	1.00011	600.0	0.50398	6.39461
12	11	1.00019	500.0	0.44926	6.21461
13	11	0.99984	350.0	0.40731	5.85793
14	8	1.00016	220.0	0.35259	5.39363
15	11	1.00003	120.0	0.28015	4.78749
16	13	0.99988	80.0	0.23119	4.38203
17	13	1.00012	50.0	0.17444	3.91202
18	11	0.99964	30.0	0.11368	3.40120
19	13	1.00016	22.0	0.07839	3.09104
20	11	0.99988	15.0	0.03724	2.70805
21	13	1.00036	12.0	0.01205	2.48491
22	13	1.00012	6.0	0.00008	1.79176

[illegible]

THE RESULTS

....

[illegible] - YSTART [illegible]

I	[illegible]	[illegible]	[illegible]	E-Yo	[illegible]
1	15	[illegible]	[illegible]	0.99999	[illegible]
2	9	[illegible]99999	12000[illegible]	[illegible]98992	[illegible]
3	7	[illegible]9996[illegible]	[illegible]	[illegible]97852	[illegible]
4	12	1.00003	2000[illegible]	0.95626	[illegible]
5	12	0.99977	15000.	0.94666	9.61[illegible]
6	12	1.00034	10000.	0.92995	9.21[illegible]34
7	11	0.99980	6000.[illegible]	0.89981	8.699[illegible]
8	13	0.99984	3000.[illegible]	0.84437	8.00637
9	11	0.99975	150[illegible]	0.77092	7.313[illegible]
10	12	0.99999	1000.[illegible]	0.72067	6.907[illegible]
11	10	0.99980	800.[illegible]	0.69080	6.684[illegible]
12	11	0.99977	500.[illegible]	0.62457	6.214[illegible]
13	12	1.00007	350.[illegible]	0.57195	5.85793
14	11	0.99974	220.[illegible]	0.50087	5.39363
15	12	0.99998	120.[illegible]	0.40612	4.76749
16	12	0.99990	80.[illegible]	0.34181	4.382[illegible]
17	12	0.99974	50.[illegible]	0.26699	3.912[illegible]
18	9	1.00006	30.[illegible]	0.18659	3.401[illegible]
19	8	0.99960	22.[illegible]	0.13898	3.091[illegible]
20	12	0.99986	16.[illegible]	0.09229	2.772[illegible]
21	13	1.00016	9.[illegible]	0.01413	2.197[illegible]
22	16	1.00028	5.[illegible]	0.00078	1.60944

THIS IS THE RESULT OF THE PROGRAM MAIN7: ONE "R",
FOR THE FOLLOWING CONDITIONS:

R= 1.000000E-02
EPS= 1.000000E-05
Initial Y(2) = YSTART(2) = -10000.000000

THE RESULTS

....

dY(2)/dt = Y(1) = YSTART(1) = 0.9966183

I	Trial(J)	Min.Hyptns.	Prtclp.	E-Yo	Ln(Prtclp
1	18	0.99716	50000.0	0.99999	10.81978
2	11	0.99970	20000.0	0.98877	9.90349
3	13	1.00025	15000.0	0.98567	9.61581
4	11	0.99967	10000.0	0.97991	9.21034
5	12	1.00016	6000.0	0.97251	8.69951
6	11	1.00007	3000.0	0.95552	8.00637
7	9	1.00039	1500.0	0.92611	7.31322
8	12	1.00036	1000.0	0.90054	6.90776
9	9	1.00039	800.0	0.88355	6.68461
10	12	1.00012	500.0	0.83980	6.21461
11	10	0.99973	350.0	0.79887	5.85793
12	10	0.99992	220.0	0.73575	5.39363
13	12	1.00001	120.0	0.63581	4.78749
14	10	1.00034	60.0	0.55925	4.38203
15	10	0.99970	50.0	0.46213	3.91202
16	10	0.99969	30.0	0.35067	3.40120
17	10	0.99984	22.0	0.28179	3.09104
18	11	1.00015	14.0	0.18303	2.63906
19	11	0.99978	9.0	0.09285	2.19722
20	8	0.99965	7.0	0.04678	1.94591
21	14	0.99964	5.0	0.01331	1.60944
22	16	1.00027	3.0	0.00463	1.09861
23	15	0.99992	2.7	0.00409	1.00000
24	16	1.00004	1.5	0.00243	0.40547
25	16	0.99998	1.0	0.00196	0.00000
26	17	0.99965	0.5	0.00157	-0.69315

[illegible]

[illegible]

Initial Y(2) = YSTART(2) = -[illegible]

THE RESULT

....

dY(2)/dt = Y(1) - YSTART(1) = [illegible]9944[illegible]

I	Trial(J)	Min.Hyptns.	Prtclp.	E-Yc	Ln(Prtclp)
1	1[illegible]	[illegible]	20000.0	[illegible]	9.90349
2	14	[illegible]	15000.0	[illegible]	9.61581
3	11	0.99974	10000.0	[illegible]	9.21034
4	12	0.99944	6000.0	[illegible]	8.69951
5	11	1.00012	3000.0	[illegible]	8.00637
6	11	0.99994	1500.0	[illegible]	7.31322
7	11	0.99979	1000.0	0.97178	6.90776
8	11	0.99994	800.0	0.96630	6.68461
9	12	1.00031	500.0	0.95123	6.21461
10	12	0.99966	350.0	0.93498	5.85793
11	13	0.99965	220.0	0.9[illegible]720	5.39363
12	10	0.99997	120.0	0.85625	4.78749
13	12	0.99964	80.0	0.81920	4.38203
14	12	0.99966	50.0	0.74204	3.91202
15	11	0.99964	30.0	0.64512	3.40120
16	12	0.99995	22.0	0.57898	3.09104
17	11	1.00034	14.0	0.46450	2.63906
18	14	1.000[illegible]	9.0	0.34226	2.19722
19	13	1.00000	5.0	0.[illegible]7136	1.60944
20	10	1.00029	2.7	0.[illegible]	1.00001
21	14	1.00012	1.5	0.02991	0.40547
22	14	0.99982	1.0	0.02283	0.00000
23	12	1.00015	0.5	0.01444	-0.69315
24	15	0.99968	0.2	0.01377	-1.60944
25	16	0.99973	0.1	0.01296	-2.30259

THIS IS THE RESULT OF THE PROGRAM MAIN?: ONE "R",
FOR THE FOLLOWING CONDITIONS:

R= 1.00000
EPS= 1.00000E-05
Initial Y(2) = YSTART(2) = -5000.00

THE RESULTS

....

dY(2)/dt = Y(2) - YSTART(1) = 0.999694

I	Trial(J)	Min.Hyptns.	Prtclp.	E-Yc	Ln(Prtclp)
1	15	0.99979	20000.0	0.99927	9.90349
2	14	0.99981	15000.0	0.99881	9.61581
3	13	0.99977	10000.0	0.99808	9.21034
4	14	0.99990	6000.0	0.99735	8.69951
5	13	0.99965	3000.0	0.99571	8.00637
6	12	1.00006	1500.0	0.99306	7.31322
7	12	0.99975	1000.0	0.98996	6.90776
8	13	0.99987	800.0	0.98804	6.68461
9	12	1.00020	500.0	0.98256	6.21461
10	13	0.99965	350.0	0.97607	5.85793
11	14	0.99968	220.0	0.96484	5.39363
12	13	0.99978	120.0	0.94310	4.78749
13	13	1.00007	80.0	0.92228	4.38203
14	7	0.99961	50.0	0.88857	3.91202
15	11	1.00022	30.0	0.83906	3.40120
16	9	0.99961	22.0	0.79960	3.09104
17	6	0.99967	14.0	0.72954	2.63906
18	10	0.99979	9.0	0.64484	2.19722
19	8	0.99980	5.0	0.51973	1.60944
20	13	1.00016	2.7	0.35835	1.00001
21	11	1.00014	1.5	0.23419	0.40547
22	14	0.99989	1.0	0.17947	0.00000
23	12	1.00022	0.5	0.13204	-0.69315
24	9	1.00002	0.2	0.11838	-1.60944
25	13	1.00010	0.1	0.11126	-2.30259
26	11	1.00015	0.05	0.10779	-2.99573

Appendix B

NOMENCLATURE

All variables in this list of symbols are dimensionless unless otherwise specified.

Symbols meaning

a = particle radius, m

b = cylinder radius, m

e = natural logarithm

$\underline{e}$ = unit velocity vector

e_{ij} = strain tensor

E = collision efficiency

$\underline{f}$ = force per unit length on the body (by fluid)

f^* = force per unit length on the fluid (by body)

$\underline{f}^*$ = line distribution of force

$\underline{i}_3$ = unit vector along the 3-direction

$\underline{I}$ = idemfactor

K_0, K_1 = modified Bessel function

l = length of the body, m

p = pressure in outer region

$\bar{p}$ = pressure in inner region

p' = pressure, N m^{-2}

p = particle parameter

Symbols meaning

$\underline{r}$ = position vector in outer region

$\bar{\underline{r}}$ = position vector in inner region

$\underline{r}'$ = position vector, m

R = Reynolds number based on radius b

Re = Reynolds number based on radius l

$\underline{R}$ = position vector

s = the ratio s'/l

s' = distance along the body from one end, m

$\hat{s}$ = distance along the body centre-line to any point

t = time variable

$\underline{t}$ = unit vector in tangent direction

U = undisturbed velocity in infinity, m sec^{-1}

Symbols	meaning
x	time variable
x_2, x_3	= distance along the 2 and 3-direction in Cartesian coordinates
x_2', x_3'	= distance along the 2 and 3-direction in Cartesian coordinates, m
y_1	= velocity in the 2-direction
y_2, y_3	= distance along the 2 and 3-direction in Cartesian coordinates
y_4	= velocity in the 3-direction
α	= one end of the body
α	= the angle between uniform velocity and the 2-axis
β	= one end of the body
γ	= Euler's constant
ε	= very small arbitrary constant
ε	= tolerance for each step
θ	= polar coordinates angle
μ	= fluid dynamic viscosity, Pa sec
κ	= the ratio b/l
λ	= cross-sectional characteristic
ν	= fluid kinematic viscosity, $m^2 sec^{-1}$
ρ	= fluid density, kg m^{-3}
ρ	= polar coordinate distance
ρ'	= polar coordinate distance, m
$\bar{\rho}$	= inner region polar coordinate distance
$\bar{\rho}'$	= inner region polar coordinate distance, m
ρ_p	= particle density, kg m^{-3}
ϕ	= polar coordinates angle
σ_{ij}	= components of stress tensor
ψ_I, ψ_{II}	= stream function
$\psi_{,i}$	= stream function derivative with respect to i